4-2019

# SYNTHESIS AND BIOLOGICAL APPLICATIONS OF SOME NOVEL UREA AND THIOUREA-BENZIMIDAZOLE DERIVATIVES

Lamia Ali Siddig Ali

United Arab Emirates University

College of Science

Department of Chemistry

# SYNTHESIS AND BIOLOGICAL APPLICATIONS OF SOME NOVEL UREA AND THIOUREA-BENZIMIDAZOLE DERIVATIVES

Lamia Ali Siddig Ali

This thesis is submitted in partial fulfillment of the requirements for the degree of Master of Science in Chemistry

Under the Supervision of Dr. Haythem Ali Mohammad Saadeh

April 2019

## Declaration of Original Work

I, Lamia Ali Siddig Ali, the undersigned, a graduate student at the United Arab Emirates University (UAEU), and the author of this thesis entitled "*Synthesis and Biological Application of Some Novel Urea and Thiourea-Benzimidazole Derivatives*", hereby, solemnly declare that this thesis is my own original research work that has been done and prepared by me under the supervision of Dr. Haythem Ali Mohammad Saadeh, in the College of Science at UAEU. This work has not previously been presented or published, or formed the basis for the award of any academic degree, diploma or a similar title at this or any other university. Any materials borrowed from other sources (whether published or unpublished) and relied upon or included in my thesis have been properly cited and acknowledged in accordance with appropriate academic conventions. I further declare that there is no potential conflict of interest with respect to the research, data collection, authorship, presentation and/or publication of this thesis.

Student's Signature: _____ Date: _____

## Advisory Committee

1) Advisor: Dr. Haythem Ali Mohammad Saadeh

Title: Associate Professor

Department of Chemistry

College of Science

2) Co-advisor: Dr. Mohammad Ahmed Khasawneh

Title: Associate Professor

Department of Chemistry

College of Science

## Approval of the Master Thesis

This Master Thesis is approved by the following Examining Committee Members:

1) Advisor (Committee Chair): Dr. Haythem Ali Saadeh
   Title: Associate Professor
   Department of Chemistry
   College of Science

   Signature _____ Date

2) Member: Na'il Ibrahim Saleh
   Title: Associate Professor
   Department of Chemistry
   College of Science

   Signature _____ Date

4) Member (External Examiner): Ideisan Abu-Abdoun
   Title: Professor
   Department of Chemistry
   Institution: University of Sharjah, UAE

   Signature _____ Date

This Master Thesis is accepted by:

Dean of the College of Science: Professor Ahmed Murad

Signature _____ Date _____

Acting Dean of the College of Graduate Studies: Professor Ali Al-Marzouqi

Signature _____ Date _____

Copy ____ of ____

## Abstract

The objective of this research is the synthesis and characterization of novel urea and thiourea-benzimidazole derivatives and to test their biological activities. The 17 novel compounds (57a-j), (58a-d), 62, 63 and 65 have been synthesized, purified by different techniques such as extraction and column chromatography and then characterized by using suitable spectroscopic techniques including $^{1}$H-NMR, $^{13}$C-NMR, fluorescence and IR spectroscopy techniques.

The biological activity of these compounds has been studied. The antibacterial activity was evaluated at different concentrations (µg/ ml) against 6 types of bacteria (*Esherichia coli*, *Pseudomonas aeruginosa*, *Salmonella enterica*, *Klebsiella pneumoniae*, *Staphylococcus aureus* and *Enterococcus fecalis*). Several compounds (57a, 57d, 57e, 57f, 57g, 57h, 57i, 58a, 58b, 58c, 62, 63 and 65) showed activity against *enterococcus 29212* and 65 showed activity against *p.aereginosa 27853* and *s.aureus 25923*, with different concentrations ranged 37.4 - 96.3µg/ ml. The antifungal activity of these 17 compounds has been tested against 4 types of fungi (*Fusarium solani, botrytis cinerea, thielaviopsis punctulate and neoscytalidium dimidiatum)* and they showed negative results at 250 µM.

In the photophysical study, the emission color of compound 65 has been studied through host-guest complexes. The fluorescence of compound 65 was switched from cyan to green upon the addition of cucurbit[7]uril of the prepared compound above by encapsulating the benzimidazole site and then with the 8-hydroxyqunioline site in compound 65. The cyan fluorescence was restored by the addition of cadaverine due to the replacement of benzimidazole site with cadaverine in the CB7 cavity.

**Keywords:** Urea, thiourea, benzimidazole, piperazine, anti-bacterial, antifungal, host-guest complexe.

**Title and Abstract (in Arabic)**

## تحضير مركبات وايجاد التطبيقات البيولوجية من مشتقات اليوريا والثيوريا مع البينزميدازول


الملخص

يهدف هذا البحث إلى تركيب مشتقات جديدة من اليوريا والثيوريا بنزيميدازول واختبار تطبيقاتها البيولوجية. تم تركيب 17 مركباً جديداً وتنقيتهم باستخدام التقنيات المناسبة. كما تم استخدام الرنين المغناطيسي النووي (البروتون والكاربون) للتأكد من بنية المركبات، بالإضافة لتقنيات التحليل الطيفي بالأشعة تحت الحمراء.

تمت دراسة فاعلية المركبات التي تم تصنيعها كمضادات بيكتيريا، حيث تم اختبارها على 6 أنواع مختلفة من البيكتيريا (الإشريكية القولونية، الزائفة الزنجارية، السالمونيلا المعوية، كليبسيلا الالتهاب الرئوي، المكورات العنقودية الذهبية والبيكتيريا المكورات العنقودية الذهبية). وأظهرت الدارسات أن عدد من المركبات لديه فعالية كمضادات لبيكتيريا المكورات المعوية 29212، ومركب 65 كمضاد لبكتريا الزائفة الزنجارية 27853 ولبكتريا المكورات العنقودية الذهبية 25923، بتركيزات مختلفة تراوحت بين 33.4- 96.3 ميكروغرام / مل. كما تم اختبار نشاط هذه المركبات كمضاد للفطريات حيث تم دراستها على 4 أنواع من الفطريات بتركيز 250 مايكرومولر، وأظهرت الدراسات أن المركبات ليس لديها أي فعالية كمضاد للفطريات.

تمت دراسة الخصائص الضوئية لأحد المركبات 65 باستخدام تجربة المُضاف-المُضِيف. تم إخماد انبعاث ضوء المركب عند ارتباطه بالمُضِيف CB7 حيث ارتبط من جهة البنزيميدازول و مع زيادة التركيز ارتبط من جهة الهيدروكسي كوينولين. كما تمت استعادة انبعاث الضوء بإضافة الكادافيرين بسبب ارتباط الCB7 مع الكادافرين بدلاً من البينزميدازول.



**مفاهيم البحث الرئيسية:** اليوريا، الثيوريا، البنزيميدازول، البيبرازين، مضاد للبكتيريا، مضاد للفطريات، الفيزيائية الضوئية.

## Acknowledgements

I'm very grateful to ALLAH for making me strong enough to reach this point. I would like to thanks United Arab Emirates University and chemistry department to give us this great opportunity.

I am extremely grateful to my all family members. I must express profound gratitude to my parents for providing me with continuous encouragement and unfailing support throughout my years of master, and for believing on me and my dreams. My father, for helping me and always be at my side. My mother, for giving me the hope and love and inspiring me. Special thanks to my old brother Amro Ali Siddig, for his help and support and his advice whenever I need it. My sister Reem Ali Siddig, for always being at my side and her endless love. My young brothers Ahmed Ali Siddig, Ayman Ali Siddig and Siddig Ali Siddig for their support. This accomplishment would not have been done without them.

I would acknowledge with much appreciation to my supervisor Dr. Haythem Saddeh for his great supervision through my master and for his support, criticisms and suggestions to finish the research and writing, thank you for motivation that you give it to us when we frustrating. I am also thankful for his time and guidance he gave me.

Many thanks go to my co-supervisor Dr. Mohameed Khasawneh whose have invested his full effort in guiding me to achieving the goal, and for his patient especially in the writing times. Thanks for his encouragement and support throughout the thesis.

My deep thanks to Dr. Abdelouhed Samdi I have to appreciate his guidance. His office was always open when I ran into a trouble or had a question about the research or writing. He guided me to the right the direction whenever I needed it.

A special thank for photophysical research group Dr. Nail I learnt a lot about photophysical by working in his lab, provided me with knowledge and help me through the experiments. Also I would like to thank my friends in physical lab Reem and Ola for their great help and support through the experiments.

I will not forget our collaborator Dr. Agness Sonnevend and her student Dania Darwich in Medicine & Health Science department for their valuable work in Antibacterial part. Also, I would like to thanks our collaborator in biology department Dr. Khaled A. El-Tarabily, Dr. Synan Abu Qamar and Dr. Esam Eldin Saeed for their endless help and gaudiness to finish the antifungal part.

I would like to express my thank to Dr. Ahmed Alzamly for his help through the years and in facilitating in performing NMR samples during the critical. Also, I would like to thank Mr. Bassam Al-Hindawi and Ragish for his help especially in the instruments.

I would like to express my deep gratitude to my friend Aysha Alkabbi who was there with me through those years of master, and for motivate me and make me happy. Also, I would like to thank my friend Ranem Kaddoura for her help and support. I will not forget to thank my supportive friends: Reem, Noura, Khadeja, Salwa, Maram, Sulafa, Areej, Ghada, Fajr and Mihad.

Finally, my thank go to all people who supported me and provided me to complete the research work directly or indirectly.

## Dedication

*To my beloved parents and family*

# Table of Contents

Title ..... i
Declaration of Original Work ..... ii
Copyright ..... iii
Advisory Committee ..... iv
Approval of the Master Thesis ..... v
Abstract ..... vii
Title and Abstract (in Arabic) ..... viii
Acknowledgements ..... ix
Dedication ..... xi
Table of Contents ..... xii
List of Tables ..... xiv
List of Figures ..... xv
Chapter 1: Introduction ..... 1
1.1 Overview ..... 1
1.2 Imidazole ..... 2
1.3 Benzimidazole ..... 3
1.3.1 Biological activity of benzimidazole derivatives ..... 5
1.4 Urea chemical and application ..... 9
1.4.1 Biological activity of urea derivatives ..... 11
1.5 Thiourea ..... 12
1.5.1 Biological activity of thiourea ..... 13
1.6 Piperazine ..... 14
1.6.1 Biological activity of piperazine ..... 15
1.7 The aim of this project ..... 17
Chapter 2: Methods ..... 21
2.1 Materials and Methods ..... 21
2.1.1 Synthesis of tert-butyl 4-(1H-benzo[d]imidazol-2-yl)piperazine-1-carboxylate 55 ..... 21
2.1.2 General synthesis of benzoimidazol-carbothioamide (57a-57j) and benzoimidazol-carboxamide derivatives (58a-58d) ..... 23
2.1.3 tert-butyl (2-((1H-benzo[d]imidazol-2-yl)amino)ethyl)carbamate 60 ..... 31
2.1.4 N1-(1H-benzo[d]imidazol-2-yl)ethane-1,2-diamine 61 ..... 31

2.1.5 General synthesis of benzoimidazol-carbothioamide (62) and benzoimidazol- carboxamide derivatives 63 ..... 32
2.1.6 Biological activity ..... 33

Chapter 3: Results and Discussion ..... 36
3.1 Synthesis of urea and thiourea-benzimidazole derivatives with piperazine linker ..... 36
3.1.1 Synthesis of key intermediate (56) ..... 36
3.1.2 Synthesis of urea and thiourea-piperazine benzimidazole (57a-57j) and (58a-58d) ..... 39
3.2 Synthesis of urea and thiourea-benzimidazole derivatives with ethylenediamine linker ..... 43
3.2.1 Synthesis of key intermediate (61) ..... 44
3.2.2 Synthesis of urea and thiourea-piperazine ethylenediamine. ..... 46
3.3.1 Antibacterial activity ..... 48
3.3.2 In vitro Antifungal activity ..... 51

Chapter 4: Photochemistry ..... 53
4.1 Introduction ..... 53
4.2 Experimental part ..... 55
4.2.1 Chemistry ..... 55
4.2.2 Photochemistry ..... 56
4.3 Results and discussion ..... 58
4.3.1 Chemistry ..... 58
4.3.2 Photochemistry ..... 59

Chapter 5: Conclusion ..... 66
5.1 Recommendation and Future work ..... 66

References ..... 68

Appendix ..... 74

## List of Tables

Table 1: MIC (µg/ml) of compounds (57a-57j), (58a-58d), 62, 63 and 65 ..... 50
Table 2: MIC of compounds (57a-57j), (58a-58d), 62, 63 and 65..... 52
Table 3: NMR chemical shift of compound 65 upon addition of CB7 and CAD ..... 64

## List of Figures

Figure 1: The molecular structure of imidazole 1, pyridine 2, benzimidazole 3, cimetidine 4, omeprazole 5, imazapic 6, carbendazim 7 ..... 1
Figure 2: Condensation of nitriles with 1,2- ethylene diamine and wallach synthesis for imidazole derivatives ..... 2
Figure 3: Oroidin 8, temozolomide 9, stevensine 10, clotrimazole 11, isoconazole 12 and butoconazole 13 ..... 3
Figure 4: Synthesize of 2, 5-dimethylbenzimidazole and 2-substituted-1H-benzimidazoles by HCl ..... 4
Figure 5: Tautomers of benzimidazole ..... 5
Figure 6: Structure of N-ribosyl-dimethylbenzimidazole ..... 5
Figure 7: N-(4-nitro benzylidine)-4-(1H-benzo[d] imidazol-2-yl)benzenamine(17), 3-(4-(1H-benzo[d]imidazol-2-yl)phenyl)-2(4-methoxy phenyl)thiazolidin-4-one (18) and 1-(4-(1H-benzo[d]imidazol-2-yl)phenyl)-3chloro-4-p-tolyl azetidin-2-one (19) ..... 6
Figure 8: The molecular structure of maribavir (20), clemizole (21), emedastine (22), mizolastine (23) and astemizole (24) ..... 7
Figure 9: The molecular structure of thiabendazole 25, fenbendazole 26, albendazole 27 and mebendazole 28 ..... 8
Figure 10: The molecular structure of nocodazole ..... 8
Figure 11: The molecular structure of 2-(1-methyl-1-H-benzimidazol-2-yl)phenyl)imino)methyl) naphthol (HL1) ..... 9
Figure 12: The molecular structure of urea ..... 9
Figure 13: The molecular structure of MMU ..... 11
Figure 14: The molecular structure of thiourea ..... 12
Figure 15: Synthesis of Thioureas ..... 13
Figure 16: The molecular structure of 1-(2-(4-(2,3-dichlorophenyl)piperazin-1-yl)-2-oxoethyl)-3-(4-fluorophenyl)thiourea ..... 13
Figure 17: The molecular structure of methimazole 37, propylthiouracil 38, thioacetazone 39 and Ambazone 40 ..... 14
Figure 18: Synthesis of 3,4- dehydropiperazine-2-one 43 ..... 15
Figure 19: The molecular structure of amoxapine 44, trazodone 45, buclizine 46 and cyclizine 47 ..... 16
Figure 20: The molecular structure of fluphenazine 48, thiothixene 49, perphenazine 50, prochlorperazine 51 and trifluoperazine 52 ..... 17
Figure 21: General synthesis of benzoimidazol-carbothioamide (57a-j) and benzoimidazol- carboxamide derivatives (58a-d) ..... 19

Figure 22: General synthesis of benzoimidazol- carboxamide derivatives (62 and 63) ..... 20
Figure 23: Synthesis of key intermediate 57 and dimer 63 ..... 37
Figure 24: Synthesis of tert-butyl 4-(1H-benzo[d]imidazol-2-yl) piperazine-1-carboxylate 55 ..... 37
Figure 25: Synthesis of key intermediate 56 (method a) ..... 38
Figure 26: Mechanism of key intermediate 56 (method b) ..... 39
Figure 27: Synthesis of benzoimidazol-carbothioamide (57a-j) and benzoimidazol- carboxamide derivatives (58a-d) ..... 40
Figure 28: General synthesis of benzoimidazol- carboxamide derivatives (62-63) ..... 43
Figure 29: Synthesis of key intermediate 61 and dimer 69 ..... 44
Figure 30: Synthesis of tert-butyl (2-((1H-benzo[d]imidazol-2-yl)amino)ethyl)carbamate 60 ..... 45
Figure 31: Mechanism of key intermediate 61 ..... 46
Figure 32: Synthesis of benzoimidazol- carboxamide derivatives ..... 47
Figure 33: Chemical structure of cucurbiturils molecular containers (CB5, CB6 and CB7) ..... 54
Figure 34: Mechanism reaction of compound 65 ..... 58
Figure 35: Compound 65 (1), the complex of 65 with CB7 (2) and the complex of 65 with CB7 and CAD (3) under UV lamb ..... 59
Figure 36: $^{1}$H-NMR (400MHz) titration of 65 [1mM] with CB7 (0-2.9 equiv.) in $D_2O$ at pD 2.9 ..... 60
Figure 37: $^{1}$H-NMR aromatic region: Biding of compound 65/CB7 (1: 4.4 equiv.) with CAD (0.5 equiv.) in $D_2O$ ..... 62
Figure 38: $^{1}$H-NMR aliphatic region: Biding of compound 65 with CB7 (0- 4.4 equiv.) and CAD (0.5 equiv.) in $D_2O$ ..... 63
Figure 39: Binding titration ..... 65
Figure 40: $^{1}$H and $^{13}$C spectrum and IR for 55 ..... 74
Figure 41: $^{1}$H and $^{13}$C spectrum for 56 ..... 75
Figure 42: $^{1}$H and $^{13}$C spectrum for 57a ..... 76
Figure 43: $^{1}$H and $^{13}$C spectrum for 57b ..... 77
Figure 44: $^{1}$H and $^{13}$C spectrum for 57c ..... 78
Figure 45: $^{1}$H and $^{13}$C spectrum for 57d ..... 79
Figure 46: $^{1}$H and $^{13}$C spectrum for 57e ..... 80
Figure 47: $^{1}$H and $^{13}$C spectrum for 57f ..... 81
Figure 48: $^{1}$H and $^{13}$C spectrum for 57g ..... 82
Figure 49: $^{1}$H and $^{13}$C spectrum for 57h ..... 83
Figure 50: $^{1}$H and $^{13}$C spectrum for 57i ..... 84
Figure 51: $^{1}$H and $^{13}$C spectrum for 57j ..... 85
Figure 52: $^{1}$H and $^{13}$C spectrum for 58a ..... 86
Figure 53: $^{1}$H and $^{13}$C spectrum for 58b ..... 87
Figure 54: $^{1}$H and $^{13}$C spectrum for 58c ..... 88

Figure 55: $^{1}H$ and $^{13}C$ spectrum for 58d.....89
Figure 56: $^{1}H$ and $^{13}C$ spectrum for 62.....90
Figure 57: $^{1}H$ and $^{13}C$ spectrum for 63.....91
Figure 58: $^{1}H$ and $^{13}C$ spectrum for 64.....92
Figure 59: $^{1}H$ and $^{13}C$ spectrum for 65.....93
Figure 60: Infrared spectra for (55), (56) and (57a).....94
Figure 61: Infrared spectra for (57b), (57c) and (57d).....95
Figure 62: Infrared spectra for (57e), (57g) and (57f).....96
Figure 63: Infrared spectra for (57h), (57i) and (57j).....97
Figure 64: Infrared spectra for (58a), (58b) and (58c).....98
Figure 65: Infrared spectra for (58d), (60) and (61).....99
Figure 66: Infrared spectra for (62), (63) and (65).....100

## List of Abbreviations

| | |
|---|---|
| 8-HQ | 8-Hydroxyquniloine |
| BZ | Benzimidazole |
| CAD | Cadaverine |
| CB7 | Cucurbit[7]uril |
| CFU | Colony-Forming Unit |
| HIV | Human Immunodeficiency Viruses |
| IR | Infrared Spectra |
| MHA | Mueller Hinton Agar |
| N-Boc | Tert-Butyloxycarbonyl |
| NMR | Nuclear Magnetic Resonance |
| pD | P1otential of Deuterium |
| PDA | Potato Dextrose Agar |
| $R_f$ | Reflective Index |
| TFA | Trifluoroacetic Acid |
| THF | Tetrahydrofuran |

# Chapter 1: Introduction

## 1.1 Overview

Heterocyclic compounds are a class of cyclic organic compounds that have one or more heteroatoms such as O, N or S. Heterocycles are found in several groups of naturally occurring compounds (natural products). Imidazole 1, piperazine 2 and benzimidazole 3 are heterocyclic core scaffolds widely present in many classes of marketed drugs that exhibit large spectrum of interesting biological activities (Mantu et al. 2016). Examples of heterocyclic compounds which are given in Figure 1, include cimetidine 4 and omeprazole 5 which inhibit stomach acid production; imazapic 6 is a herbicide and carbendazim 7 is a fungicide.

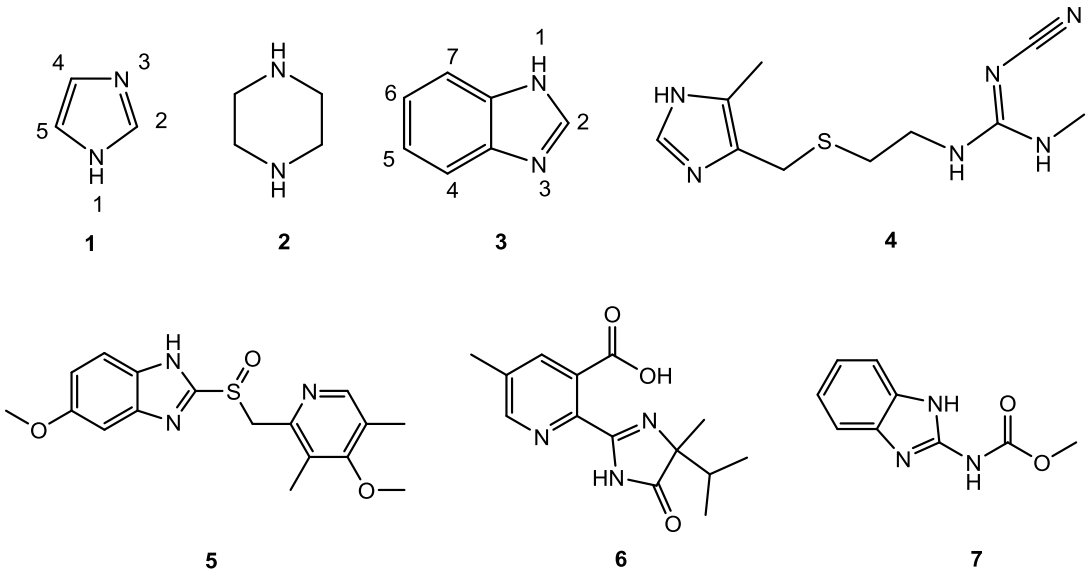


Figure 1: The molecular structure of imidazole 1, pyridine 2, benzimidazole 3, cimetidine 4, omeprazole 5, imazapic 6, carbendazim 7

In this thesis, several compound containing imidazole, benzimidazole, piperazine, ethylenediamine, urea and thiourea moieties are synthesized, characterized and their antibacterial, antifungal activity is evaluated.

### 1.2 Imidazole

There are several methods for the synthesis of imidazole and its derivatives. Example include the condensation of nitriles with 1,2- ethylene diamine followed by the dehydrogenation with $BaMnO_4$ (Figure 2 a) (Elderfield, 1975). The second example is the Wallach synthesis which involves the reaction of N,N-dimethyloxamide with phosphorus pentachloride, followed by reduction with hydroiodic acid (Figure 2 b) (Wallach & Schuelze, 1881). Other methods for the synthesis of imidazole derivatives are also reported in recent reviews (Manocha et al. 2016).

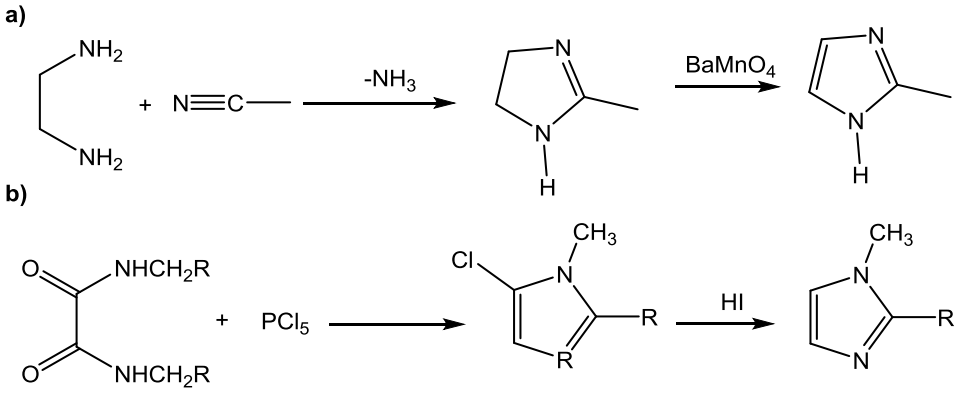


Figure 2: a) Condensation of nitriles with 1,2-ethylene diamine b) Wallach synthesis for imidazole derivatives

Natural products containing imidazole moiety include oroidin 8, temozolomide 9 and stevensine 10 which are isolated from marine sponge (Dyson et al. 2014; Albizati et al. 1985). On the other hand, imidazole scaffold is found in

several synthetic drugs such as clotrimazole 11, isoconazole 12 and butoconazole 13 which are used as antifungal drugs (Figure 3).

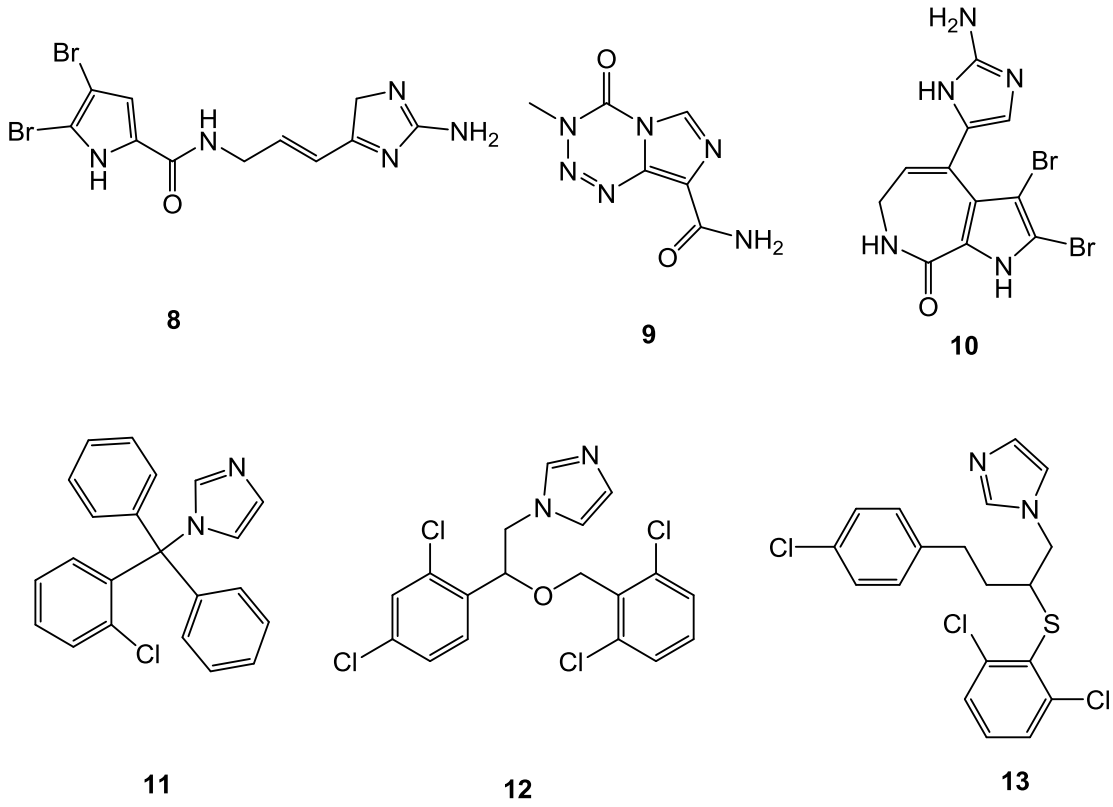


Figure 3: Oroidin 8, temozolomide 9, stevensine 10, clotrimazole 11, isoconazole 12 and butoconazole 13

Imidazole derivatives have important biological activities such as anti-cancer, antifungal, antiviral, antiinflammatory and anti-diabetic activities (Kale et al. 2016). This explains the intensive synthetic interest and the attention of many research groups around the world (Romero et al. 2014).

### 1.3 Benzimidazole

Benzimidazole is a derivative of imidazole and plays an important role in organic chemistry due to its high degree of chemical stability. Oxidation and reduction of benzimidazole require vigorous conditions (Srestha et al. 2014).

Benzimidazole became an attractive compound and several reports containing the synthesis of benzimidazole derivatives appeared in the literature (Salahuddin et al. 2017; Alaqeel, 2017; Akhtar et al. 2017).

The first derivatives of benzimidazole 2,5-dimethylbenzimidazole was synthesized by Hoebrecker in 1872 following a reduction, cyclization and aromatization reaction of 2-nitro-4-methylacetanilide (Figure 4 a) (Wright, 1951). Another method involves the coupling of o-phenylenediamine with p-amino benzoic acid followed by aromatization (Figure 4 b) (Panneerselvam et al. 2011).

**a)**

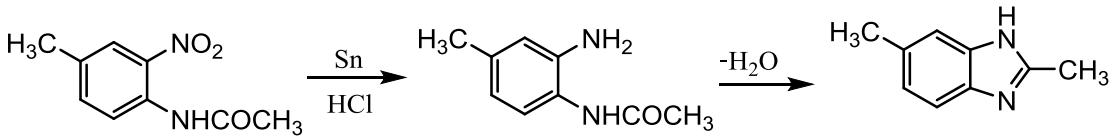


**b)**

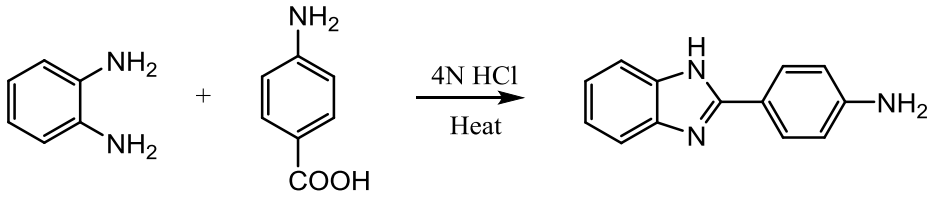


Figure 4: (a) Scheme for synthesized 2,5-dimethylbenzimidazole, (b) Synthesis of 2-substituted-1H-benzimidazoles by HCl

Due to electronic resonance, positions 1 and 2 of the benzimidazole ring are the most important positions in terms of reactivity. Position 1 is highly reactive due to the nucleophilicity of the nitrogen, while the carbon in position 2 is electrophilic due to presence of two nitrogens attached to it. There are two equivalent tautomeric forms of benzimidazole as outlined in Figure 5 (Wright, 1951).

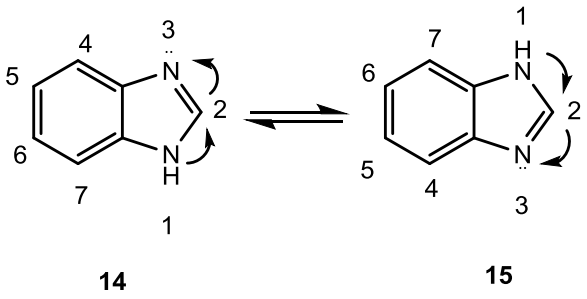


Figure 5: Tautomers of benzimidazole

The most notable natural benzimidazole derivative is probably N-ribosyl-dimethylbenzimidazole 16 (Figure 6) which works as a ligand in vitamin $B_{12}$ by binding the nitrogen atom in benzimidazole with cobalt atom in porphyrin (Srestha et al., 2014).

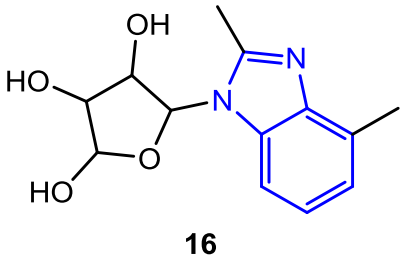


Figure 6: Structure of N-ribosyl-dimethylbenzimidazole

### 1.3.1 Biological activity of benzimidazole derivatives

Benzimidazole bioactivities were recently reviewed by several groups around the world (Manocha et al. 2017; Akhtar et al., 2017; Salahuddin et al. 2017; Shrivastava et al., 2017). Compounds containing benzimidazole have been widely used in drug development and researchers around the world are actively seeking new uses and applications of benzimidazole.

Benzimidazole derivatives were reported to possess antimicrobial activity

(Negi et al. 2017); for example, the synthetic compound 17 (N-(4-nitrobenzylidine)-4-(1H-benzo[d] imidazol-2-yl) benzenamine) (Figure 7) shows potent antimicrobial activity against *S.epidermidis* (Gram-positive bacterium), with minimum inhibitory concentrations (MIC) of 9 µg/mL. Compound 18 (3-(4-(1H-benzo[d]imidazol-2-yl)phenyl)-2(4-methoxyphenyl)thiazolidin-4-one) showed significant activity (MIC= 12 µg/mL) against both *K. pneumoniae* (Gram-negative bacterium) and A. niger (fungus). Compound 19 (1-(4-(1H-benzo[d]imidazol-2-yl)phenyl)-3chloro-4-p-tolylazetidin-2-one) showed significant activity (MIC = 12 µg/mL) against *E. coli* bacteria (Panneerselvam & Kumar, 2011).

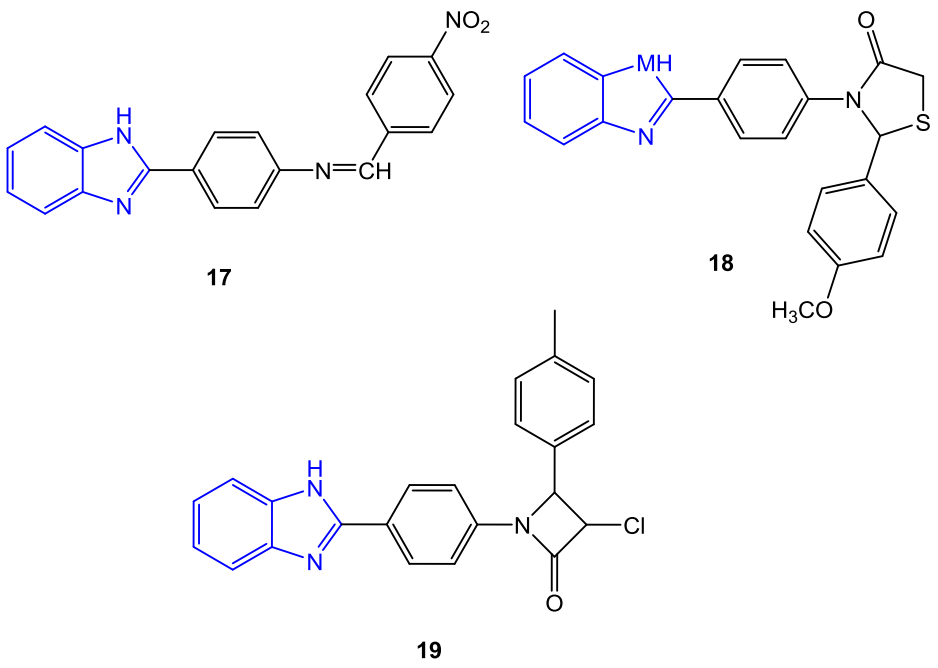


Figure 7: N-(4-nitro benzylidine)-4-(1H-benzo[d] imidazol-2-yl) benzenamine(17), 3-(4-(1H-benzo[d]imidazol-2-yl)phenyl)-2(4-methoxy phenyl)thiazolidin-4-one (18) and 1-(4-(1H-benzo[d]imidazol-2-yl)phenyl)-3chloro-4-p-tolyl azetidin-2-one (19)

Some benzimidazole derivatives were reported to exhibit antiviral activity such as, human cytomegalovirus (HCMV), HIV, RNA, and influenza. Maribavir 20, an oral drug containing benzimidazole, is used to treat human cytomegalovirus

(HCMV) disease in stem cell/bone (Soni, 2014). It contains substitutions at the positions 1, 2, 5 and 6. Several benzimidazole derivatives such as 21, 22, 23 and 24 have been found in several allergy drugs due to their antihistamine activity (Figure 8).

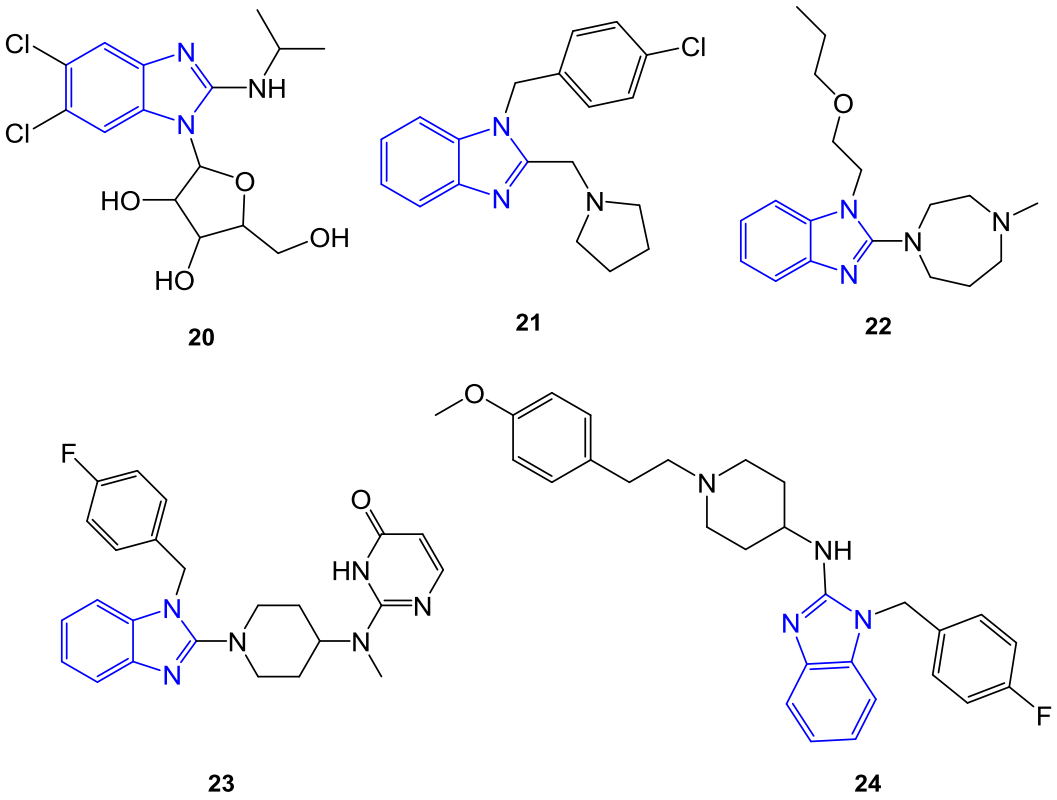


Figure 8: The molecular structure of maribavir (20), clemizole (21), emedastine (22), mizolastine (23) and astemizole (24)

Drugs containing benzimidazole are the most common drugs used to treat infections associated with helminthes which are common in developing countries (Horton, 2000). In 1961, synthesis of thiabendazole 25 opened the door for more potent antihelminthic drugs (Brown et al., 1962). Since 1960s more than twenty antihelminthic benzimidazole compounds were used in medical and veterinary practices (Cazajous et al., 2018). Fenbendazole 26, albendazole 27 and mebendazole 28 are examples of antihelminthic drugs (Figure 9).

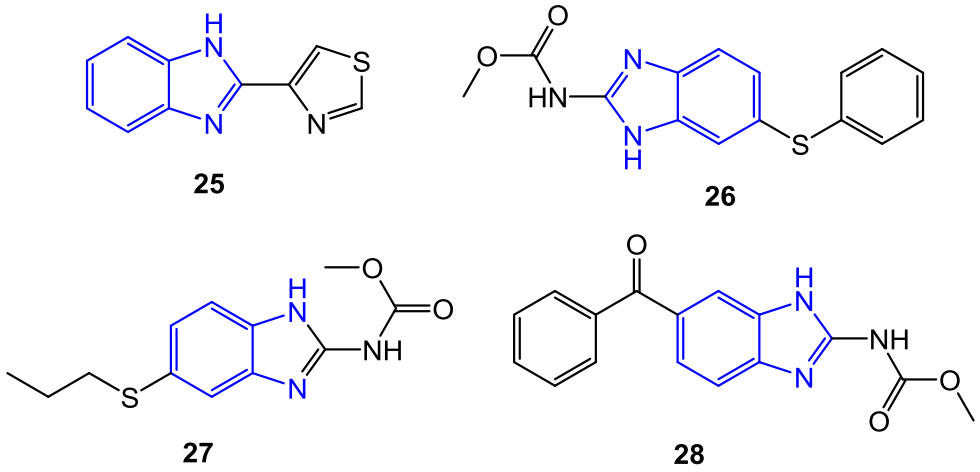


Figure 9: The molecular structure of thiabendazole 25, fenbendazole 26, albendazole 27 and mebendazole 28

Benzimidazole derivatives were also reported to exhibit anticancer activity. Figure 10 shows nocodazole 29 (antineoplastic drug) which inhibits various cancer-related kinases, it is type of cancer that is related to transduction process (Shrivastava et al., 2017).

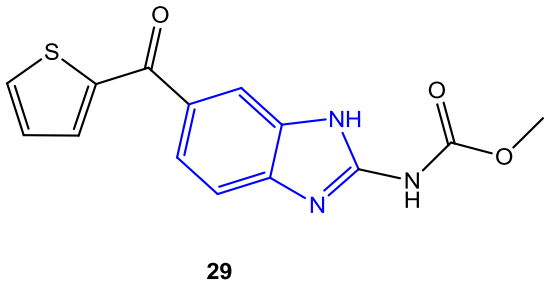


Figure 10: The molecular structure of nocodazole

Metal chelation is one of the properties that are exhibited by compounds with activity against Alzheimer, cancer and Parkinson diseases (Drew, 2017; Flora & Pachauri, 2010). Therefore metal chelation is usually studied for some newly synthesized compounds. Structure 30 (Figure 11) shows a 2-(1-methyl-1-H-

benzimidazol-2-yl)phenyl)imino)methyl) naphthol (HL1) this compound chelates with Cu(II), and exhibits a significant inhibitory effect on lung carcinoma cancer cells (A-549), and is more potent ($IC_{50}$=16.7 µM) than the cisplatin drug ($IC_{50}$ = 27.2 µM) under the same experimental conditions.

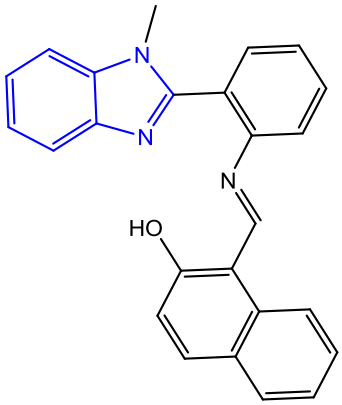


30

Figure 11: The molecular structure of 2-(1-methyl-1-H-benzimidazol-2-yl)phenyl)imino)methyl) naphthol (HL1)

**1.4 Urea chemical and application**

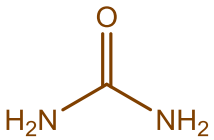


31

Figure 12: The molecular structure of urea

Urea 31 (Figure 12) is a colorless, odorless natural compound produced in the metabolism process of mammals and excreted with urine. Urea was synthesized for the first time by Friedrich Wohler in 1828, by combining ammonium chloride and cyanic acid (Wöhler, 1828). Another method involves the reaction between ammonia

and carbon dioxide to form ammonium carbamate, which is dehydrated in order to produce urea (Shibata et al. 1995) (Equation 1).

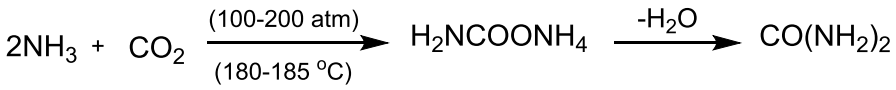


Equation 1: Synthesis of urea by ammonia and carbon dioxide

There are several ways to synthesize organic urea listed in the Equation 2. (Zhao et al., 2016; Min, 2018). Urea is used as a fertilizer, and as livestock feed additive. It is also used in the production of synthetic resins in as adhesives, plastics, moldings, plywood, laminates, particleboard, coatings and textiles. Minor uses of urea includes as rehydrating lotions, cold-compresses, deicers and diuretics.

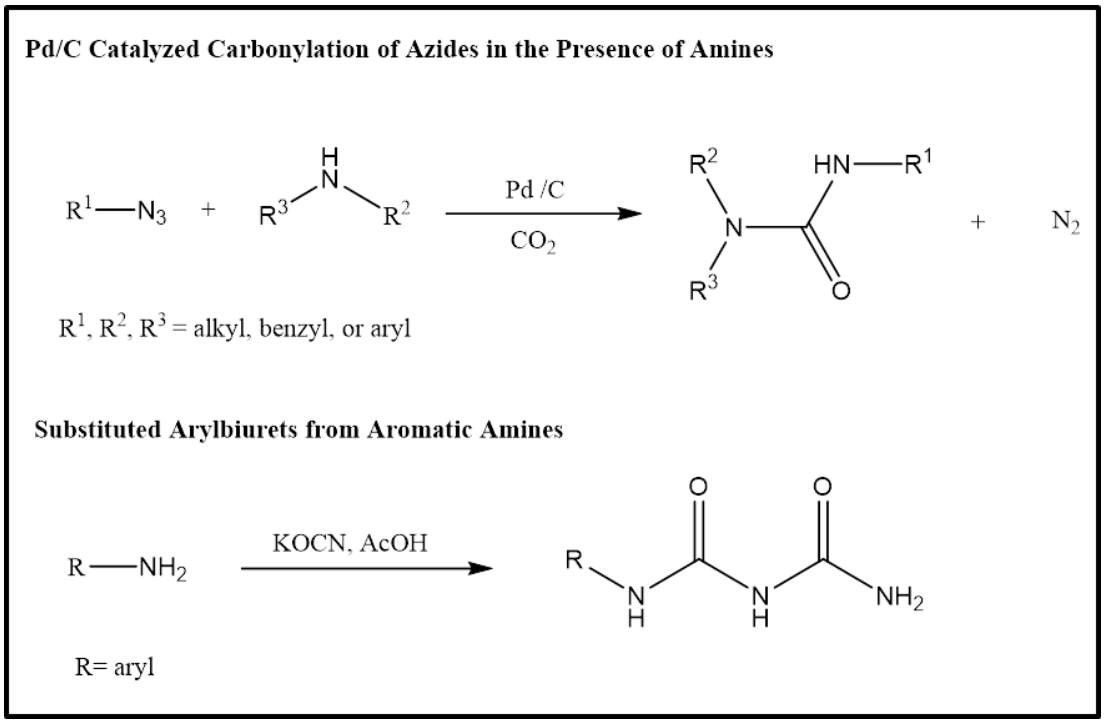


Equation 2: General synthetic approach towards ureas

### 1.4.1 Biological activity of urea derivatives

Urea is used in many marketed treatments such as ure-Na (oral treatment) to treat hyponatremia, and carmol drug that is used to treat dermatological disorders and dry skin. The most popular derivatives of urea are thiourea, sulphur urea, phenyl urea, etc. Urea and its derivatives have been shown to exhibit a number of biological activities including antibiotic, hypoglycaemic and antiatherosclerotic effect, in addition to antitumour activities. They also could be used as sedatives, hypnotics, and antibacterial, anticonvulsants and anticancer agents (Sikka, 2015).

The naturally-occurring urea derivative 1,3-bis (4-methoxybenzyl) urea (MMU) extracted from plant *Pentadiplandra brazzeana* root showed a significant soluble epoxide hydrolase (sEH) inhibitory effect. sEH is an enzyme found in mammals, and plays a major role in the metabolism of endogenous lipid epoxides. Those lipids play a role in pain, asthma and inflammation. This compound 32 (Figure 13) showed a significant sEH inhibitory activity that significantly reduce inflammatory pain in nociceptive pain assay in rats ($IC_{50}$ of 92 nM) via fluorescent assay on human sEH (Kitamura et al., 2015).

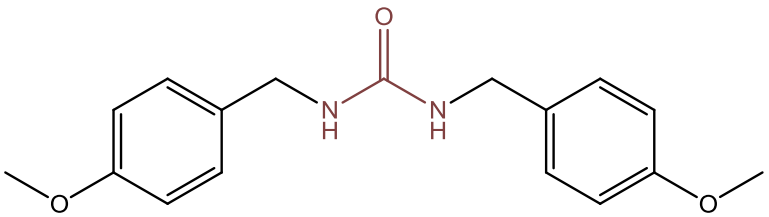


**32**

Figure 13: The molecular structure of MMU

## 1.5 Thiourea

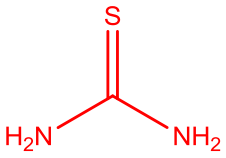


33

Figure 14: The molecular structure of thiourea

Thiourea 33 (Figure 14) is one of the most important nitrogen and sulfur-containing compounds. Despite the structural similarity between thiourea and urea, properties of these two compounds differ significantly, mostly due to the difference in electronegativity between sulfur and oxygen atoms.

Thiourea is synthesized by several methods including the reaction of isothiocyanates (mustard oils) with ammonia, primary amines, or secondary amines to produce N-alkylated thioureas 34 (Figure 15 a). Kurzer synthesized 1-(o-chlorophenyl)-2-thiourea from amine and ammonium thiocyanate 35 (Figure 15 b) (McEwen, 1991).

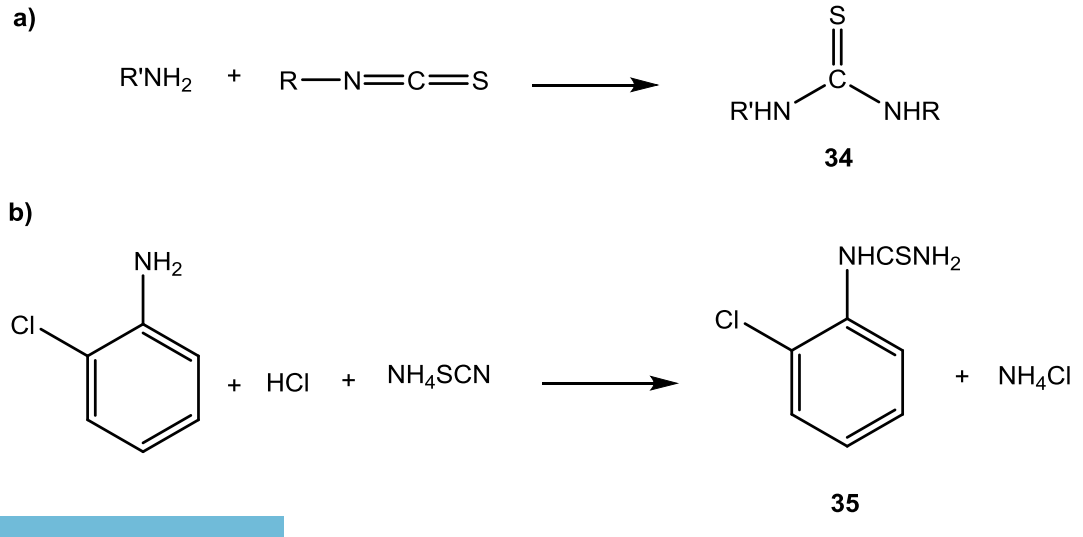

Figure 15: Synthesis of Thioureas from Mustard Oils and b) Synthesis of 1-(o-chlorophenyl)-2-thiourea

### 1.5.1 Biological activity of thiourea

Recently, thiourea proved to be useful in drug research (Shakeel et al. 2017). It works as control of plant pathogens like *Fusarium oxysporum* and *Penicillum expansum*. Thiourea is naturally occurring in laburnum shrubs (Nguyen, 2018). Research revealed that urea or thiourea with 2,3-dichlorophenyl piperazine show variation in the anti-inflammatory activity depending on the substitution group. Compounds with halogens (Cl, F and Br) in *para* position on the phenyl ring or electron withdrawing groups show high activity. Compound of structure 36 (1-(2-(4-(2,3-dichlorophenyl)piperazin-1-yl)-2-oxoethyl)-3-(4-fluoropheny8l)thiourea), which contains F as substitution group in para position gave good activity with $IC_{50}$= 30 µg/mL (Figure 16) (Vardhan et al. 2017).

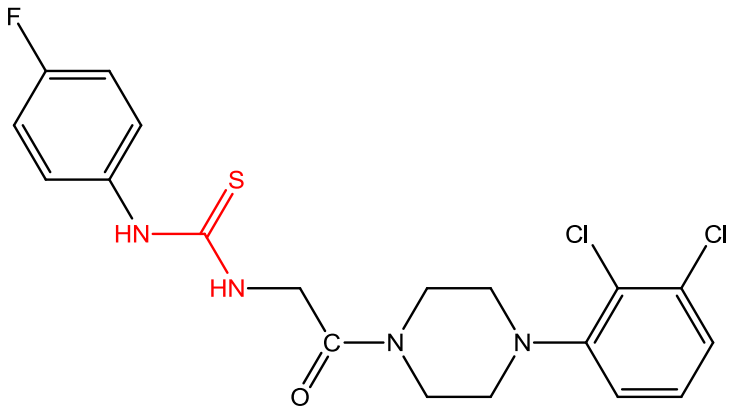


**36**

Figure 16: The molecular structure of 1-(2-(4-(2,3-dichlorophenyl)piperazin-1-yl)-2-oxoethyl)-3-(4-fluorophenyl)thiourea

Derivatives of thiourea have also been used to treat the excessive activity of thyroid gland, as in methimazole 37 and propylthiouracil 38 (Chakraborty et al. 2018). It has been found in oral antibiotic drugs such as thioacetazone 39 (Shakeel et al., 2017). Furthermore, thiourea can work as antiseptic as in Ambazone 40 (Choi & Jee, 2015) (Figure 17).

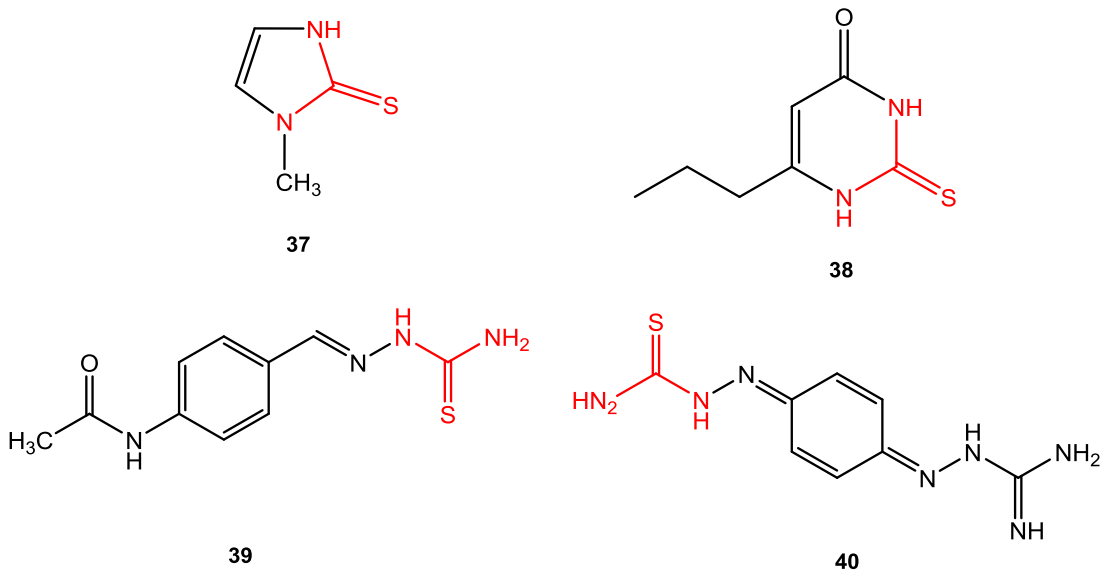


Figure 17: The molecular structure of methimazole 37, propylthiouracil 38, thioacetazone 39 and Ambazone 40

**1.6 Piperazine**

Piperazine 2 is a saturated heterocyclic organic compound that contains two atoms of nitrogen at opposite positions, 1 and 4. Piperazine has been widely used in the manufacture of resins, plastics, brake fluid, and pesticides. Synthesis of piperazine could be done by combining 1,2-dichloroethane with ammonia, and by catalyzed reaction of ethylene diamine in the presence of nickel or cobalt (Loo

et al. 2017). The most popular method for the synthesis of piperazine involves the reaction of α-keto ester 41 with substituted or unsubstituted ethylenediamine 42 to produce 3,4- dehydropiperazine-2-one 43 (Figure 18) (Sebastian at al. 2003).

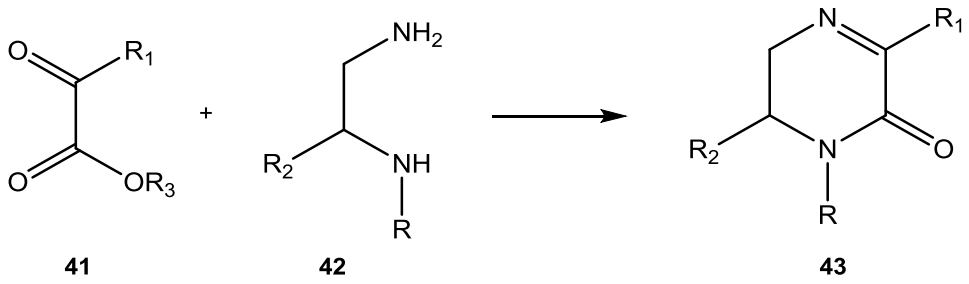


Figure 18: Synthesis of 3,4- dehydropiperazine-2-one 43

### 1.6.1 Biological activity of piperazine

Piperazine and its derivatives have important pharmacological properties, including antihelminthic activity, antibacterial activity, antifungal activity and antitubercular activity (Ismail et al. 2017). There are several antidepressant drugs that contain piperazine including amoxapine 44 and trazodone 45. In addition piperazine can be found in antihistamine drugs such as buclizine 46 and cyclizine 47 (Figure 19).

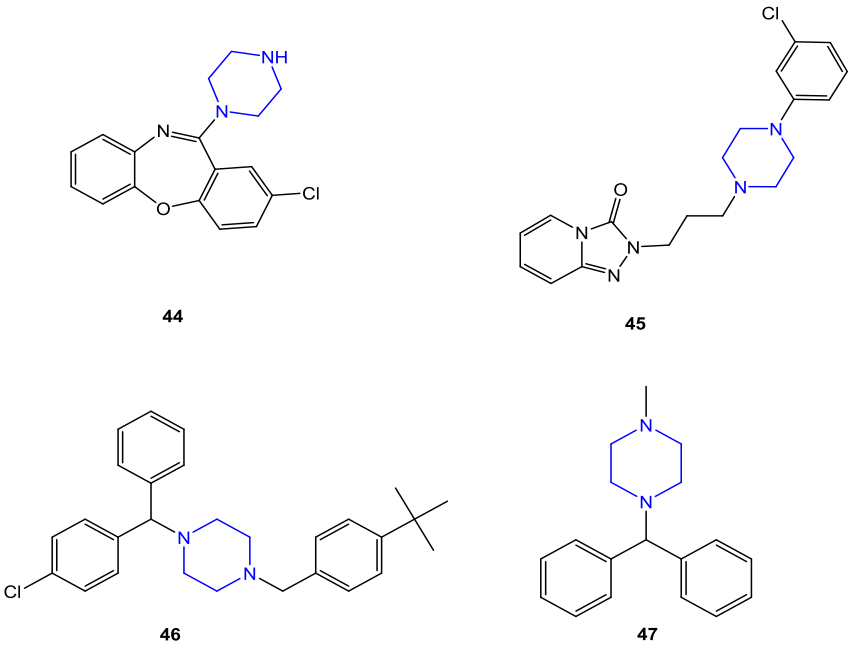


Figure 19: The molecular structure of amoxapine 44, trazodone 45, buclizine 46 and cyclizine 47

Piperazine derivatives also show antipsychotics activity and it include in several antipsychotic drugs (including hallucinations, delusions and paranoia). Examples of Piperazine derivatives drugs include fluphenazine 48, thiothixene 49, perphenazine 50, prochlorperazine 51 and trifluoperazine 52 (Figure 20).

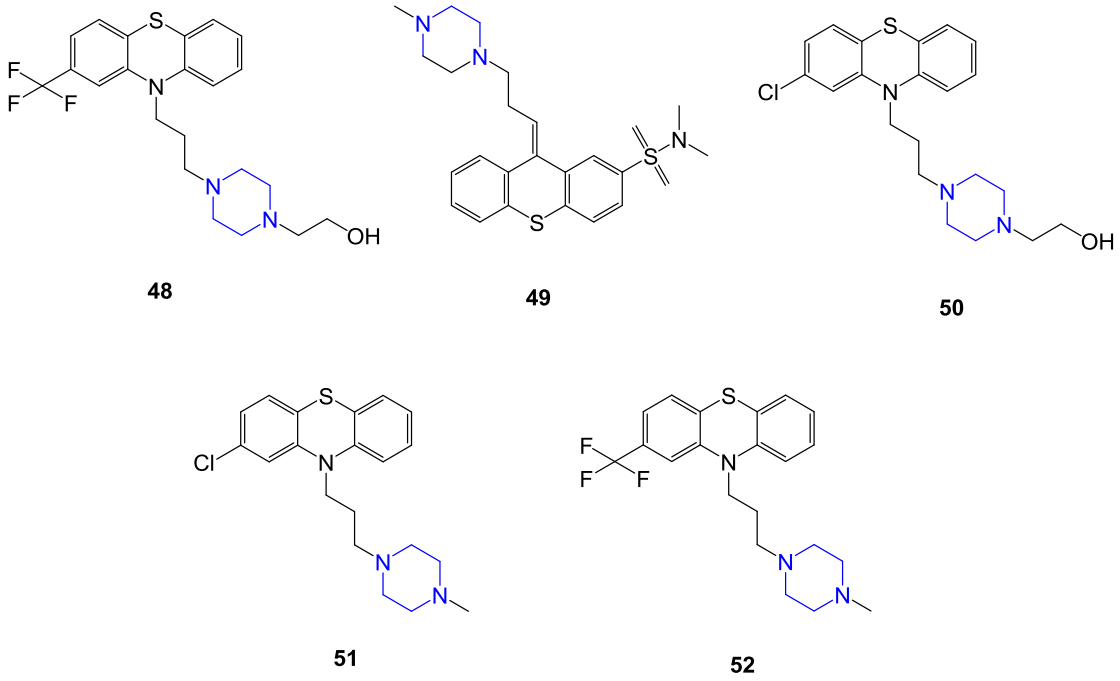


Figure 20: The molecular structure of fluphenazine 48, thiothixene 49, perphenazine 50, prochlorperazine 51 and trifluoperazine 52

Piperazine and its derivatives have also been used in anthelmintic drugs (antiparasitic drugs that treat infections of parasitic worms) (Gokbulut & Mckellar, 2018). Generally, piperazine derivatives have anthelmintic activity by paralyzing parasites which allows the host to remove the invading organisms easily. Piperazine in the form of piperazine citrate and piperazine hydrate is used to treat partial intestinal obstruction caused by Ascaris worms, a disease common for children.

### 1.7 The aim of this project

Drug resistance problem is the ability of microbes to mutate in order to resist the drug effect, and grow in the presence of a drug that usually will kill them. Drug resistance problem results from overuse and misuse of antibiotics. Alexander

Fleming pointed to the overuse of antibiotics problem in 1945. Drug resistance problem triggered research to produce new compounds to replace the inactive drugs (Pandurangan et al. 2017).

Based on the biological activities of the benzimidazole, piperazine, urea and thiourea discussed earlier in this chapter, the following scheme synthesis of a series of derivatives containing those moieties as outlined in Figure 21.

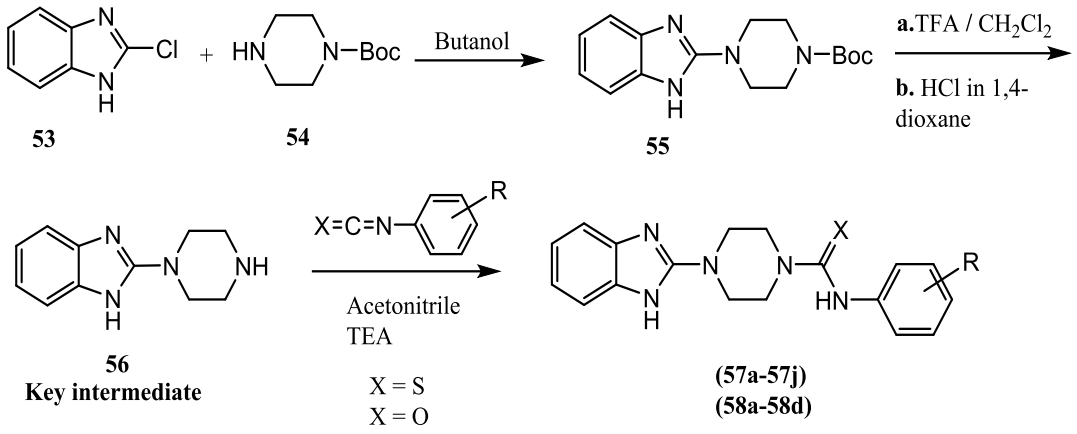


| X | | | |
|---|---|---|---|
| S | | O | |
| **Code** | **R** | **Code** | **R** |
| **57a** | H | **58a** | 4-$CH_3$ |
| **57b** | 4-$CH_3$ | **58b** | 4-$OCH_3$ |
| **57c** | 4-$OCH_3$ | **58c** | 3-Cl |
| **57d** | 3-Cl | **58d** | 4-Cl |
| **57e** | 4-Cl | | |
| **57f** | 4-$NO_2$ | | |
| **57g** | 2-F | | |
| **57h** | 3-F | | |
| **57i** | 4-F | | |
| **57j** | 4-$CF_3$ | | |

Figure 21: General synthesis of benzoimidazol-carbothioamide (57a-j) and benzoimidazol- carboxamide derivatives (58a-d)

The diversity of the proposed compounds in this scheme is evident from the different functional groups on the phenyl ring including activating and deactivating groups. Activating groups such as $OCH_3$ strongly increase the electron density on the phenyl ring by resonance effect, while $CH_3$ weakly increases electron density on the phenyl ring by inductive effect. On the other hand, deactivating groups such as F, Cl and $CF_3$ will affect the ring by decreasing the electron density making the ring less electron rich by inductive withdrawing effect. $NO_2$ group is a strongly electron

withdrawing group by resonance and inductive effect. Those different functional groups are expected to affect the biological activity of the proposed compounds.

The structure activity relationship will be further investigated, by replacing the piperazine with ethylenediamine in order to study the possible effect of the piperazine ring conformation. A series of compounds with ethylenediamine moiety is outlined in Figure 22.

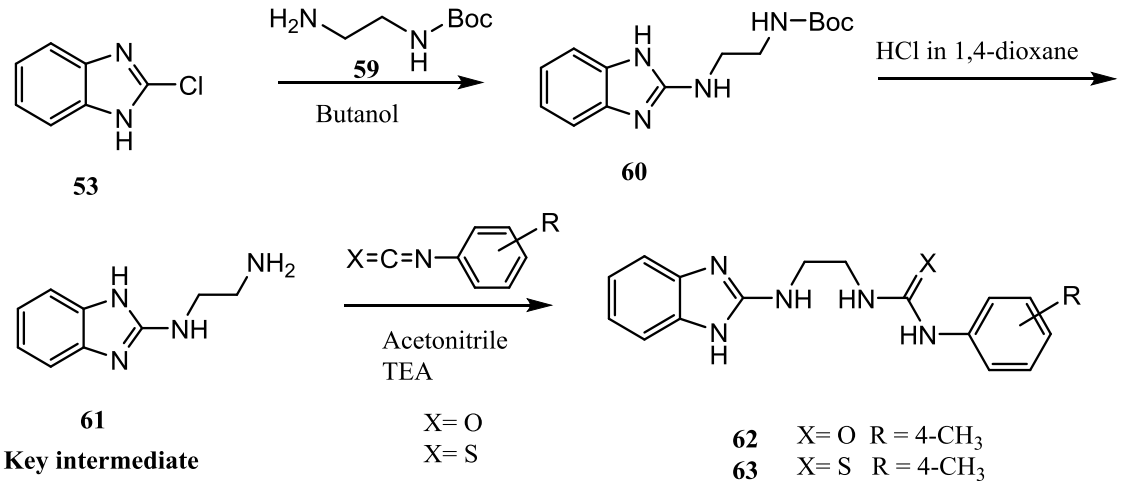


Figure 22: General synthesis of benzoimidazol- carboxamide derivatives (62 and 63)

# Chapter 2: Methods

## 2.1 Materials and Methods

Melting points were determined in open capillary tube on a Sanyo Gallenkamp MPD 350-BM 3.5 Melting Point apparatus (UK), and are uncorrected. FT-IR spectra were recorded in a Thermo Nicolet Nexus 470 FT-IR spectrophotometer (USA). $^{1}$H NMR and $^{13}$C NMR spectra were recorded, using Varian-400 MHz (USA), at room temperature in $CDCl_3$ or DMSO-$d_6$ at 400 MHz using solvent peaks [$CDCl_3$: 7.26 (*D*), 77.2 (*C*) ppm and DMSO-$d_6$ 2.50 (D) and 39.7 (C) ppm] as internal references. The assignment of chemical shifts is based on standard NMR experiments ($^{1}$H, $^{13}$C, $^{1}$H-$^{1}$H COSY, $^{1}$H-$^{13}$C HSQC, HMBC). TLC analyses were performed on silica F254 and detection by UV light at 254 nm. Column chromatographies were performed on silica Gel 60 (230 mesh). Chemicals and reagents were purchased from Sigma Aldrich Chemical Co. and ACROS ORGANICS, USA. All chemicals and reagents were used as received without further purification.

### 2.1.1 Synthesis of tert-butyl 4-(1H-benzo[d]imidazol-2-yl)piperazine-1-carboxylate 55

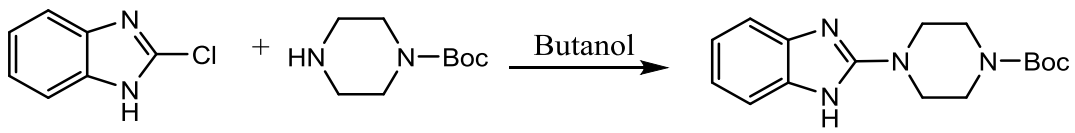


**53** **54** **55**

A mixture of 2-chrolobenzimidazole (3.0 g, 19.6 mmol) and N-tert-butoxycarbonyl piperazine (3.7 g, 20 mmol) in 1-butanol (40 mL) was heated to reflux overnight. After finishing, the precipitate was collected and rinsed with ether

and dried over high vacuum to obtain tert-butyl 4-(1H-benzimidazol-2-yl)piperazine-1-carboxylate (Lv et al. 2015). White solid, (m = 5.603g, 94.5%); mp 317-319 °C; $R_f$ = 0.8 (1:1 Ethyl acetate/ Hexane); IR (KBr, $cm^{-1}$) 1650 (C=O), 3407(NH); $^1$H NMR (400 MHz, $CDCl_3$) δ 7.49 (dd, J = 5.9, 3.2 Hz, 2H), 7.15 (dd, J = 5.9, 3.2 Hz, 2H), 4.04 – 3.83 (m, 4H), 3.74 – 3.53 (m, 4H), 1.45 (s, 9H); 13C-NMR (101 MHz, $CDCl_3$)

**Synthesis of 2-(piperazin-1-yl)-1*H*-benzo[d]imidazole 56**

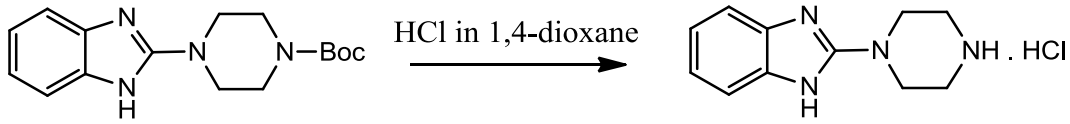


**55** **56**

A mixture of N-Boc protected amine 55 (5.3 g, 1 eq) in dioxane (10 mL) was added to 4M of HCl in dioxane (106 mL). The reaction mixture was stirred at room temperature for 3h. After completion of the reaction, the precipitate was filtered and dried under high vacuum to obtain 2-(piperazin-1-yl)-1H-benzimidazole 56 in quantitative yield (Lv et al., 2015; Wang et al. 2015). White solid, (m = 4.82g, 96%); mp 317-319 °C; $R_f$ = 0.25 (Ethyl acetate),IR (KBr, $cm^{-1}$) 3380 (NH);1H NMR (400 MHz, $CD_3OD$) δ: 7.50 – 7.41 (m, 2H), 7.38 – 7.32 (m, 2H), 4.01 – 3.91 (m, 4H, 4x Pip-H), 3.55 – 3.46 (m, 4H, 4x Pip-H). $^{13}$C NMR (101 MHz, $CD_3OD$) δ 149.91, 129.72, 124.11, 111.38, 43.25, 41.92.

### 2.1.2 General synthesis of benzoimidazol-carbothioamide (57a-57j) and benzoimidazol-carboxamide derivatives (58a-58d)

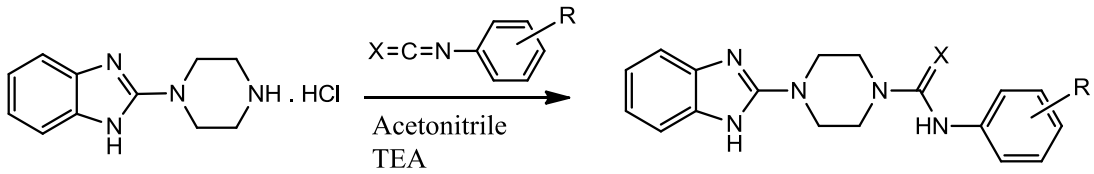


**56**
**Key intermediate**

X = S
X = O

**(57a-57j)**
**(58a-58d)**

| X | | | |
|---|---|---|---|
| S | | O | |
| **Code** | **R** | **Code** | **R** |
| **57a** | H | **58a** | 4-$CH_3$ |
| **57b** | 4-$CH_3$ | **58b** | 4-$OCH_3$ |
| **57c** | 4-$OCH_3$ | **58c** | 3-Cl |
| **57d** | 3-Cl | **58d** | 4-Cl |
| **57e** | 4-Cl | | |
| **57f** | 4-$NO_2$ | | |
| **57g** | 2-F | | |
| **57h** | 3-F | | |
| **57i** | 4-F | | |
| **57j** | 4-$CF_3$ | | |

To a stirred solution of 2-(piperazin-1-yl)-1H-benzo[d]imidazole 56 (1.1 mmol) in dry acetonitrile (10 mL), was added excess triethylamine (460 µL, 4 mmol) and the corresponding isothiocyanatobenzene or isocyanatobenzene (1.1 mmol). The mixture was stirred at room temperature overnight. The solvent was removed under vacuum, dissolved in ethyl acetate (20 mL) then washed with water. The organic layer was dried over anhydrous sodium sulfate, the solvent was evaporated leaving a small quantity of solvent. Then hexane was added. The precipitate formed was filtered and dried to obtain the desired compounds (57a-j and 58a-d).

**4-(1H-benzo[d]imidazol-2-yl)-N-phenylpiperazine-1-carbothioamide 57a**

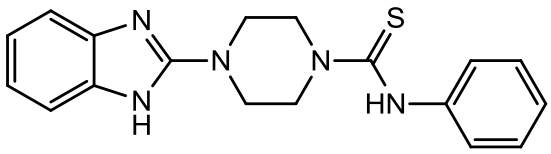

**57a**

Off white solid, (0.53 g, 86%); mp 229-231 °C; $R_f$ = 0.74 (9:1 Dichloromethane/ Methanol), IR (KBr, $cm^{-1}$) 1530 (S=C), 3399 (NH); $^1$H-NMR (400 MHz, DMSO-d6) δ 9.49 (s, 1H), 7.32-7.28 (m, 5H), 7.27 – 7.14 (m, 3H), 7.15 – 7.10 (m, 1H), 7.07-7.15 (m, 2H), 4.11 – 4.09 (m, 4H), 3.68 – 3.66 (m, 4H). $^{13}$C NMR (101 MHz, DMSO-d6) δ 182.04, 155.66, 141.35, 128.48, 125.84, 124.90, 120.48, 47.66, 46.02.

**4-(1H-benzo[d]imidazol-2-yl)-N-(p-tolyl)piperazine-1-carbothioamide 57b**

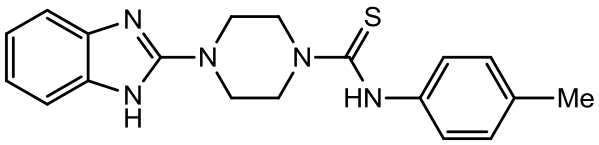

**57b**

Off white solid (m = 0.28g, 72%); mp 231-233 °C; $R_f$ = 0.72 (9:1 Dichloromethane/ Methanol), IR (KBr, $cm^{-1}$) 1523 (S=C), 3430 (NH); $^1$H-NMR (400 MHz, DMSO-d6) δ 11.53 (s, 1H), 9.37 (s, 1H), 7.33 (d, J = 8.4 Hz, 1H), 7.27 – 7.14 (m, 3H), 7.13 – 7.06 (m, 1H), 6.95 (dd, J = 5.8, 3.2 Hz, 1H), 4.16 – 3.95 (m, 4H), 3.67 – 3.47 (m, 4H), 2.28 (s, 3H). $^{13}$C NMR (101 MHz, DMSO-d6) δ 182.07, 155.98, 138.73, 134.10, 130.78, 128.96, 126.22, 126.03, 120.26, 47.63, 46.00, 21.00.

**4-(1H-benzo[d]imidazol-2-yl)-N-(4-methoxyphenyl)piperazine-1-carbothioamide 57c**

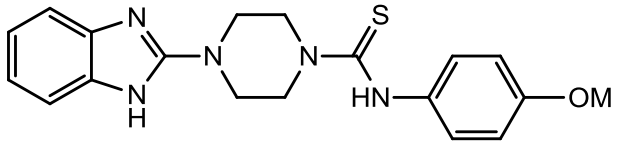


**57c**

White solid, (0.381 g, 57%); mp 285-287 °C; $R_f$ = 0.77 (9:1 Dichloromethane/ Methanol), IR (KBr, $cm^{-1}$) 1527 (S=C), 3413(NH); $^1$H-NMR (400 MHz, DMSO-d6) δ 11.46 (s, 1H), 9.31 (s, 1H), 7.16 (d, J = 9.0 Hz, 3H), 6.86 (d, J = 9.0 Hz, 4H), 4.13 – 3.94 (m, 4H), 3.73 (s, 3H), 3.64 – 3.52 (m, 4H). $^{13}$C-NMR (101 MHz, DMSO-d6) δ 182.24, 156.92, 155.99, 134.24, 127.90, 120.22, 113.64, 55.62, 47.61, 46.10.

**4-(1H-benzo[d]imidazol-2-yl)-N-(3-chlorophenyl)piperazine-1-carbothioamide 57d**

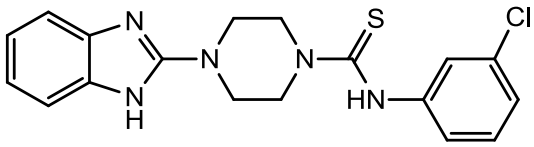


**57d**

Off white solid, (0.2 g, 74%); mp 248-250 °C; $R_f$ = 0.74 (9:1 Dichloromethane/ Methanol), IR (KBr, $cm^{-1}$) 1529 (C=S), 3428(NH); $^1$H-NMR (400 MHz, DMSO-d6) δ 11.56 (s, 1H), 9.54 (s, 1H), 7.46 (t, *J* = 2.0 Hz, 1H), 7.37 – 7.27 (m, 2H), 7.25 – 7.20 (m, 2H), 7.17 (dt, *J* = 7.3, 1.9 Hz, 1H), 6.95 (dd, *J* = 5.8, 3.2 Hz, 2H), 4.11 – 4.02 (m, 4H), 3.69 – 3.54 (m, 4H). $^{13}$C-NMR (101 MHz, DMSO-d6) δ 181.71, 155.95, 142.94, 132.55, 130.03, 125.13, 124.41, 123.92, 120.27, 47.84, 45.99.

**4-(1H-benzo[d]imidazol-2-yl)-N-(4-chlorophenyl)piperazine-1-carbothioamide 57e**

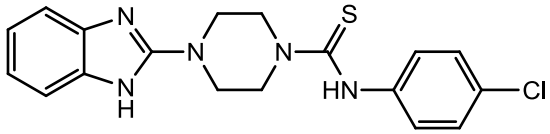


**57e**

Off white solid (0.532 g, 79%); mp 246-248 °C; $R_f$ = 0.71 (9:1 Dichloromethane/ Methanol), IR (KBr, $cm^{-1}$) 1524 (C=S), 3399(NH); $^1$H NMR (400 MHz, DMSO-$d_6$) δ 11.48 (s, 1H, NH), 9.50 (s, 1H, NH), 7.63 – 7.40 (m, *J* = 9.6 Hz, 1H), 7.34 (d, *J* = 9.4 Hz, 2H), 7.22 (dd, *J* = 17.7, 7.5 Hz, 1H), 6.94 (dd, *J* = 13.7, 7.7 Hz, 1H), 4.17 – 3.98 (m, 4H), 3.70 – 3.51 (m, 4H). 13C NMR (101 MHz, DMSO-$d_6$) δ 181.83, 156.09, 140.36, 128.77, 128.34, 127.37, 47.78, 45.98.

**4-(1H-benzo[d]imidazol-2-yl)-N-(4-nitrophenyl)piperazine-1-carbothioamide 57f**

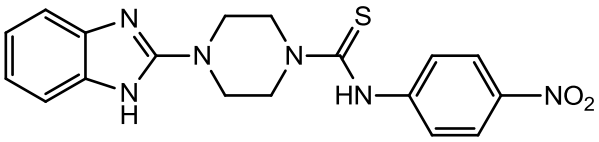


**57f**

Yellow solid, (0.252 g, 91%); mp 2041-206 °C; $R_f$ = 0.84 (9:1 Dichloromethane/ Methanol), IR (KBr, $cm^{-1}$) 1530 (C=S), 3435 (NH); $^1$H NMR (400 MHz, DMSO-$d_6$) δ 11.63 (br s, 1H, NH), 9.96 (s, 1H, NH), 8.18 (d, J = 9.2 Hz, 2H), 7.63 (d, J = 9.1 Hz, 2H), 7.23 (dd, J = 5.4, 3.5 Hz, 2H), 6.96 (dd, J = 5.8, 3.2 Hz, 2H), 4.13 – 4.06 (m, 4H), 3.68 – 3.60 (m, 4H). $^{13}$C NMR (101 MHz, DMSO-d6) δ 181.34, 155.70, 148.15, 142.59, 128.77, 124.41, 123.18, 120.43, 48.26, 46.00.

**4-(1H-benzo[d]imidazol-2-yl)-N-(2-fluorophenyl)piperazine-1-carbothioamide 57g**

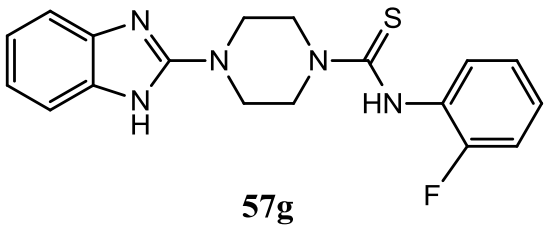

**57g**

Yellowish solid, (0.206 g, 80%); mp 268-270 °C; $R_f$ = 0.8 (9:1 Dichloromethane/ Methanol)IR (KBr, $cm^{-1}$) 1528 (C=S), 3458 (NH); $^1$H-NMR (400 MHz, DMSO-d6) δ 11.82 (s, 1H), 9.30 (s, 1H), 7.32 – 7.21 (m, 5H), 7.21 – 7.13 (m, 1H), 7.04 – 6.94 (m, 2H), 4.17 – 3.96 (m, 4H), 3.74 – 3.58 (m, 4H). $^{13}$C NMR (101 MHz, DMSO-d6) δ 182.67, 159.03, 156.58, 154.74, 151.88, 136.89, 130.56, 129.16, 129.04, 128.24, 128.17, 124.53, 124.49, 121.06, 116.26, 116.06, 112.45, 47.52, 45.97.

**4-(1H-benzo[d]imidazol-2-yl)-N-(3-fluorophenyl)piperazine-1-carbothioamide 57h**

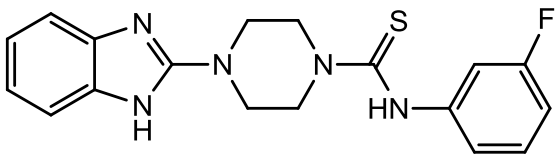

**57h**

White solid, (0.52 g, 80%); mp 229-231 °C; $R_f$ = 0.71 (9:1 Dichloromethane/Methanol) IR (KBr, $cm^{-1}$) 1535 (C=S), 3410 (NH); $^1$H NMR (400 MHz, DMSO-$d_6$) δ 11.58 (s, 1H), 9.55 (s, 1H), 7.33 (td, *J* = 8.2, 6.8 Hz, 1H), 7.26 (dt, *J* = 11.2, 2.3 Hz, 1H), 7.24 – 7.19 (m, 2H), 7.16 (ddd, *J* = 8.1, 2.0, 0.9 Hz, 1H), 7.00 – 6.89 (m, 3H), 4.10 – 4.04 (m, 4H), 3.66 – 3.58 (m, 4H). $^{13}$C NMR (101 MHz,

DMSO-$d_6$) δ 181.74, 163.24, 160.83, 155.59, 143.37, 143.26, 138.21, 129.87, 129.77, 121.06, 121.03, 120.48, 112.57, 112.28, 112.04, 111.19, 110.98, 47.91, 46.14.

**4-(1H-benzo[d]imidazol-2-yl)-N-(4-fluorophenyl)piperazine-1-carbothioamide 57i**

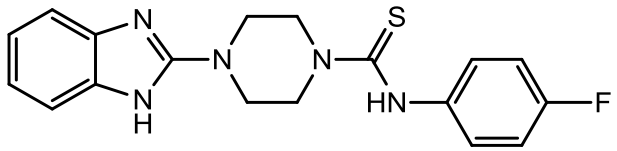

**57i**

Beige solid (0.64 g, 98%); mp 284-250°C; $R_f$ = 0.78 (9:1 Dichloromethane/ Methanol), IR (KBr, $cm^{-1}$) 1569 (C=S), 3193(NH); $^1$H NMR (400 MHz, DMSO-$d_6$) δ 11.48 (s, 1H), 9.44 (s, 1H), 7.31 (dd, *J* = 9.0, 5.1 Hz, 1H), 7.22 (dd, *J* = 17.5, 7.6 Hz, 2H), 7.14 (t, *J* = 8.9 Hz, 1H), 6.94 (dq, *J* = 14.9, 7.4 Hz, 2H), 4.28 – 3.89 (m, 4H), 3.79 – 3.50 (m, 4H). $^{13}$C NMR (101 MHz, DMSO-$d_6$) δ 182.15, 160.91, 158.51, 155.28, 137.63, 137.60, 128.25, 128.17, 120.76, 115.21, 114.99, 47.51, 45.96.

**4-(1H-benzo[d]imidazol-2-yl)-N-(4-(trifluoromethyl)phenyl)piperazine-1-carbothioamide 57j**

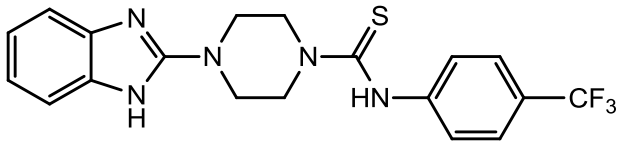

**57j**

white solid, (0.248 g, 84%); mp 246-244 °C; $R_f$ = 0.78 (9:1 Dichloromethane/ Methanol), IR (KBr, $cm^{-1}$) 1529 (C=S), 3423 (NH); $^1$H-NMR (400 MHz, DMSO-d6) δ 9.73 (s, 1H), 8.95 (s, 1H), 7.66 (d, J = 8.5 Hz, 1H), 7.58 (d, J = 8.5 Hz, 1H), 7.27 (dd, J = 5.8, 3.2 Hz, 1H), 7.02 (dd, J = 5.7, 3.2 Hz, 1H), 4.20 – 4.00 (m, 4H), 3.76 –

3.58 (m, 4H). $^{13}$C NMR (101 MHz, DMSO-$d_6$) δ 181.78, 155.97, 145.29, 128.96, 126.26, 125.65, 125.61, 125.57, 125.53, 124.78, 124.42, 124.10, 123.78, 123.56, 120.86, 119.39, 48.02, 46.03

**4-(1H-benzo[d]imidazol-2-yl)-N-(p-tolyl)piperazine-1-carboxamide 58a**

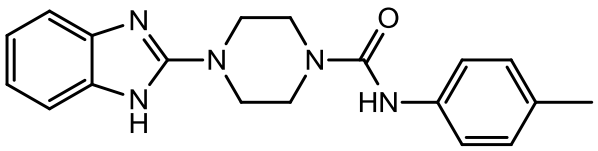

**58a**

Beige solid (0.335g, 55%); mp 298-300 °C; $R_f$ = 0.74 (9:1 Dichloromethane/ Methanol), IR (KBr, cm$^{-1}$) 1637 (C=O), 3407 (NH); $^1$H NMR (400 MHz, DMSO-d6) δ 11.46 (s, 1H), 8.55 (s, 1H), 7.34 (dd, J = 13.8, 8.2 Hz, 2H), 7.21 (s, 2H), 7.06 (t, J = 8.5 Hz, 3H), 7.00 – 6.85 (m, 2H), 3.59 (dd, J = 7.1, 3.4 Hz, 4H), 3.53 (dd, J = 7.1, 3.6 Hz, 4H), 2.23 (s, 3H). $^{13}$C NMR (101 MHz, DMSO-$d_6$) δ 156.39, 155.53, 138.22, 137.66, 131.10, 129.60, 129.20, 120.29, 118.63, 46.37, 43.57, 20.80.

**4-(1H-benzo[d]imidazol-2-yl)-N-(4-methoxyphenyl)piperazine-1-carboxamide 58b**

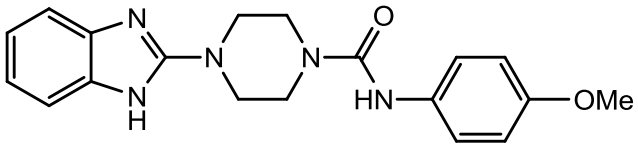

**58b**

Off white solid, (0.16 g, 63%); mp 297-299 °C; $R_f$ = 0.75 (9:1 Dichloromethane/ Methanol), IR (KBr, cm$^{-1}$) 1634 (C=O), 3467(NH); $^1$H NMR (400 MHz, DMSO-$d_6$) δ 11.55 (s, 1H), 8.48 (s, 1H), 7.39 – 7.31 (m, 1H), 7.21 (dd, *J* = 5.5, 3.4 Hz, 1H), 6.94 (dd, *J* = 5.8, 3.1 Hz, 1H), 6.88 – 6.80 (m, 1H), 3.70 (s, 3H), 3.61 – 3.55 (m, 4H), 3.55

– 3.49 (m, 4H). $^{13}$C NMR (101 MHz, DMSO-$d_6$) δ 156.25, 155.66, 154.94, 133.73, 122.04, 120.30, 114.37, 113.96, 55.53, 46.35, 43.51.

**4-(1H-benzo[d]imidazol-2-yl)-N-(3-chlorophenyl)piperazine-1-carboxamide 58c**

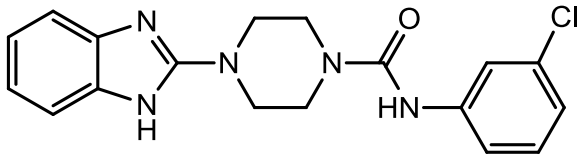

**58c**

White solid, (0.41 g, 63%); mp 287-289 °C; $R_f$ = 0.68 (9:1 Dichloromethane/ Methanol), IR (KBr, cm$^{-1}$) 1636 (C=O), 3434(NH); $^1$H NMR (400 MHz, DMSO-$d_6$) δ 11.46 (s, 1H, NH), 8.82 (s, 1H, NH), 7.67 (s, 1H), 7.42 (d, *J* = 8.8 Hz, 1H), 7.27 (t, *J* = 8.1 Hz, 1H), 6.99 (d, *J* = 8.4 Hz, 1H), 3.63 – 3.57 (m, 4H), 3.56 – 3.50 (m, 4H). $^{13}$C NMR (101 MHz, DMSO-$d_6$) δ 156.31, 155.03, 142.50, 133.17, 130.43, 121.78, 119.20, 118.11, 46.31, 43.58.

**4-(1H-benzo[d]imidazol-2-yl)-N-(4-chlorophenyl)piperazine-1-carboxamide 58d**

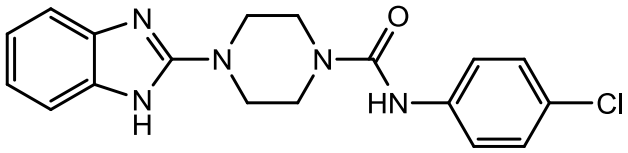

**58d**

Off white solid (m = 0.304g, 50%); mp 287-289 °C; $R_f$ = 0.70z (9:1 Dichloromethane/ Methanol), IR (KBr, cm$^{-1}$) 1642 (C=O), 3259(NH); $^1$H NMR (400 MHz, DMSO-$d_6$) δ 11.46 (s, 1H), 8.77 (s, 1H), 7.59 – 7.45 (m, 2H), 7.29 (d, *J* = 8.9 Hz, 1H), 7.21 (dd, *J* = 18.0, 7.7 Hz, 2H), 7.08 – 6.75 (m, 2H), 3.59 (dd, *J* = 7.1, 3.6 Hz, 4H), 3.53 (dd, *J* = 6.8, 3.7 Hz, 4H.

### 2.1.3 tert-butyl (2-((1H-benzo[d]imidazol-2-yl)amino)ethyl)carbamate 60

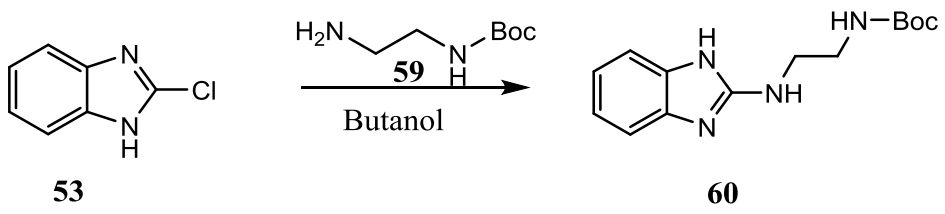


A mixture of 2-chrolobenzimidazole (1.52 g, 10mmol) and tert-butyl (2-aminoethyl) carbamate (1.74 g, 11 mmol) in 1-butanol (40 mL) was heated to reflux for 24 hours. After finishing, the reaction was evaporated. And to the oily crude was added diethyl ether, evaporated and the obtained solid was purified by column chromatography using as eluyent Chlorofom/Methanol (95/5, v/v) to afford the final product tert-butyl 4-(1H-benzimidazol-2-yl)piperazine-1-carboxylate 60 (Zhu et al., 2013). Beige solid, (2.6g, 94%); mp 164-166 °C; IR (KBr, $cm^{-1}$) 1640 (C=O), 3381 (NH); $^{1}H$ NMR (400 MHz, $CD_3OD$) δ 7.28 (dd, *J* = 5.9, 3.2 Hz, 2H), 7.14 (dd, *J* = 5.9, 3.2 Hz, 2H), 3.47 (t, *J* = 6.0 Hz, 2H), 3.35 – 3.27 (m, 4H), 1.39 (s, 9H). $^{13}C$ NMR (101 MHz, $CD_3OD$) δ 157.34, 152.58, 133.12, 121.88, 111.07, 78.97, 42.75, 39.37, 27.24.

### 2.1.4 N1-(1H-benzo[d]imidazol-2-yl)ethane-1,2-diamine 61

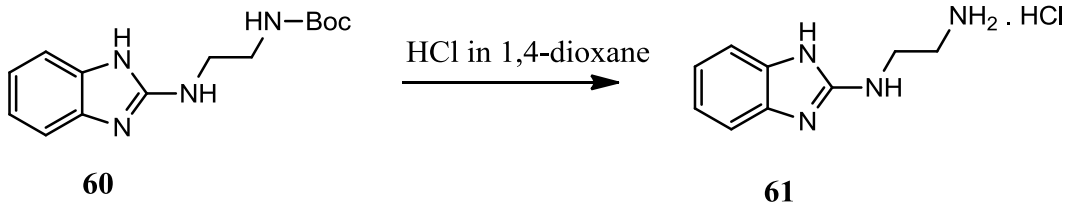


A mixture of N-Boc protected amine 60 (0.4 g,1.5 mmol) in dioxane (4 mL) was added to 4M of HCl in dioxane (8 mL). The reaction mixture was stirred at room temperature for 3 hours. After finishing, the solvent was evaporated and wash it with hexane and dried under high vacuum to obtain N-(2-aminoethyl)-1H-

benzo[d]imidazol-2-amine 61 in quantitative yield. White solid, (m = 0.263g, 73%); mp 295-297 °C; IR (KBr, $cm^{-1}$) 3404(NH);

### 2.1.5 General synthesis of benzoimidazol-carbothioamide (62) and benzoimidazol- carboxamide derivatives 63

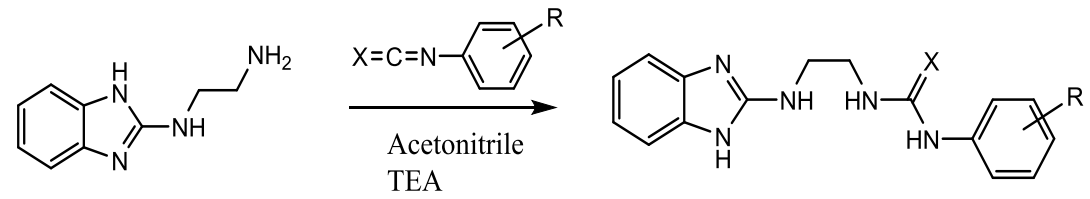


**61**
**Key intermediate**

X= O
X= S

**62** X= O R = 4-$CH_3$
**63** X= S R = 4-$CH_3$

A mixture N-(2-aminoethyl)-1H-benzo[d]imidazol-2-amine **61** (1eq) and isocyanatobenzene and isocyanatobenzene (1eq) in acetonitrile (10 ml) and Triethylamine (6 eq) stirred on ice (0°C) overnight. After finishing, the solvent was evaporated and extracted with ethyl acetate (20 ml). The organic phase was evaporated, and diethyl ether was added. And the product was obtained.

**1-(2-(1H-benzo[d]imidazol-2-ylamino)ethyl)-3-p-tolylurea 62**

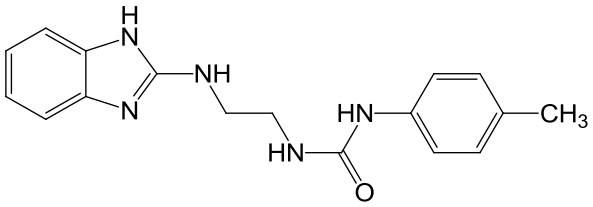


**62**

Beige solid (m = 0.069g, 77%); mp 100-102; IR (KBr, $cm^{-1}$) 1705 (C=O), 3370(NH); $^1$H NMR (400 MHz, $CD_3OD$) δ 8.33 (s, 1H), 7.38 – 7.31 (m,, 2H), 7.26 – 7.19 (m, 2H), 7.18 – 7.11 (m, 2H), 7.10-7.08 (m, 1H), 7.08 – 7.01 (m, 3H), 6.42 (s, 1H), 3.57-3.54 (m, 2H), 3.50-3.47 (m, 2H), 2.24 (s, 3H).

**1-(2-(1H-benzo[d]imidazol-2-ylamino)ethyl)-3-p-tolylthiourea 63**

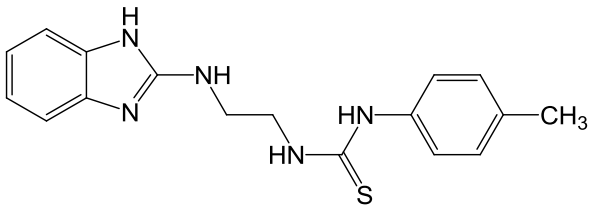

**63**

Beige solid (m = 0.182g, 97%); mp 165-167, IR (KBr, $cm^{-1}$) 1684 (C=S), 3271(NH); $^1$H NMR (400 MHz, Methanol-$d_4$) δ 9.32 (s, 1H), 7.45 (s, 1H), 7.33-7.31 (m, 2H), 7.24 – 7.21-7.19 (m, 2H), 7.12-7.10 (m, 2H), 7.04-7.02 (m, 2H), 3.94 – 3.87 (m, 2H), 3.64-3.61 (m, 2H), 2.27 (s, 3H).

### 2.1.6 Biological activity

#### 2.1.6.1 Antibacterial activity

**Measurement of minimum inhibitory concentration (MIC) by agar dilution**

The compounds (57a-j), (58a-d), 62, 63 and 65 were tested toward different types of bacteria. They dissolved in dimethyl sulfoxide (DMSO) (Sigma-Aldrich, France) in concentration of 2500µM. Ten step serial dilution of this solution was prepared in Mueller Hinton Broth (Himedia Laboratories, Mumbai, India) resulting in concentrations of 1250, 625, 312.5, 156.25, 78.125, 39.1, 19.5, 9.8 and 4.9µM of each compounds. One ml from each solution was added to 24 ml of molten Mueller Hinton Agar (MHA) (MAST, Merseyside, UK) in order to prepare MHA containing 100, 50, 25, 12.5, 6.25, 3.125, 1.6, 0.8, 0.4 and 0.2µM of each compounds tested. Furthermore, plates containing only DMSO corresponding to the DMSO concentration of each dilution were also used as control.

The effects of compounds were tested on the following bacteria: *Esherichia coli* ATCC25922, *Pseudomonas aeruginosa* ATCC27853, *Salmonella enterica* sv. *Braenderup H9812* (ATCC BAA-664), *Klebsiella pneumoniae* ATCC700603, *Staphylococcus aureus* ATCC25923 and *Enterococcus fecalis* ATCC29212.

Bacterial suspension containing approximately $10^4$ CFU/ml were prepared in phosphate buffered saline, of which a 10 µl drop (approximately 100 bacterial cell) was placed on the surface of MHA plates containing the above described concentrations of the chemical compounds tested. A MHA plate without any chemicals was used as a growth control in each experiment. Plates were incubated for 18 hours at 37°C in a humidified atmosphere of ambient air. The bacterial growth after this incubation was checked and recorded.

### 2.1.6.2 Antifungal activity

**In-vitro evaluation of some synthetic chemical compounds on the mycelial growth of some selected plant diseases causal fungi:**

The evaluation of the synthetic chemical compounds (57a-j), (58a-d), 62, 63 and 65 are in-vitro evaluated on the mycelial growth (mm) of four selected fungi (*Fusarium solani, Neocystalidium dimediatum, Botrytis cinerea, and Thielaviopsis punctulata*). The 17 compounds were dissolved in dimethyl sulfoxide (DMSO) in concentration of 100µM.

The potato dextrose agar medium (PDA) supplied with 1ml of antibiotic (Chloramphenicol 50mg/ml) to inhibit the bacterial growth was prepared, autoclaved and poured into sterile petri dishes. Then the selected fungi were grown on the above mentioned medium and incubated at 27ºC for 7 days.

Moreover, holes of about 10-mm were made on newly prepared PDA medium using sterile cork-borer (4 holes were made per each petri plate dish), and then 0.2 ml from each compound was poured in each hole, and incubated in the refrigerator (4ºC) for one hour. A sterile cork-borer (5-mm in diameter) was used to introduce the tested pathogens on the middle of each petri-dish plate contains the selected synthetic chemical compounds. Finally, all petri-dish plates were kept in the incubator for 7 days at 27ºC.

# Chapter 3: Results and Discussion

## 3.1 Synthesis of urea and thiourea-benzimidazole derivatives with piperazine linker

Compounds synthesized in this project (57a-57j), (58a-58d), 62, 63 and 65 are hybrid compounds of benzimidazole, piperazine, ethylenediamine and urea or thiourea as outlined in Figures 23 and 24. Our aim is to study the effect of structural variation (oxygen with sulfur in urea vs. thiourea) and the effect of substituents on the benzene ring attached to their moieties on the bioactivity of these compounds. Substituents on the benzene ring were selected based on their electronic properties including groups that are electron donors through inductive effect (e.g $–OCH_3$) and groups that are electron acceptors through the resonance effect and electron withdrawing through the inductive effect (e.g $CF_3$). The nitro group ($NO_2$) is electron acceptor through inductive and resonance effect. All these structural changes are expected to provide good understanding of the effect electronic properties have on the bioactivity properties of these compounds. The synthesis of piprazine–urea and thiourea derivatives is outlined in Figure 21.

### 3.1.1 Synthesis of key intermediate (56)

The original plan for the synthesis of key intermediate 56 was outlined in Figure 21. However, several attempts to affect this synthesis resulted in the dimer 67 as the side product (Figure 23).

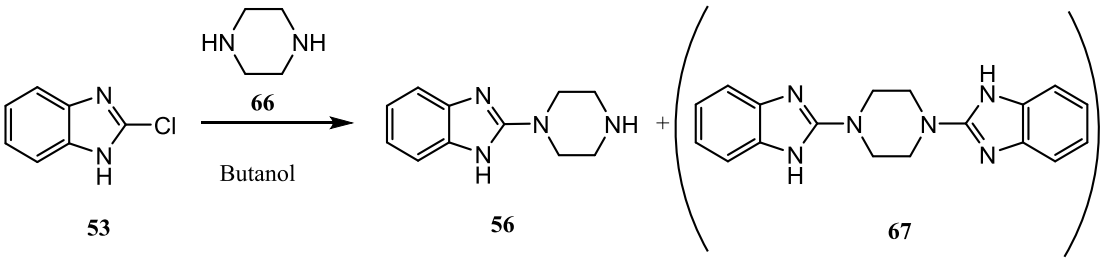


Figure 23: Synthesis of key intermediate 57 and dimer 63

Therefore N-Boc piprazine (tert-butyloxycarbonyl protecting group) was used to in order to get the desired product N-Boc piperazine-benzoimidazole 55. Compound 55 was obtained from 2-chloro-benzoimidazole 53 by nucleophilic aromatic substitution of the chlorine atom with N-Boc piperazine 54 in butanol accordance to previously published method (Lv et al., 2015), as a white solid with a good yield (94%) (Figure 24).

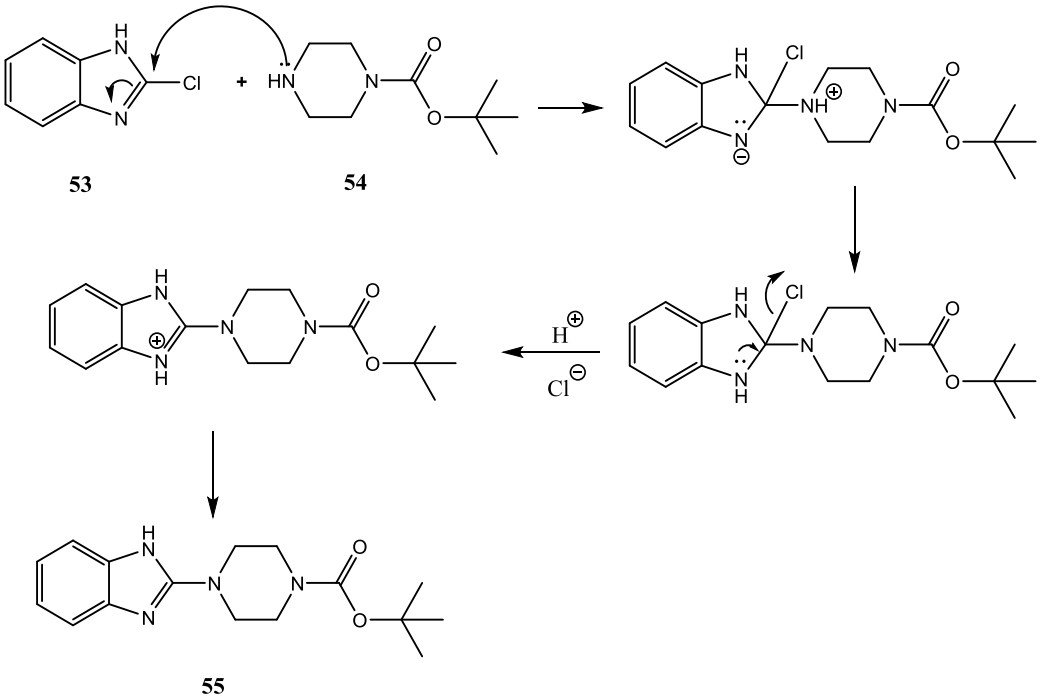


Figure 24: Synthesis of tert-butyl 4-(1H-benzo[d]imidazol-2-yl) piperazine-1-carboxylate 55

Subsequent removal of the N-Boc moiety was performed with two different procedures (a) and (b), (Figures 25 and 26).

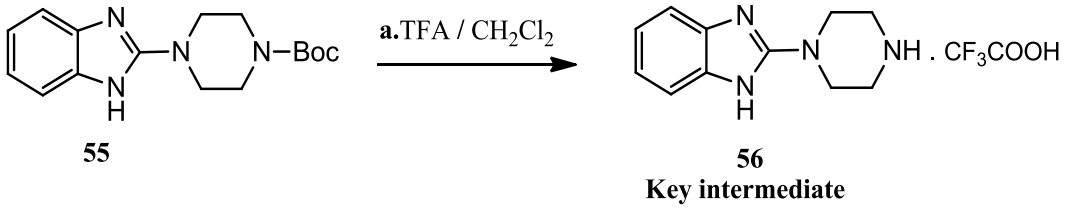


**55** **56**
**Key intermediate**

Figure 25: Synthesis of key intermediate 56 (method a)

The first method (Figure 25) involves the use of trifluoroacetic acid in dichloromethane for two hours. This reaction gave the product 2-(piperazin-1-yl)-1H-benzo[d]imidazole (56) with very low yields. Modification of the reaction conditions (increasing the amount of acid and increasing reaction time) did not improve the yield appreciably.

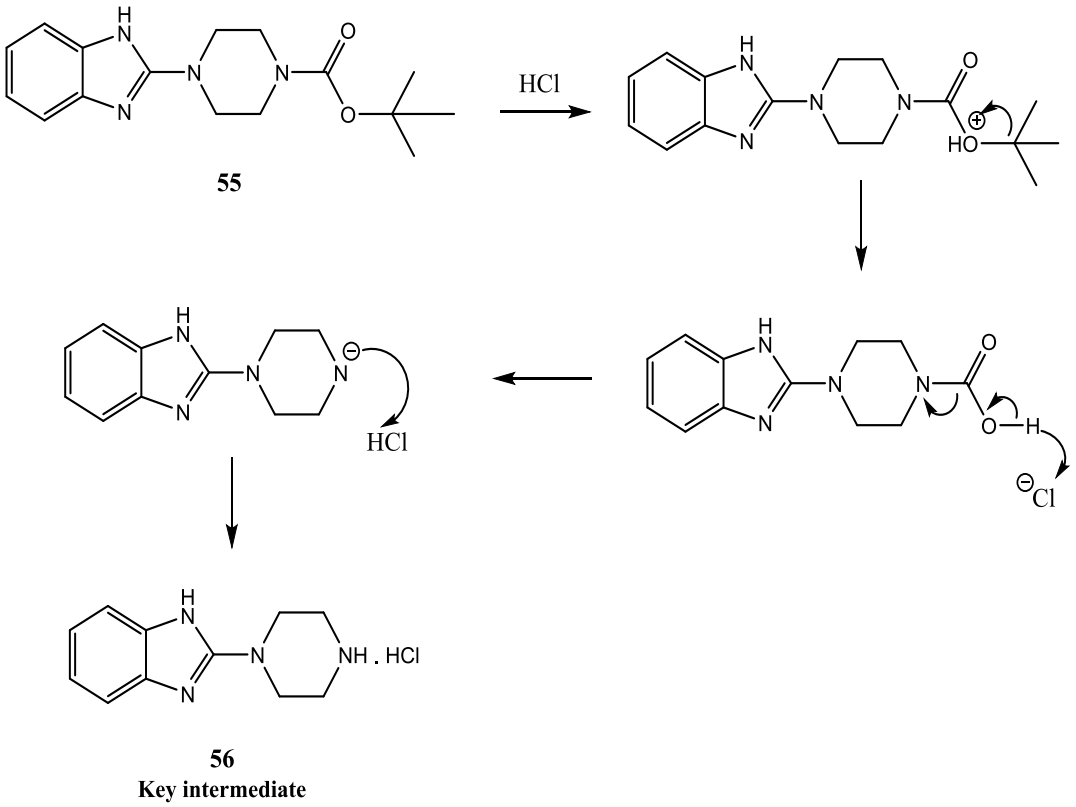


Figure 26: Mechanism of key intermediate 56 (method b)

The second method (Figure 26) involves HCl in 1,4-dioxane for two hours, this reaction gave high yield (90%) of the key intermediate 56, which was confirmed using $^{1}H$ NMR and $^{13}C$ NMR spectroscopy, this method is more efficient, and it have been used in next step to produce the final products.

### 3.1.2 Synthesis of urea and thiourea-piperazine benzimidazole (57a-57j) and (58a-58d)

A series of 14 novel Benzoimidazol-carbothioamide (57a-57j) and benzoimidazol-carboxamide derivatives (58a-58d) were synthesized as outlined in Figure 21, were obtained by the nucleophilic addition in which the amine group in key intermediate (56) react with the electrophilic carbon of in isothiocyanatobenzene (S) or isocyanatobenzene (O) in the presence of acetonitrile, according to reported

procedure. Final products (57a-j) and (58a-d) were obtained with good yields (50% - 63%) and (57% - 98%) for urea and thiourea compounds, respectively. Figure 27 shows the mechanism of the reaction.

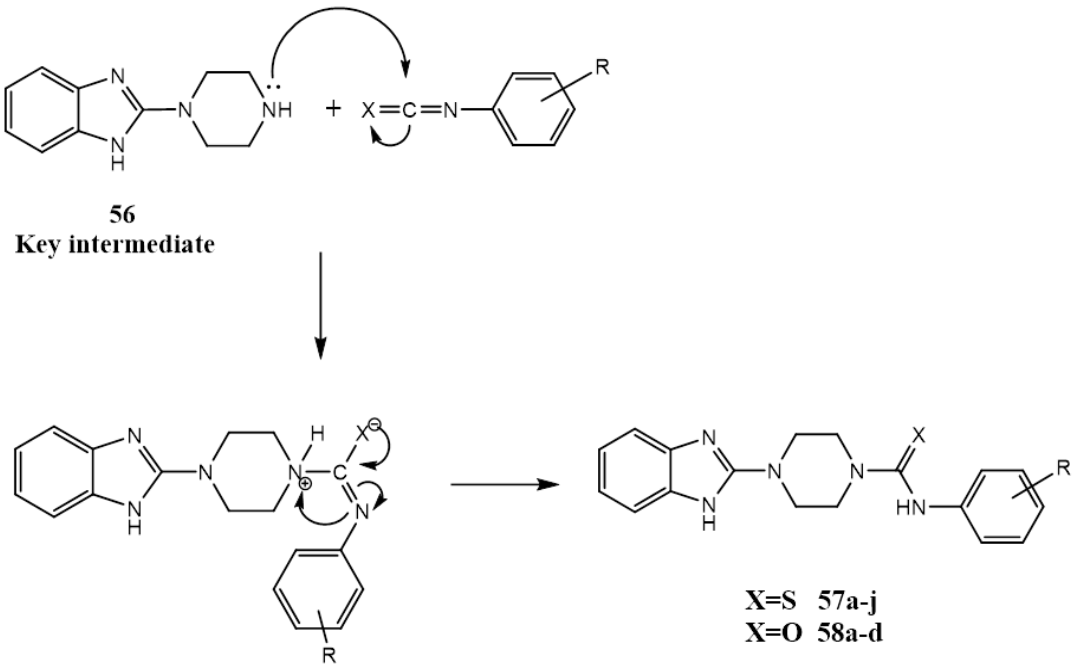


| X | | | |
|---|---|---|---|
| S | | O | |
| **Code** | **R** | **Code** | **R** |
| **57a** | H | **58a** | 4-$CH_3$ |
| **57b** | 4-$CH_3$ | **58b** | 4-$OCH_3$ |
| **57c** | 4-$OCH_3$ | **58c** | 3-Cl |
| **57d** | 3-Cl | **58d** | 4-Cl |
| **57e** | 4-Cl | | |
| **57f** | 4-$NO_2$ | | |
| **57g** | 2-F | | |
| **57h** | 3-F | | |
| **57i** | 4-F | | |
| **57j** | 4-$CF_3$ | | |

Figure 27: Synthesis of benzoimidazol-carbothioamide (57a-j) and benzoimidazol-carboxamide derivatives (58a-d)

### 3.1.2.1 Thiourea-piperazine benzimidazole derivatives (57a-j)

The suggested structures of compounds 57a-j were confirmed based on the spectral results from $^{1}H$ NMR, $^{13}C$ NMR and IR. In $^{1}H$ NMR spectra of the synthesized compounds 57a-j the benzimidazole protons appeared around 7 ppm and 7.2 ppm. The piperazine protons appeared around 3-3.6 ppm and 4- 4.6 ppm. While the H-N in benzimidazole appeared at high ppm around 9. However the N-H in thiourea it more deshield and appeared at 11.5 ppm.

The proton signals of benzene in thiourea derivatives appeared at aromatic region as a typical two doublets with different ppm in the range of 7.00-7.50 ppm depending on the nature of R group. While the two compounds 57j and 57f have more downfield peaks, the peaks for 57j appeared in the range of 7.5-8.00 ppm due to the $CF_3$ group on aromatic ring and compound 57f appeared in the range of 7.0-8.50 due to the nitro group.

The $^{13}C$ NMR spectra of compounds 57a-j showed the exact number of carbon atoms. The carbon of piperazine appeared around 46 ppm and 48 ppm, quaternary carbon of thiourea around 181.6 ppm. The methyl in compound 57c appeared at 55.62, while compound in 57b appeared at 20 ppm, depending on the R group attached to benzene ring. If the R is electron-donating (57a, 57b and 57c), the aromatic region will be in the range of 110-140 ppm. On the other hand, the compounds 57d-j the electron-withdrawing groups is shifting the δ-value down field to the range of 110-160 ppm. The quaternary carbon of thiourea around 181.6 ppm.

The IR spectra of compounds 57a-j showed N-H band around 3399-3458 $cm^{1}$. The thiourea is confirmed by bands around 1523-1535 $cm^{-1}$ which is the C=S stretching bands.

### 3.1.2.2 Urea-piperazine benzimidazole derivatives (58a-d)

The structures of compounds 58a-d were confirmed by spectral results from $^{1}H$ NMR, $^{13}C$ NMR and IR.

The $^{1}H$ NMR spectra of compounds 58a-d showed the same peaks of benzimidazole in thiourea which around is 7ppm and 7.2 ppm. The peaks of piperazine protons appeared in the range of 3.6-4.1 ppm. The H-N in benzimidazole appeared around 9 ppm. While the N-H in urea is more deshield and appeared at 11.5 ppm. The methyl in compound 58a and 58b appeared at 2.3 ppm and 3.7ppm respectively.

The aromatic region showed the proton of benzene that attached to urea derivatives as a typical two doublets with different ppm in the range of 7.00-7.50 ppm depending on the R group. While the two compounds 58c and 58d showed slightly downfield peaks in the range of 7.00-7.70 ppm due to the electron-withdrawing effect of the Cl atom.

The $^{13}C$ NMR spectra of compounds 58a-d showed the exact number of carbon atoms. The carbon of piperazine appeared around 43 ppm and 46 ppm, quaternary carbon of urea at 155 ppm. The methyl in compound 58a appeared at 20 ppm, while compound in 58b appeared at 55.62 ppm due to the Oxygen in the methoxy group. Depending on the R group attached to benzene ring. If the R is electron-donating (58a and 58b), the range of aromatic region will be 110-140 ppm.

While the electron-withdrawing groups shifting the δ-value down field to the range of 110-160 ppm. The quaternary carbon of urea at 155 ppm.

The IR spectra of compounds 58a-d showed N-H band around 3259-3407 $cm^{-1}$. The urea is confirmed by bands around 1636-1642 $cm^{-1}$ which is the C=O stretching bands.

### 3.2 Synthesis of urea and thiourea-benzimidazole derivatives with ethylenediamine linker

The structural similarity between the synthesized series carbothioamide (57a-57j) and (58a-58d) required that another series of compounds to be synthesized including compounds having ethylenediamine linker in place of the piperazine linker as outlined in the following Figure 28.

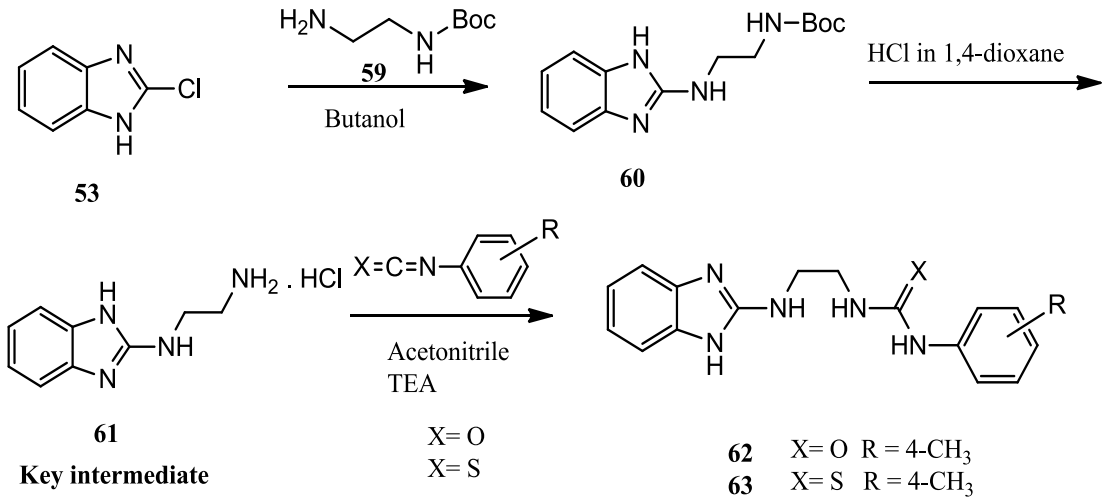


Figure 28: General synthesis of benzoimidazol- carboxamide derivatives (62-63)

The series including piperazine moiety is presumed to have a more rigid configuration compared to those having the configurationally flexible

ethylenediamine moiety. Ethylenediamine is less nucleophilic because it is primary amine comparing to piperazine which is secondary amine.

### 3.2.1 Synthesis of key intermediate (61)

Starting with 53 and ethylenediamine, the result is a mixture of desired product 61 and the dimer 69 (Figure 29).

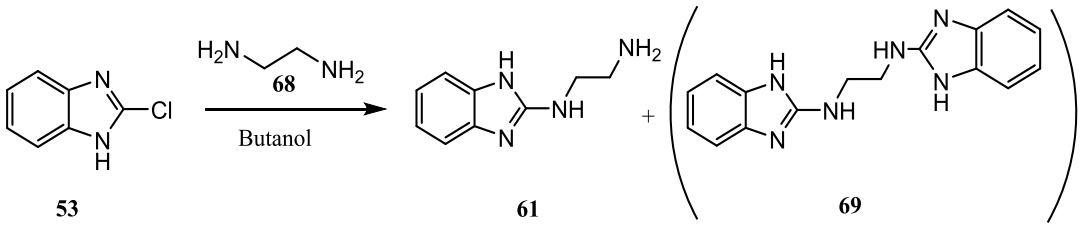


Figure 29: Synthesis of key intermediate 61 and dimer 69

Therefore, N-Boc ethylene diamine (tert-butyloxycarbonyl protecting group), was used instead. Compound 60 was obtained from 2-chloro-benzoimidazole 53 by nucleophilic substitution of the chlorine atom with N-Boc ethylene diamine 59 in accordance with previously published method (Zhu et al., 2013). Figure 30 shows the mechanism of the reaction.

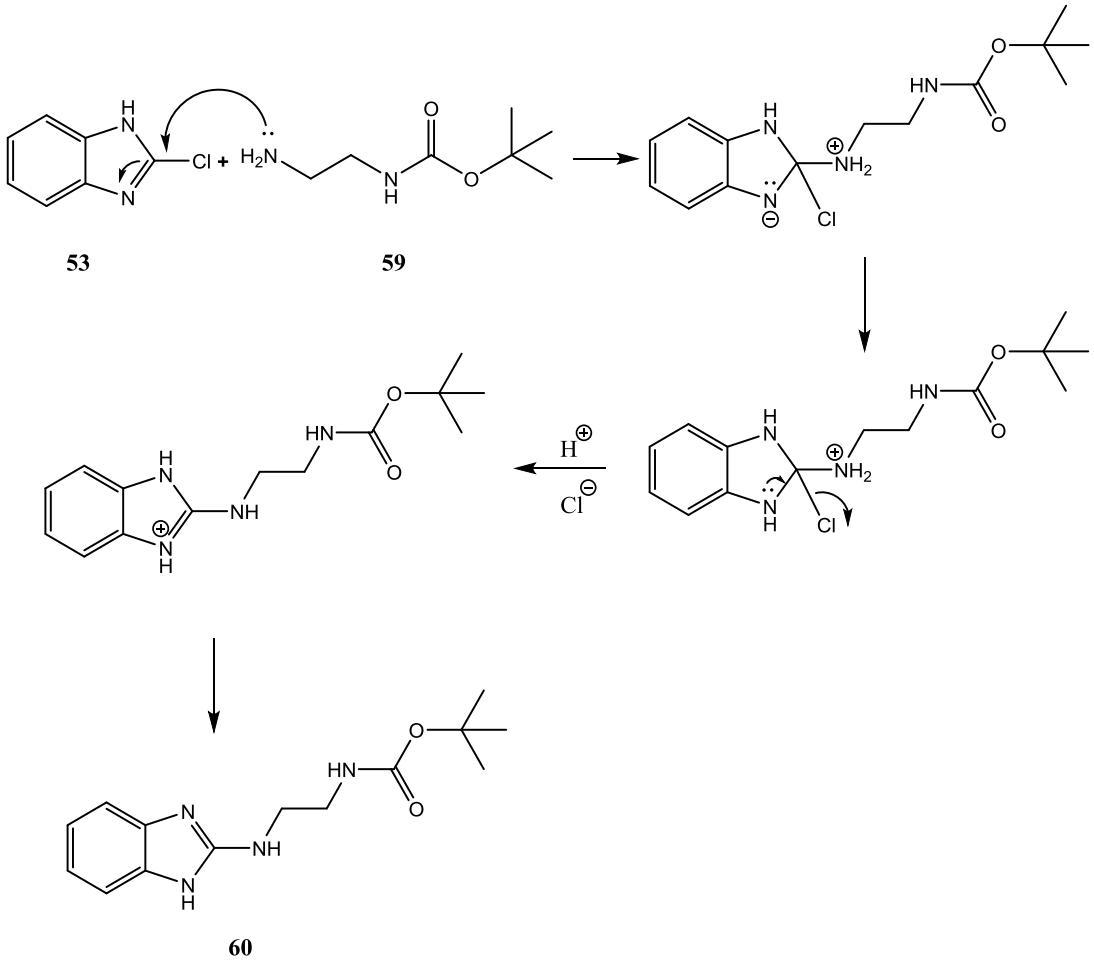


Figure 30: Synthesis of tert-butyl (2-((1H-benzo[d]imidazol-2-yl)amino)ethyl)carbamate 60

In this step ethylenediamine takes longer time to react with protecting group which shows a lower yield than the reaction of piprazine compound with protecting group. This because the ethylenediamine is primary amine which make it less nucleophile comparing with the piprazine (secondary amine).

The crude oily product was first solidified by diethyl ether and purified by column chromatography (eluent chloroform/methanol (95/5, v/v)). Subsequent removal of the N-Boc moiety with 4M HCl in dioxane gave 2-(aminoethyl)-1H-benzo[d]imidazol-2-amine (61) with yields (73%) (Figure 31).

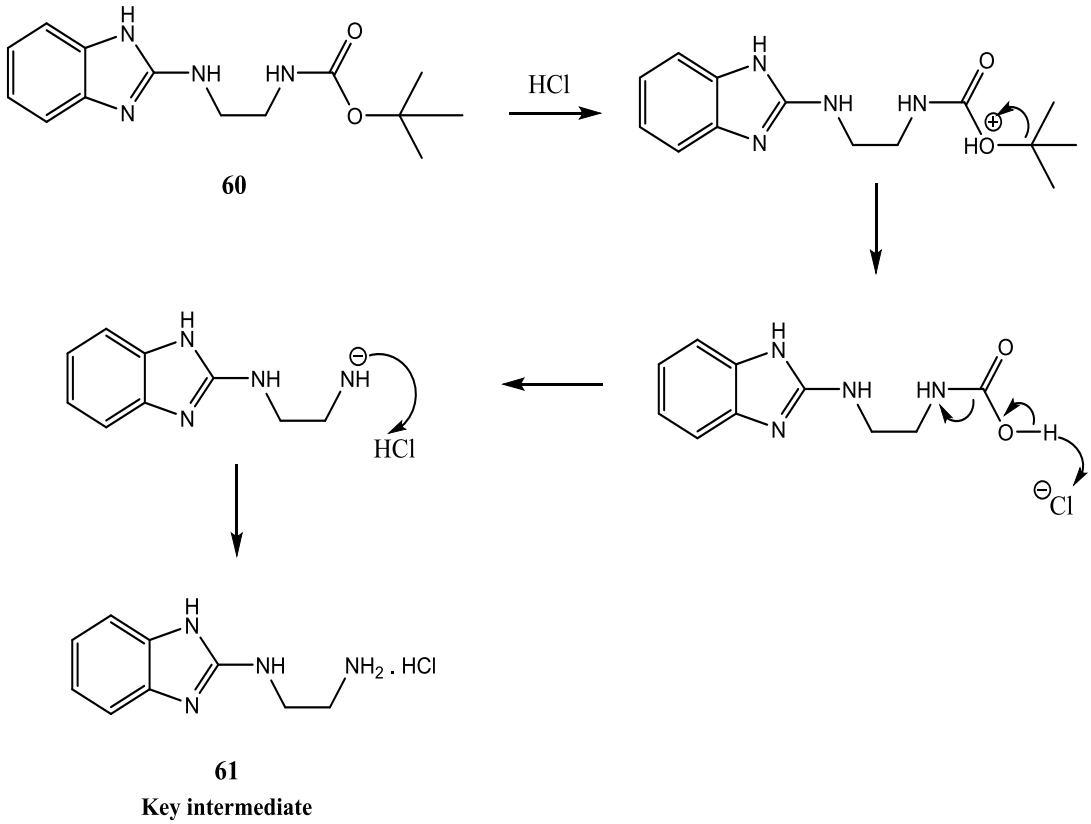


Figure 31: Mechanism of key intermediate 61

### 3.2.2 Synthesis of urea and thiourea-piperazine ethylenediamine.

Compounds 62 and 63 were synthesized as outlined in Figure 30, they obtained by the nucleophilic addition in which the amine group in key intermediate (61) react with the electrophilic carbon of in isothiocyanatobenzene (S) or isocyanatobenzene (O) in the presence of acetonitrile, according to reported procedure in experimental part. Figure 32 shows the mechanism of the reaction.

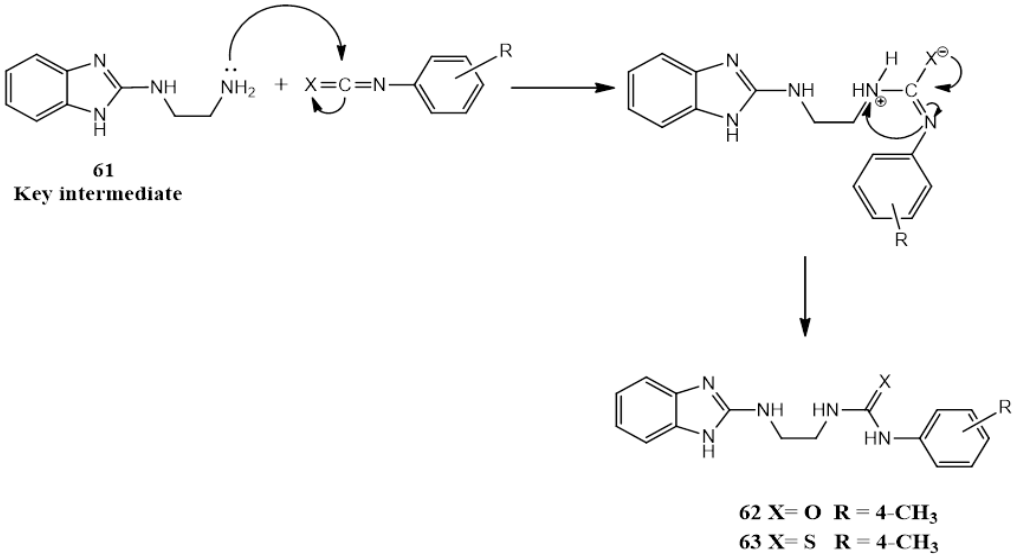


| | 62 | 63 | 70 | 71 | 72 | 73 | 74 |
|---|---|---|---|---|---|---|---|
| **X** | O | S | O | O | O | S | S |
| **R** | 4-$CH_3$ | 4-$CH_3$ | 4-$NO_2$ | 3-Cl | 4-OMe | 3-Cl | H |

Figure 32: Synthesis of benzoimidazol- carboxamide derivatives

The synthesize compounds 62-74 was attempted by the reaction of key intermediate, (61) with isothiocyanatobenzene and isocyanatobenzene respectively. Two out of the seven compounds 62 (urea) and 63 (thiourea) with a substituent group (-$CH_3$) were obtained in good yield 95% and 77%, respectively. Those products were pure and their structures were confirmed using $^{1}H$ NMR and $^{13}C$ NMR.

Compounds (70-74) were achieved with lower yields and purities. Repeated recrystallization with several solvents and preparative TLC did not achieve the desired purity criterion. Therefore, these compounds have not been pursued for synthesis and purification.

### 3.2.2.1 1-(2-(1H-benzo[d]imidazol-2-ylamino)ethyl)-3-p-tolylurea 62

The suggested structures of 62 were confirmed based on the $^{1}H$ NMR, $^{13}C$ NMR and IR results. $^{1}H$ NMR spectrum shows the signals of ethylenediamine at 3.4 ppm and 3.5 ppm. The methyl group appeared at low ppm 2.24. In the aromatic region the proton signals of benzene that attached to urea derivative appeared in the range of 7.20-7.30 ppm. While signals of benzimidazole group appeared around 7 ppm and 7.2 ppm. The IR spectra showed N-H band at 3370 $cm^{-1}$. The urea is confirmed by bands at 1705 $cm^{-1}$ which is the C=O stretching bands.

### 3.2.2.2 1-(2-(1H-benzo[d]imidazol-2-ylamino)ethyl)-3-p-tolylthiourea 63

The structures of 63 were confirmed based on the spectral results of $^{1}H$ NMR, $^{13}C$ NMR and IR results. In the $^{1}H$ NMR spectrum the signals of ethylenediamine appeared at 3.6 ppm and 3.9 ppm. The methyl group appeared at low ppm 2.27. In the aromatic area the signals of benzimidazole group appeared around 7 ppm and 7.2 ppm. While signals of benzene that attached to urea derivative appeared in the range of 7.20 -7.40 ppm. The IR spectrum showed N-H band at 3271 $cm^{-1}$. The urea is confirmed by bands at 1684 $cm^{-1}$ which is the S=O stretching bands.

## 3.3 Biological activity

### 3.3.1 Antibacterial activity

**Measurement of minimum inhibitory concentration (MIC) by agar dilution method**

Compounds (57a-57j), (58a-58d), 62, 63 and 65 were tested for antibacterial activity using the agar dilution method against six types of resistance gram positive

and gram negative bacteria including *E.coli 25922, P.aereginosa 27853, Salmonella H9812, K.pneumoniae 700603, S.aureus 25923* and *Enterococcus 29212.*

*E.coli* is a gram negative bacterium that causes of the gastrointestinal tract and central nervous system (Kaper et al. 2004). *P.aereginosa* is a gram negative bacteria able to cause nosocomial infections such as wound infections and urinary tract infections (Rustini et al. 2017). *Salmonella* is a gram negative bacteria and it is the second predominant cause of foodborne gastroenteritis (Mahmoud, B., 2012). *K.pneumoniae* is a gram negative bacteria that causes nosocomial infections, pneumonia, and sepsis in patients (Mei et al. 2017). *S.aureus* is a gram positive bacterium that causes both community-acquired and hospital infections such as meningitis and pneumonia (Bacci & Boncompain, 2017). *Enterococcus* it is a gram positive bacteria that cause line-associated bloodstream infections (Woods et al. 2007). Those pathogens are considered as life-threatening bacteria and they innate resistance to many antibiotics which make them target for many research groups.

Table 1 shows the MIC (µg/ml) results of the 17 compounds tasted against the 6 bacteria. 13 out of 17 compounds showed a good to moderate activity against *enterococcus 29212* at different concentrations ranged between 37.1 – 92.7 µg/ml. In addition 2 compounds (65 and 57e) out of the 13 compounds showed a moderate activity against the *S.aureus 25923* (gram positive bacteria) with concentration 88 µg/ml and 92.7µg/ml respectively. While bacteria *P.aereginosa 27853* has been inhibited by compound 65 and 57e with concentration 88 µg/ml and 92.7 µg/ml, respectively. The rest 4 compounds showed negative results against the 6 type of bacteria.

Table 1: MIC (µg/ml) of compounds (57a-57j), (58a-58d), 62, 63 and 65

| | **E.coli** | **P.aereginosa** | **Salmonella** | **K.pneumoniae** | **S.aureus** | **Enterococcus** |
|---|---|---|---|---|---|---|
| **DMSO** | GROWING | GROWING | GROWING | GROWING | GROWING | GROWING |
| **57a** | >83.6 | >83.6 | >83.6 | >83.6 | >83.6 | 66.9 |
| **57b** | >88 | >88 | >88 | >88 | >88 | >88 |
| **57c** | >92.7 | >92.7 | >92.7 | >92.7 | >92.7 | >92.7 |
| **57d** | >89 | >89 | >89 | >89 | >89 | 71.3 |
| **57e** | >92.7 | 92.7 | >92.7 | >92.7 | 92.7 | 92.7 |
| **57f** | >96.3 | >96.3 | >96.3 | >96.3 | >96.3 | 77 |
| **57g** | >89 | >89 | >89 | >89 | >89 | 71.3 |
| **57h** | >89 | >89 | >89 | >89 | >89 | 71.3 |
| **57i** | >89 | >89 | >89 | >89 | >89 | 89 |
| **57j** | >101.8 | >101.8 | >101.8 | >101.8 | >101.8 | >101.8 |
| **58a** | >83.6 | >83.6 | >83.6 | >83.6 | >83.6 | 66.9 |
| **58b** | >88 | >88 | >88 | >88 | >88 | 70.4 |
| **58c** | >92.7 | >92.7 | >92.7 | >92.7 | >92.7 | 37.1 |
| **58d** | >89 | >89 | >89 | >89 | >89 | >89 |
| **62** | >78.2 | > 78.2 | >78.2 | > 78.2 | >78.2 | 78.2 |
| **63** | > 61.8 | > 61.8 | > 61.8 | > 61.8 | > 61.8 | 49.4 |
| **65** | >88 | 88 | >88 | >88 | 88 | 88 |
| **2-Cl BZ** | > 38.1 | > 38.1 | > 38.1 | > 38.1 | > 38.1 | > 38.1 |
| **8-HQ** | 29 | > 36.2 | 36.2 | 29 | 14.4 | > 36.2 |
| **MHA** | GROWING | GROWING | GROWING | GROWING | GROWING | GROWING |

### 3.3.2 In vitro Antifungal activity

**In vitro -evaluation of the minimum effective concentration in vitro**

Compounds (57a-57j), (58a-58d), 62, 63 and 65 were tested against 4 types of fungi which are Fusarium solani, botrytis cinerea, thielaviopsis punctulate and neoscytalidium dimidiatum.

Fusarium solani is a fungus that causes blindness in subtropical and tropical areas (Zwart et al. 1973). Botrytis cinerea is a fungus responsible of gray mold disease on over 200 plants and kills the host plant through the production of reactive oxygen species and toxin (Choquer et al. 2007). Thielaviopsis punctulate is a type of fungus that causes serious diseases on date palm such as black scorch and rhizosis, which could affect the economic value of these trees (Saeed et al. 2016). Neoscytalidium dimidiatum is a mold that causes dermatomycosis, onychomycosis, and pulmonary fungal infection (Dionne et al., 2015).

The 17 compounds were tested at 100 µM concentration, after 10 days in this incubation the fungus growth was checked and recorded. In the plates of compounds and control (DMSO) the fungi grow normally, therefor compounds did not show antifungal activity at ≥ 100 µM (Table 2).

Table 2: MIC of compounds (57a-57j), (58a-58d), 62, 63 and 65

| | Fusarium solani | botrytis cinerea | thielaviopsis punctulate | neoscytalidium dimidiatum. |
|---|---|---|---|---|
| DMSO | GROWING | GROWING | GROWING | GROWING |
| **57a** | >100µM | >100µM | >100µM | >100µM |
| **57b** | >100µM | >100µM | >100µM | >100µM |
| **57c** | >100µM | >100µM | >100µM | >100µM |
| **57d** | >100µM | >100µM | >100µM | >100µM |
| **57e** | >100µM | >100µM | >100µM | >100µM |
| **57f** | >100µM | >100µM | >100µM | >100µM |
| **57g** | >100µM | >100µM | >100µM | >100µM |
| **57h** | >100µM | >100µM | >100µM | >100µM |
| **57i** | >100µM | >100µM | >100µM | >100µM |
| **57j** | >100µM | >100µM | >100µM | >100µM |
| **58a** | >100µM | >100µM | >100µM | >100µM |
| **58b** | >100µM | >100µM | >100µM | >100µM |
| **58c** | >100µM | >100µM | >100µM | >100µM |
| **58d** | >100µM | >100µM | >100µM | >100µM |
| **62** | >100µM | >100µM | >100µM | >100µM |
| **63** | >100µM | >100µM | >100µM | >100µM |
| **65** | >100µM | >100µM | >100µM | >100µM |

# Chapter 4: Photochemistry

## 4.1 Introduction

Luminescence is the emission of visible, ultraviolet or infrared photons by some substances in their excited states upon the exposure to a light source at a shorter wavelength (Lakowicz, 2006). It is divided into two types depending on the route of deactivation of the energy at the excited state, namely, fluorescence and phosphorescence (Valeur & Santos, 2001). The environment plays an important role in modulating the fluorescence emission originated from some organic molecules, so called fluorescent probes, which are used to report information about the structure and dynamics of the surrounding microhetergenous systems, such as biological receptors in medicinal applications (Shaikh et al. 2008). Fluorescent dyes can be used to relocate and detect some biological substrates in cellular media, micelles, membranes, polymers, and more (Hamilton et al. 2015). In many occasions, host-guest complexes of several fluorescent probes were employed in biological application (Dsouza et al. 2011).

Supramolecular photochemistry was first developed by Lehn, Cram and Pedesen in 1987. Since then this field has seen an evolution in different application such as biomedicine and chemical sensing (Saleh et al. 2013). Supramolecular photochemistry is the study of the properties of molecular assemblies through intermolecular interactions in their excited states (Ramamurthy & Mondal, 2015). Supramolecular chemistry is the study of host-guest complexes (Dsouza et al. 2011), which occurs when a small molecule (guest) inters the cavity of a larger molecule (host) and interact by non-covalent bonds (Wagner, 2009). The non-covalent

interactions are hydrogen bonding, electrostatic interaction, cation- π and anion-π interaction, hydrophobic interaction, and other aromatic interaction (Shumilova et al. 2018).

Cucurbit[n]urils (CBn) consisted of glycoluril group that are connected to methylene groups. The applications of cucurbit[n]urils complexes in supramolecular chemistry has come into a form of stable complexes with different guests, including amino acids, drug molecules, dyes, saccharides, hydrocarbons, and proteins, which have number of applications in health, environment and energy (Assaf & Nau, 2014). Figure 33 represents cucurbit[n]urils structures, including three examples: CB5, CB6 and CB7.

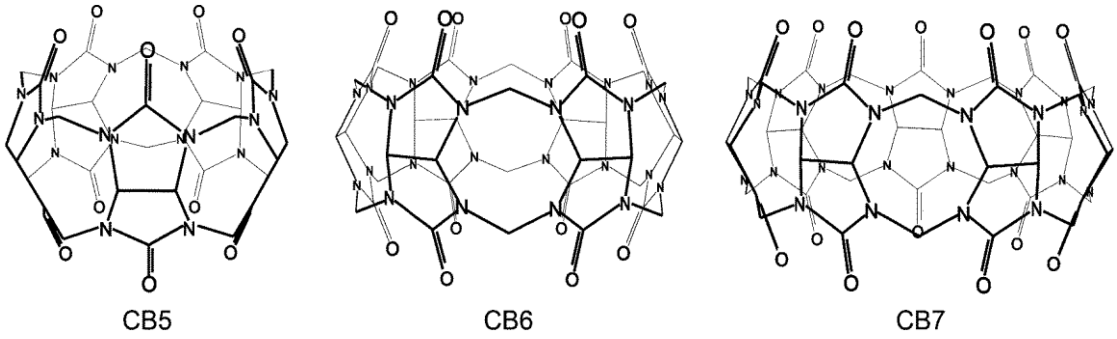


Figure 33: Chemical structure of cucurbiturils molecular containers (CB5, CB6 and CB7)

Based on the important and applications of the fluorescent dyes and supramolecular photochemistry as discussed earlier in the introduction, compound 65 was selected and the binding properties of the fluorescent dye with CB7 was tested by the titration method using NMR and UV-Vis techniques.

## 4.2 Experimental part

### 4.2.1 Chemistry

#### 4.2.1.1 Preparation of 5-chloromethyl-8-quinolinol hydrochloride 64

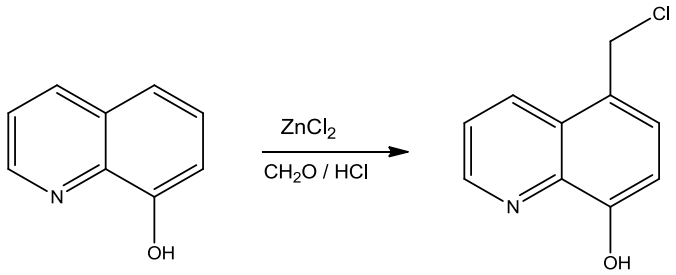


**64**

A mixture of 8-hydroxyquine (5.84 g, 70.0 mmol), with zinc chloride (1.05 g, 29.6 mmol) in 50 ml of concentrated hydrochloric acid, and 6.4 ml of 37% formaldehyde was stirred overnight. The mixture was filtered, washed with acetone and dried to obtain the desired compounds. The yellow solid obtained (7.94g, 86%). $^{1}$H NMR (400 MHz, Deuterium Oxide) δ 9.06 (dd, J = 8.7, 1.4 Hz, 1H), 8.81 (dd, J = 5.4, 1.4 Hz, 1H), 7.90 (dd, J = 8.7, 5.4 Hz, 1H), 7.53 (d, J = 8.0 Hz, 1H), 7.18 (d, J = 8.0 Hz, 1H), 4.87 (d, J = 0.6 Hz, 2H). $^{13}$C NMR (101 MHz, $D_2O$) δ 145.96, 143.02, 141.86, 129.99, 127.84, 127.36, 127.15, 121.70, 115.05, 59.77.

#### 4.2.1.2 Synthesis of 5-((4-(1H-benzo[d]imidazol-2-yl)piperazin-1-yl)methyl)quinolin-8-ol 65

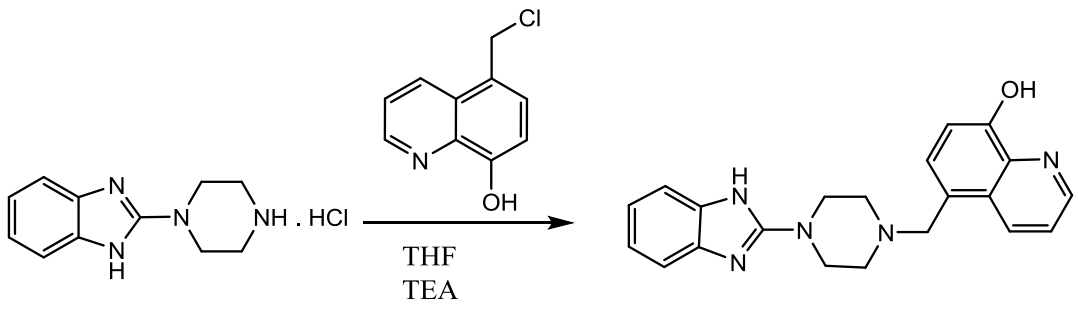


**56** **65**

To a stirred solution of 2-(piperazin-1-yl)-1H-benzo[d]imidazole 56 (0.5 mmol) in tetrahydrofuran (10 mL), triethylamine (460 µL, 4 mmol) was added 5-chloromethyl-8-quinolinol hydrochloride 64 (0.5 mmol). The mixture was stirred at room temperature overnight. After completion, the solvent was removed under vacuum, dissolved in ethyl acetate (20 mL) then washed with water. The organic layer was dried over anhydrous sodium sulfate, the solvent was evaporated, the crude was crystalized over ethyl acetate and the precipitate formed was filtered and dried to obtain the desired compounds. White solid, (0.115 g, 63%); mp 276-278 $^{0}$C; $R_f$ = 0.44 (Ethyl acetate) IR (KBr, $cm^{-1}$) 3077(NH), 3326 (OH); $^{1}$H NMR (400 MHz, DMSO-$d_6$) δ 11.34 (s, 1H), 9.76 (s, 1H), 8.86 (dd, *J* = 4.1, 1.6 Hz, 1H), 8.69 (dd, *J* = 8.6, 1.7 Hz, 1H), 7.60 (dd, *J* = 8.6, 4.1 Hz, 1H), 7.37 (d, *J* = 7.8 Hz, 1H), 7.16 (dd, *J* = 18.9, 7.6 Hz, 2H), 7.01 (d, *J* = 7.7 Hz, 1H), 6.97 – 6.84 (m, 2H), 3.83 (s, 2H), 3.43 (t, *J* = 5.0 Hz, 4H), 2.53 (d, J = 4.3 Hz, 4H). $^{13}$C NMR (101 MHz, DMSO) δ 156.49, 153.41, 148.24, 139.32, 134.27, 129.52, 128.34, 124.21, 121.93, 110.43, 60.04, 52.36, 46.47.

### 4.2.2 Photochemistry

#### 4.2.2.1 Binding titration experiment

Samples: CB7 (purity > 99.9%) was purchased from sigma-Aldrich

UV−vis absorption spectra and fluorescence spectra were measured by Cary-300 instrument (Varian) and Cary-Eclipse instrument respectively with slit widths 10 nm for both the excitation and emission monochromator or 5 nm and 10 nm for excitation and emission monochromator. In the titration experiment, the concentrations of the guest were kept constant and the host was gradually increased. The spectra were plotted as a function of the host concentrations at a given

wavelength. In the binding experiment of compound 65 with CB7, the following procedure was used at pH 7.4; 35 µM of 65 solution was placed in cuvette with 1-cm optical path length and small amounts of the CB7 solution (1 mM) were gradually added with micropipette. For theinteraction of 65/CB7 complex with CAD at pH 7.4, and 35 µM of 65 and 350 µM of CB7 solution was placed in the same cuvette and small amounts of the CAD solution (1 mM) were gradually added with micropipette (Saleh et al. 2015).

#### 4.2.2.2 NMR titration

All $^{1}$H NMR spectra were recorded, using Varian-400 MHz (USA), at room temperature in $D_2O$. The pH values of the solutions were adjusted by adding HCl (DCl) and recorded using a pH meter (WTW 330i equipped with a WTW SenTix Mic glass electrode). For the NMR titration experiment of compound 65 with CB7 complex, first the pD of $D_2O$ was adjusted to 2.9 in which a stock solution of 65 was prepared with a final concentration of ~2 mM. Then a calculated weight of CB7 (0.2 equivalent) was added to compound 65 solution in the NMR tube. The 0.2 equivalent of CB7 were gradually added to the solution to complete the titration. The NMR spectra were measured for each solution (Saleh et al. 2015).

However, for the titration experiment of 65/CB7 complex with CAD at pH 1.3, a stock solution of 65 (2 mM) and CB7 (4 mM) complex was prepared. Then a calculated weight of CAD (1 equivalent) was added to the complex in the NMR tube.

## 4.3 Results and discussion

### 4.3.1 Chemistry

#### 4.3.3.1 Synthesis of 5-((4-(1H-benzo[d]imidazol-2-yl)piperazin-1-yl)methyl)quinolin-8-ol (65)

Compound 65 was prepared by $S_N2$ reaction of 5-chloromethyl-8-quinolinol hydrochloride 64 with the key intermediate 56, in the presence of triethylamine and THF. Figure 34 shows the mechanism of the reaction.

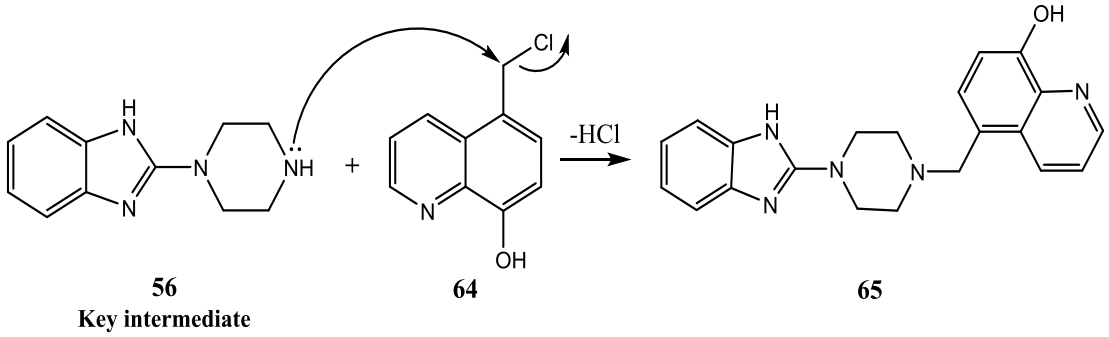


Figure 34: Mechanism reaction of compound 65

Suggested structures of compound 65 were confirmed based on the $^1$H NMR, $^{13}$C NMR and IR results. The $^1$H NMR spectrum showed the piperazine protons of benzimidazole around 3.43 ppm and 3.83 ppm. The N-H and O-H peaks appeared at 9.76 ppm and 11.34 ppm. In the aromatic region the benzimidazole protons appeared at 6.9 ppm and 7.16. While the 8-Hydroxyquniolne protons appeared around at 7 ppm and 9 ppm.

The $^{13}$C NMR spectrum showed the exact number of carbon atoms. The carbon of piperazine appeared around 52.36 ppm and 46.47 ppm. The methyl group

appeared at 60.04 ppm, the range of aromatic region will be 148.24- 110.43 ppm. The IR spectrum showed N-H band at 3077 $cm^{-1}$ and O-H band appeared at 3326 $cm^{1}$.

### 4.3.2 Photochemistry

Compound 65 in aqueous solution (pH 7.4) emit cyan color (first cuvette). The color of this emission was switched to green upon the addition of CB7 (second cuvette), the color has then been restored with the addition of CAD (third cuvette) (Figure 35).

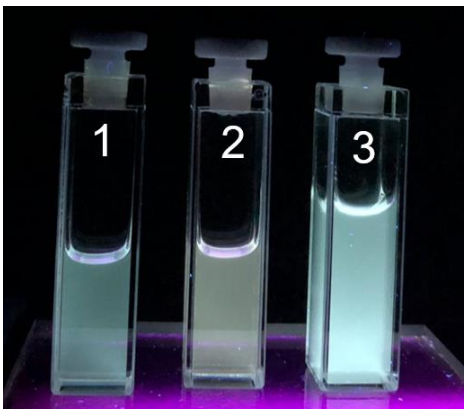


Figure 35: Compound 65 (1), the complex of 65 with CB7 (2) and the complex of 65 with CB7 and CAD (3) under UV lamb

#### 4.3.2.1 NMR titration of 65 with CB7

One of most common method for quantifying the interaction of supramolecular components is the titration of the guest compound in the solution with the host and tracking the changes in physical properties through NMR and UV-Vis absorption techniques. In this work, the interaction of compound 65 with CB7 was examined, and utilize of this supramolecular approach with CAD stimulus (as a model drug for biosensing) was checked (Figure 36).

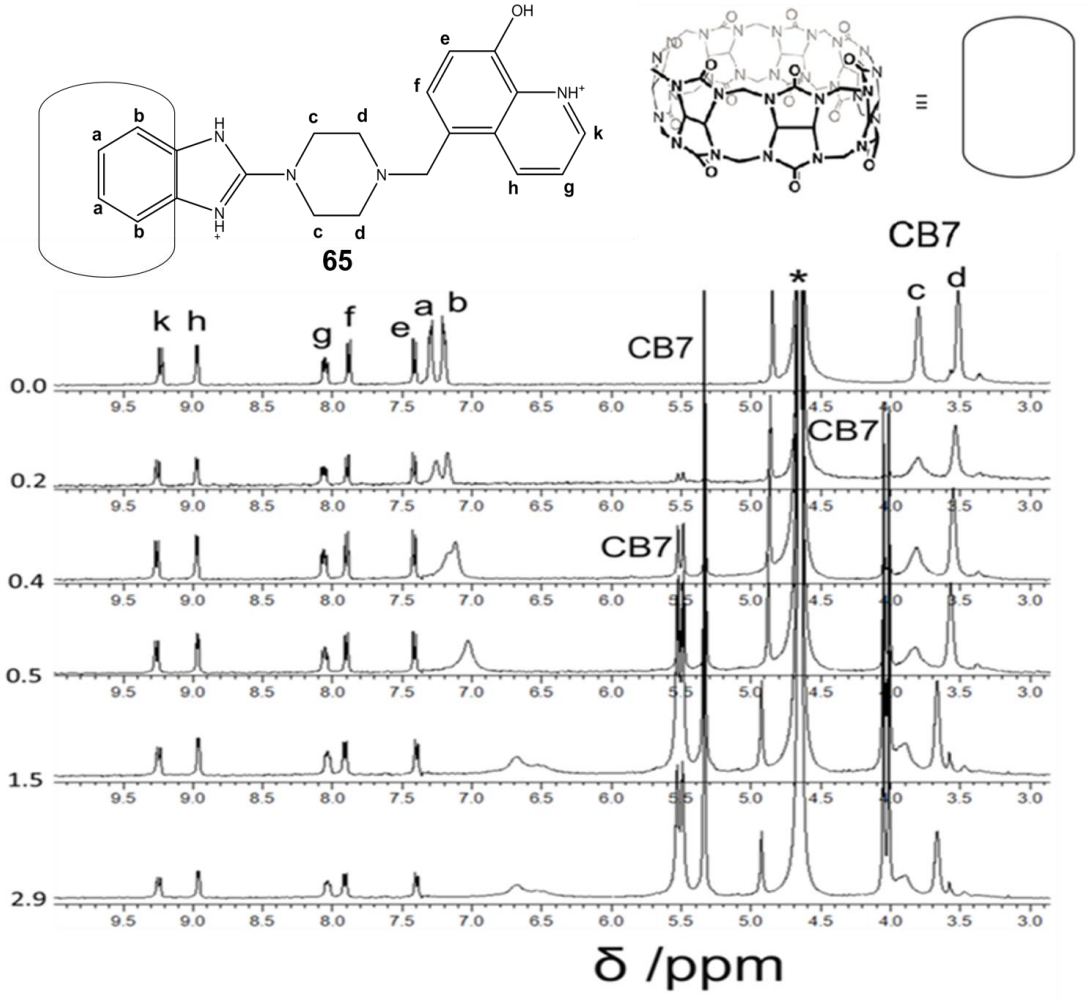


Figure 36: $^{1}$H-NMR (400MHz) titration of 65 [1mM] with CB7 (0-2.9 equiv.) in $D_2O$ at pD 2.9

In the first experiment, NMR titration was conducted in order to study the binding mode of 65 with CB7 at pD 2.9 (potential of Deuterium). In Figure 36, in the absence of CB7, 65 peaks were labeled a-k. (0.2, 0.4, 0.5, 1.5 and 2.9 equivalent) of CB7 were gradually added. The upfield shift in the peaks of benzimidazole ring (a and b) upon the increase of the CB7 equivalent.

This upfield shift also confirms the binding of CB7 to benzimidazole ring. It is known that CB7 prefers to bind to protonated guests because of preferential ion-dipole interaction (Atwood et al. 2017). At pD 2.9 the benzimidazole group is

expected to be protonated, which explains the observe NMR trend in the binding pattern.

### 4.3.2.2 Host-guest interaction of the complex 65/CB7 and cadaverine

NMR titration of 65/CB7 complex at 1:2 equivalents with CAD was conducted at acidic media in order to show the binding mode of CAD to CB7 and to establish the stimuli-responsiveness of the host-guest system.

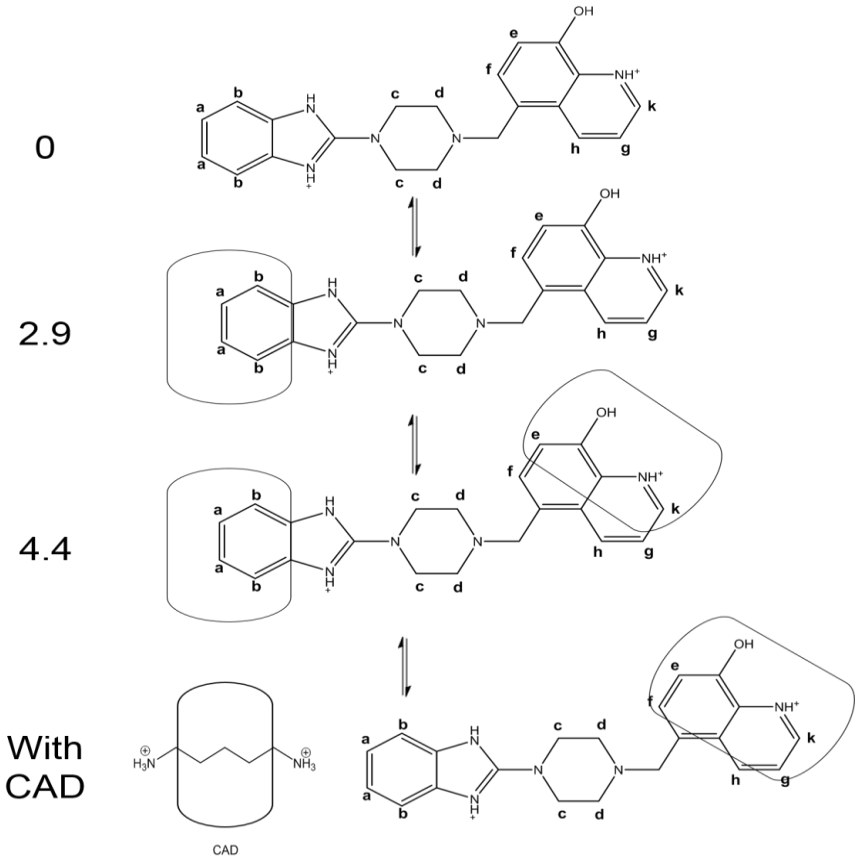


Figure 37: $^{1}$H-NMR aromatic region: Biding of compound 65/CB7 (1: 4.4 equiv.) with CAD (0.5 equiv.) in $D_2O$

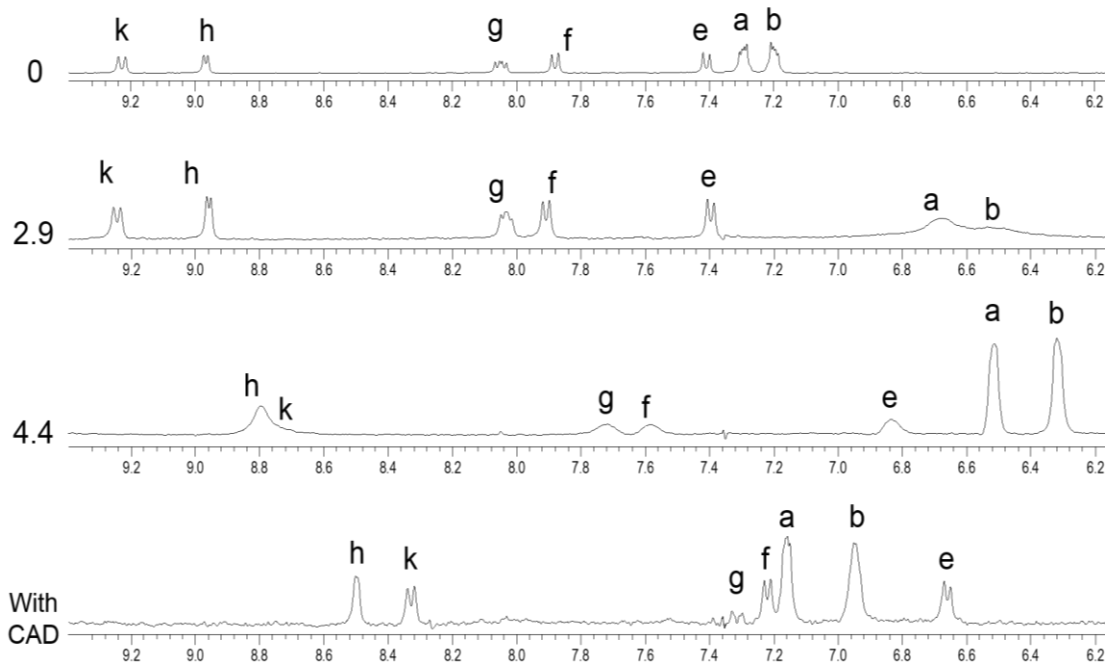


Figure 37: $^{1}$H-NMR aromatic region: Biding of compound 65/CB7 (1: 4.4 equiv.) with CAD (0.5 equiv.) in $D_2O$ (continued)

As can be seen in Figure 37, the equilibrium between compound 65 with CB7 is changed upon the addition of different equivalents. At 2.9 equivalent of CB7 the capsulation has occurred at benzimidazole site, as manifested in the up field shifted of a and b peaks. However with the addition of >2 equivalents, both the benzimidazole unit and 8-HQ units were encapsulated by CB7 cavity leading to the maximum shift of a and b peaks to 6.5 ppm and 6.3 ppm respectively. However, 8-HQ protons (e - h) where not shifted at >1 equivalent of CB7, but then after adding more than 2 equivalents of CB7 the peaks were shifted to lower ppm. The amount of the shift depends on the monitored proton, which confirms the selectivity of this host-guest system. For example, the CB7 prefer to initially binds to k and e protons over the other protons (g, h and f). Table 3 shows the chemical shifts in the peaks of compound 65, upon the addition of CB7.

The position of the peaks a and b were recovered after the addition of CAD, which clearly means that BZ is not encapsulated and that the CAD competes with BZ towards the CB7 cavity. Moreover, this addition allowed the fully encapsulation of 8-HQ site. Before the addition of CAD, the CB7 was partially engulfing the 8-HQ, but the competitive displacement of BZ by CAD enables the fully encapsulation resulting in a full shift to lower ppm of all protons except h. Overall, the results might be rational by the thermodynamics preference toward CAD when competing with BZ units, which needs further investigation. While c and d protons represent the piperazine peaks (Figure 38).

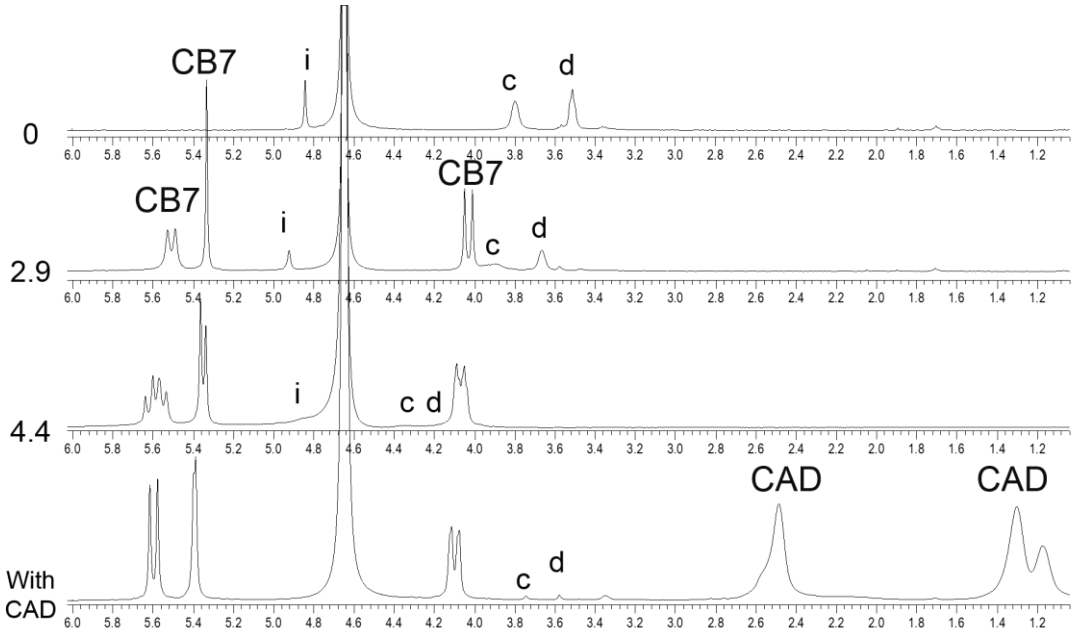


Figure 38: $^{1}$H-NMR aliphatic region: Biding of compound 65 with CB7 (0- 4.4 equiv.) and CAD (0.5 equiv.) in $D_2O$

Table 3: NMR chemical shift of compound 65 upon addition of CB7 and CAD

| Protons | After CB7 | After CAD |
|---|---|---|
| **a** | -0.8ppm | -0.8 ppm |
| **b** | -0.9 ppm | -0.9 ppm |
| **e** | -0.6 ppm | -0.8 ppm |
| **f** | -0.3 ppm | -0.6 ppm |
| **g** | -0.4 ppm | -0.8 ppm |
| **h** | -0.2 ppm | -0.5 ppm |
| **k** | -0.5 ppm | -0.9 ppm |
| **c** | +0.7 ppm | 0 ppm |
| **d** | +0.5 ppm | 0 ppm |

Looking at aliphatic region we noticed that proton belong to the piperazine ring and methylene group were shifted to higher ppm which indicate they are outside the cavity, with the addition of more CB7 they are hidden under the CB7 peaks.

#### 4.3.2.3 UV-Vis binding titration experiment

In this experiment the titration of 65/ CB7 complex with CAD was conduct by using fluorescence techniques. In the binding titration experiment, pH 7.4 was selected because it matches the environment in medical applications in *vitro* and in *vivo*.

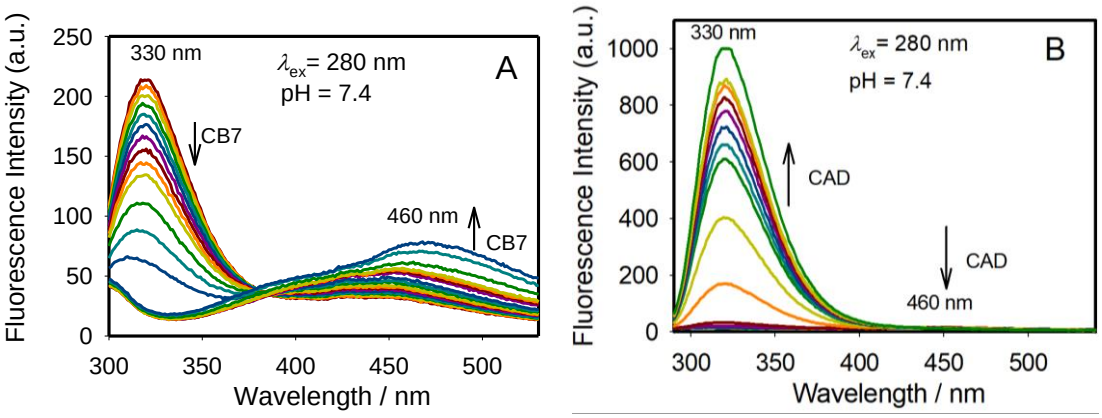


Figure 39: (A) Shows the binding titration of 65 with CB7 at pH 7.4. (B) Shows the binding titration of the complex 65 /CB7 with cadaverine at pH 7.4

Figure 39 A shows the variation the emission spectra of 65 [35 µM] upon binding to CB7 (0-500 µM). The fluorescent compound (65) has an emission around 320, however as the CB7's concentrations (0-500 µM) increase, the intensity at 320nm decreased and the intensity 460 nm increased. Leading to a shift in the color from cyan to green. The appearance of an intersection points confirms the complexion of 65 to CB7.

Figure 39 B shows the binding titration of 65 with CB7 at pH 7.4 with the gradual addition of cadaverine to the 65/CB7. It can be noticed that there is a gradual increase in the emission at 320nm, and with a decrease in the emission at 460nm. It is concluded that cadaverine replaces dye 65 and restore the cyan color.

# Chapter 5: Conclusion

This study involved the design and synthesis of 17 novel compounds (57a-57j), (58a-58d), 62, 63 and 65 that contain benzimidazole, piperazine, 8-hydroxyqunoline and urea or thiourea moieties. Those compounds were characterized by using suiTable spectroscopic techniques including $^{1}$H-NMR, $^{13}$C-NMR, and IR spectroscopy techniques.

The biological activities of the 17 synthesized compounds were evaluated for their antibacterial and antifungal activities. The antibacterial activities were evaluated against 6 types of bacteria (*E.coli 25922, P.aereginosa 27853, Salmonella H9812, K.pneumoniae 700603, S.aureus 25923 and Enterococcus 29212*). 13 compounds (57a, 57d, 57e, 57f, 57g, 57h, 57i, 58a, 58b, 58c, 62, 63 and 65) showed a positive result against *enterococcus 29212* and 65 showed activity against *p.aereginosa 27853* and *s.aureus 25923*, with different concentrations ranged 33.4 - 96.3µg/ ml. However, all compounds showed negative results when studied against selected four fungi (*Fusarium solani, botrytis cinerea, thielaviopsis punctulate and neoscytalidium dimidiatum*) at concentration 200 µM.

Compound 65 exhibited interesting photophysical properties. Fluorescence emission of this compound was switched from cyan to green. The establishment of stimuli-responsiveness system emission was checked using CAD as model drug.

## 5.1 Recommendation and Future work

The 17 novel synthetic compounds exhibit interesting biological activity, we evaluated only antibacterial. In the future we aim to examine antiviral,

antihelminthic, and anticancer activities. Moreover, more compounds can be synthesized by changing the substituent groups, in quest for future comparison.

## References

Abata´ngelo V., Peressutti N., Boncompain A., Amadio A., Carrasco S., Sua´rez C., et al. (2017) Broad-range Lytic Bacteriophages That Kill Staphylococcus Aureus Local Field Strains. *PLoS ONE, 12*(7), 1-22. doi: 10.1371/journal.pone.0181671.

Akhtar, W., Khan, M., Verma, M. Shaquiquzzaman, M. A. Rizvi, M., Mehdi, S., Akhter, M., Alam, M. (2017). Therapeutic Evolution of Benzimidazole Derivatives In The last Ouinquennial Period. *European Journal of Medicinal Chemistry, 126*, 705-753. doi:org/10.1016/j.ejmech.2016.12.010.

Alaqeel, S. (2017). Synthetic Approaches to Benzimidazoles From o-phenylenediamine: A Literature Review. *Journal of Saudi Chemical Society*, *21*(2), 229–237. doi: 10.1016/j.jscs.2016.08.001.

Albizati, K., Martin, V., Agharahimi, M., Stolze, D. (1992). *Synthesis of Marine Natural Products 1*, Germany, Springer-Verlag Berlin Heidelberg.

Assaf, K., & Nau, M. (2014). Cucurbiturils: From Synthesis To High-affinity Binding and Catalysis. *The Royal Society of Chemistry, 44*(2), 385–604. doi: 10.1039/c4cs00273c.

Atwood, J., Gokel, G., & Barbour, L. (2017). *Comprehensive Supramolecular Chemistry II* (2nd ed.). United States, Elsevier.

Brown, D., Matzuk, R., Ilves, R., Peterson, H., Harris, A., Sarett, H., Cuckler, C. (1962). Antiparastic Drugs. IV. 2-(4-thiazolyl)-benzimidazole, A New Anthelmintic. *Journal of the American Chemical Society, 83*(7), 1764–1765. doi.org/10.1021/ja01468a052.

Cazajous, T., Prevot, F., Kerbiriou, A., Milhes, M., Grisez, C., Tropee, A., … Aragon, A. (2018). Multiple-resistance To Ivermectin and Benzimidazole of A Haemonchus Contortus Population In a Sheep Flock From Mainland France, First Report, *Veterinary Parasitology : Regional Studies and Reports, 14*, 103–105. doi:10.1016/j.vprsr.2018.09.005.

Chakraborty, A., Sarkar, D., Dey, P., & Chandra, A. K. (2018). New Insights Into Morphological, Stereological and Functional Studies of The Adrenal Gland under Exposure to The Potent Goitrogen Thiourea, *Interdiscip Toxicology, 11*(1), 38–44. doi:10.2478/intox-2018-0005.

Choi, J., & Jee, J. G. (2015). Repositioning Of Thiourea-containing Drugs As Tyrosinase Inhibitors. *International Journal of Molecular Sciences*, *16*(12), 28534–28548. doi: org/10.3390/ijms161226114.

Choquer, M., Fournier, E., Kunz, C., Levis, C., Pradier, J., Simon, A., & Viaud, M. (2007). Botrytis Cinerea Virulence Factors: New Insights Into A Necrotrophic And Polyphageous Pathogen. *Federation of European Microbiological Societies*, *277*, 1–10. doi: 10.1111/j.1574-6968.2007.00930.x.

Dionne, B., Neff, L., Lee, S., Sutton, D., Wiederhold, N., Lindner, J., … Jakeman, B. (2015). Pulmonary Fungal Infection Caused by Neoscytalidium Dimidiatum. *Journal of Clinical Microbiology*, *53*(7), 2381–2384. doi: 10.1128/JCM.00206-15.

Drew, S., C. (2017). The Case For Abandoning Therapeutic Chelation Of Copper Ions in Alzheimer's Disease. *Frontiers in Neuroscience*, *11*, 1-11. doi: 10.3389/fnins.2017.00317.

Dsouza, N., Pischel, U., & Nau, W. (2011). Complexation of Fluorescent Dyes By Macrocyclic Hosts., *Supramolecular Photochemistry*,(pp. 78-114). doi: 10.1002/9781118095300.ch3.

Dsouza, N., Pischel, U., & Nau, W. (2011). Fluorescent Dyes and Their Supramolecular Host / Guest Complexes with Macrocycles in Aqueous Solution, *American Chemical Society*. *111*, 7941–7980. doi: 10.1021/cr200213s.

Dyson, L., Wright, A., Young, K., Sakoff, J., & Mccluskey, A. (2014). Bioorganic & Medicinal Chemistry Synthesis and anticancer activity of focused compound libraries from the natural product lead, oroidin. *Bioorganic & Medicinal Chemistry*, *22*(5), 1690–1699. doi:10.1016/j.bmc.2014.01.021.

Elderfield, R. (1975). *5- membered heterocycles combining two heteroatoms & their benzo derivatives*, heterocyclic compound. United Kingdom, John Wiley.

Flora, S., & Pachauri, V. (2010). Chelation in metal intoxication. *International Journal of Environmental Research and Public Health*, *7*(7), 2745–2788. doi:10.3390/ijerph7072745.

Gokbulut, C., & Mckellar, Q. (2018). Veterinary Parasitology Anthelmintic drugs used in equine species. *Veterinary Parasitology*, *261*, 27–52. doi:10.1016/j.vetpar.2018.08.002.

Hamilton, G., Sahoo, S., Kamila, S., Singh, N., Kaur, N., Hylanda, B., & Callan, J. (2015). Optical probes for the detection of protons, and alkali and alkaline earth metal cations. *The Royal Society of Chemistry*, *44*, 4415–4432. doi: 10.1039/c4cs00365a.

Horton, J. (2000). Albendazole: a review of anthelmintic efficacy and safety in humans. *Parasitology*, *121*, 113-132. doi:10.1017/S0031182000007290.

Ismail, P., Yousif, A., & Harki, H. (2017). Alterations of Some Heavy Metals and race Elements Levels in Breast. *Journal of Medicinal Chemistry* (Los Angeles), *7*(1), 758–760. doi: 10.4172/2161-0444.1000426.

Kale, S., Pawar, R., & S.Kale, A. (2016). Imidazole, Its Derivatives & Their Importance: A Review. *International Journal of Current Advanced Research, 5* (5), 906–911.

Kaper, J., Nataro, J., & Mobley, H. (2004). Pathogenic Escherichia Coli. *Nature, 2,* 123-140. doi: 10.1038/nrmicro818.

Kitamura, S., Morisseau, C., Inceoglu, B., Kamita, S., Nicola, G., Nyegue, M., & Hammock, B. (2015). Potent Natural Soluble Epoxide Hydrolase Inhibitors from Pentadiplandra brazzeana Baillon : Synthesis, Quantification, and Measurement of Biological Activities In Vitro and In Vivo, *PLoSONE 10*(2), 1-16. doi: org/10.1371/journal.pone.0117438.

Lakowicz, J. (2006). *Principles of Fluorescence Spectroscopy* (Third Edit). USA, Springer.

Loo, R., Milané, C., Sonneveld, L., & Roos, A. (2017). New Protocol for Piperazine Production Using Homogeneously Catalyzed Alcohol Amination of Diethanolamine by a Ru-PNP Pincer Complex and the Coupling Reagent Phosphorus Pentachloride for Cyclization of Aminoethyl ethanolamine. *Paper Catalysis.*

Lv, F., Li, Z., Hu, W., & Wu, X. (2015). Small Molecules Enhance Functional O - mannosylation of Alpha-dystroglycan. *Bioorganic & Medicinal Chemistry*, *23*(24), 7661–7670. doi: 10.1016/j.bmc.2015.11.011.

Mahmoud, B. (2012). *Salmonella- a Dangerous Foodbornen Pathogen*. Croatia, InTech.

Manocha, P., Kaur, A., Anand, K., & Kumar, H. (2016). A review: Imidazole Synthesis and Its Biological Activities. *International Journal of Pharmaceutical Science and Research, 1*(7), 12-16.

Mantu, D., Antoci, V., Moldoveanu, C., Zbancioc, G., & Mangalagiu, I. (2016). Hybrid Imidazole ( benzimidazole )/ Pyridine ( quinoline ) Derivatives and Evaluation of Their Anticancer and Antimycobacterial Activity, *Journal of Enzyme Inhibition and Medicinal Chemistry, 31,* 96-103. doi:10.1080/14756366.2016.1190711.

McEwen, D. (1991). Synthesis of Aliphatic Bis ( Thioureas ) (Honors Projects). Illinois Wesleyan University, Bloomington, US.

Mei, Y., Liu, P., Wan, L., Liu, Y., Wang, L., & Wei, D. (2017). Virulence and Genomic Feature of a Virulent Klebsiella pneumoniae Sequence Type 14 Strain of Serotype K2 Harboring bla NDM-5 in China, *8*(March), *Frontiers in Microbiology*, *8*, 1-9. doi:org/10.3389/fmicb.2017.00335.

Min, X. Liu, J., Dongb, Y., Hussain, M., (2018). One-Pot Assembly towards ω - Substituted Arylbiurets from Aromatic Amines, Potassium Cyanate, and Glacial Acetic Acid, *Synthesis*, *50.* 341–348. doi:10.1055/s-0036-1590934.

Negi, D., Kumar, G., Singh, M., & Singh, N. (2017). Antibacterial Activity of Benzimidazole Derivatives : A Mini Review, *Journal of Chemistry*, *6*(3), 18–28.

Nguyen, T. (2018). *Food and Cancer: A Guide to Understanding the Secondary Causes of Cancer.* EnCognitive.com.

Pandurangan, A., Ascher, D., Thomas, S., & Blundell, T. (2017). Genomes, Structural Biology and Drug Discovery: Combating the Impacts of Mutations in Genetic Disease and Antibiotic Resistance, *portland press*, *45*(2), 303–311. doi:10.1042/BST20160422.

Panneerselvam, T., & Kumar, S. (2011). Synthesis of Novel 2-substituted Benzimidazole Derivatives as Potential Anti-microbial Agents, *Research in Biotechnology*, *2*(3), 50-57.

Ramamurthy, V., & Mondal, B. (2015). Supramolecular Photochemistry Concepts Highlighted with Select Examples. *Journal of Photochemistry & Photobiology C: Photochemistry Reviews*, *23*, 68-102. doi:10.1016/j.jphotochemrev.2015.04.002.

Romero, D., Heredia, V., Barradas, O., López, M., & Pavón, E. (2014). Synthesis of Imidazole Derivatives and Their Biological Activities. *Journal of Chemistry and Biochemistry*, *2*(2), 45–83. doi:10.15640/jcb.v2n2a3.

Rustini, R., Jamsari, J., Marlina, M., Zubir, N., & Yuliandra, Y. (2017). Antibacterial Resistance Pattern of Pseudomonas Aeruginosa Isolated from Clinical Samples at A General Hospital in Padang, West Sumatra, Indonesia, *Asian Journal of Pharmaceutical and Clinical Research*, *10*(8), 158–160. doi: 10.22159/ajpcr.2017.v10i8.18539.

Saeed, E., Sham, A., El-Tarabily, K., Abu Elsamen, F., Iratni, R., & AbuQamar, S. (2016). Chemical Control of Black Scorch Disease on Date Palm Caused by the Fungal Pathogen Thielaviopsis punctulata in United Arab Emirates. *The American Phytopathological Society*, *100*(12), 2370-2376. doi:10.1094/PDIS-05-16-0645-RE.

Salahuddin, Shaharyar, M., & Mazumder, A. (2017). Benzimidazoles: A biologically Active Compounds. *Arabian Journal of Chemistry*, *10*, 157–173.

doi:10.1016/j.arabjc.2012.07.017.

Saleh, N., Al-handawi, M., Bufaroosha, M., Assaf, K., & Nau, W. (2015). Tuning Protonation States of Tripelennamine Antihistamines by Cucurbit[7]uril. *Journal of physical organic chemistry*, *29*, 101–106. doi:10.1002/poc.3504.

Sebastian, S., Patel, H., Thennati, R. (2003). United States Patent No. US 6,603,003 B2. Retrieved from https://patents.google.com/patent/US6603003B2/en.

Shaikh, M., Mohanty, J., Bhasikuttan, A., Uzunova, V., Nau, W., & Pal, H. (2008). Salt-induced Guest Relocation From a Macrocyclic Cavity into a Biomolecular Pocket Interplay Between Cucurbit7uril and Albumin, *The royal society of chemistry*, *31*, 3681–3683. doi: 10.1039/b804381g.

Shakeel, A., Altaf, A., Qureshi, A., & Badshah, A. (2017). Thiourea Derivatives in Drug Design and Medicinal Chemistry: A Short Review, *Journal of Drug Design and Medicinal Chemistry*, *2*(1):10-20 doi:10.11648/j.jddmc.20160201.12.

Shibata, M., Yoshida, K., & Furuya, N. (1995). Electrochemical synthesis of urea on reduction of carbon dioxide with nitrate and nitrite ions using Cu-loaded gas-diffusion electrode, *Journal of Electroanalytical Chemistry*, *387*, 143-145.

Shrivastava, N., Naim, M., Alam, M., Nawaz, F., Ahmed, S., & Ozair Alam, O. (2017). Benzimidazole Scaffold as Anticancer Agent: Synthetic Approaches and Structure–Activity Relationship, *Archiv der Pharmazie, 350,* 1–80. doi:10.1002/ardp.201700040.

Shumilova, T. A., Tobias, R., Lang, H., & Kataev, E. A. (2018). Straightforward Design of Fluorescent Receptors for Sulfate : Study of Non-Covalent Interactions Contributing to Host – Guest Formation. *Chemistry a European Journal Communication, 24*, 1500–1504. doi: org/10.1002/chem.201704098

Sikka1, P., Sahu1, J., Mishra, A., & Hashim, S. (2015). Role of Aryl Urea Containing Compounds in Medicinal Chemistry. *Medicinal Chemistry*, *5*(11), 479–483. doi:10.4172/2161-0444.1000305.

Singla, P., Luxami. V., & Paul, K. (2014). Benzimidazole-biologically Attractive Scaffold For Protein Kinase Inhibitors Prinka, *The Royal Society of Chemistry*, *4*, 12422–12440. doi:10.1039/c3ra46304d.

Soni, B. (2014). A short review on potential activities of benzimidazole derivatives. *PharmaTutor*, *2*(8), 110–118.

Srestha, N., Banerjee, J., & Srivastava, S. (2014). A Review on Chemistry and Biological Significance of Benzimidaole Nucleus, *Journal Of Pharmacy*, *4*(12), 28–41.

Valeur, B., Santos, M. (2001). *Molecular Fluorescence Principles and Applications* (2nd Ed.). France, Wiley-VCH .

Vardhan, D., Kumara, H., Sridhara, M., & Gowda, D. (2017). Urea/thiourea Derivatives of Gly/Pro Conjugated 2,3-dichlorophenyl Piperazine As Potent Anti-inflammatory Agents: SAR studies. *Indian Journal of Chemisty, 56B*(11), 1207–1211.

Wagner, B. (2009). The Use of Coumarins as Environmentally-Sensitive Fluorescent Probes of Heterogeneous Inclusion Systems. *Molecules, 14*, 210–237. doi:10.3390/molecules14010210.

Wallach, O., & Schulze, E. (1881). Ueber Basen der Oxalsäurereihe. *Berichte Der Deutschen Chemischen Gesellschaft, 14*(1), 420–428. doi:10.1002/cber.18810140195 .

Wang, L., Kofler, M., Brosch, G., Melesina, J., Sippl, W., Martinez, E., & Easmon, J.(2015).2-Benzazolyl-4-Piperazin1Ylsulfonylbenzenecarbohydroxamic Acidsas Novel Selective Histone Deacetylase-6 Inhibitors with Antiproliferative Activity. *PLoS ONE, 10* (12), 1–22. doi:10.1371/journal.pone.0134556.

Woods SE, Lieberman MT, Lebreton F, Trowel E, de la Fuente-Nu´ñez C, Dzink-Fox J, et al. (2017) Characterization of Multi-Drug Resistant Enterococcus faecalis Isolated from Cephalic Recording Chambers in Research Macaques (Macaca spp.). *PLoS ONE, 12*(1), 1-20. doi:10.1371/journal.pone.0169293.

Wright, J. (1951). The chemistry of the benzimidazoles. *The Royal Socity of Chemistry, 48* (3), 397-541. doi: 101.1021/cr60151a002.

Wöhler. (1828). Ueber künstliche Bildung des Harnstoffe. *Pogg Ann Phys Chem, 88* (2), 253-256. doi:10.1002/andp.18280880206.

Zhao, J., Li, Z., Yan, S., Xu, S., Wang, M., Fu, B., & Zhang, Z. (2016). Pd/C Catalyzed Carbonylation of Azides in the Presence of Amines. *Organic Letters, 18*(8), 1736−1739. doi:10.1021/acs.orglett.6b00381.

Zwart, P., Verwer, M., Vries, G., Hermandies-Nijhof, E., & Vries, H. (1973). Fungal infection of the eyes of the snake Epicrates chenchria maurus : Enucleation under Halothane narcosis. *Journal of Small Animal Practice, 14*, 773–779.

Zhu, J., Wu, C., Li, X., Wu, G., Xie, S., Hu, Q., … Hong, X. (2013). Synthesis, Biological Evaluation and Molecular Modeling of Substituted 2-aminobenzimidazoles as Novel Inhibitors of Acetylcholinesterase and Butyrylcholinesterase. *Bioorganic & Medicinal Chemistry, 21*(14), 4218-4224. doi:10.1016/j.bmc.2013.05.001.

# Appendix

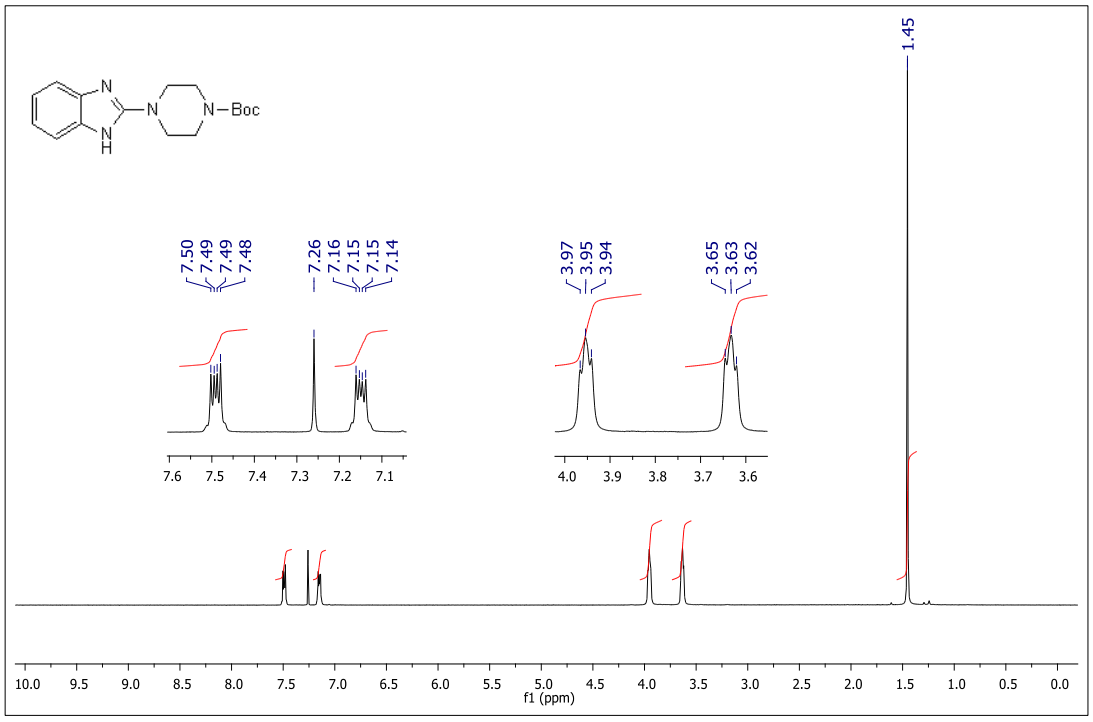


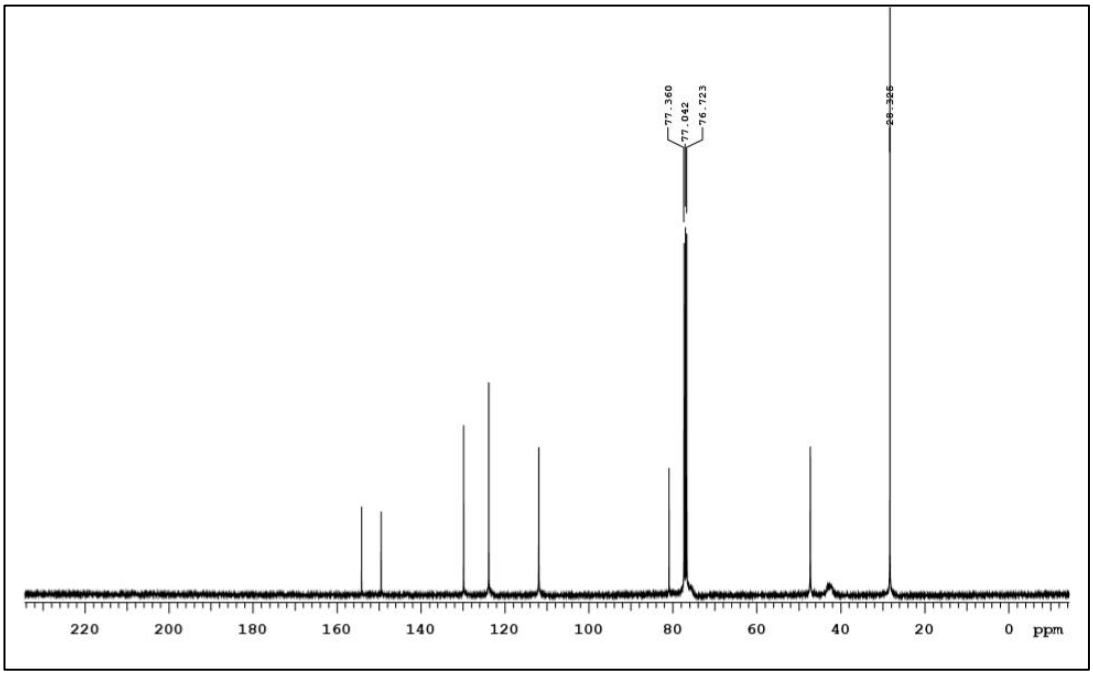


Figure 40: $^{1}H$ and $^{13}C$ spectrum and IR for 55

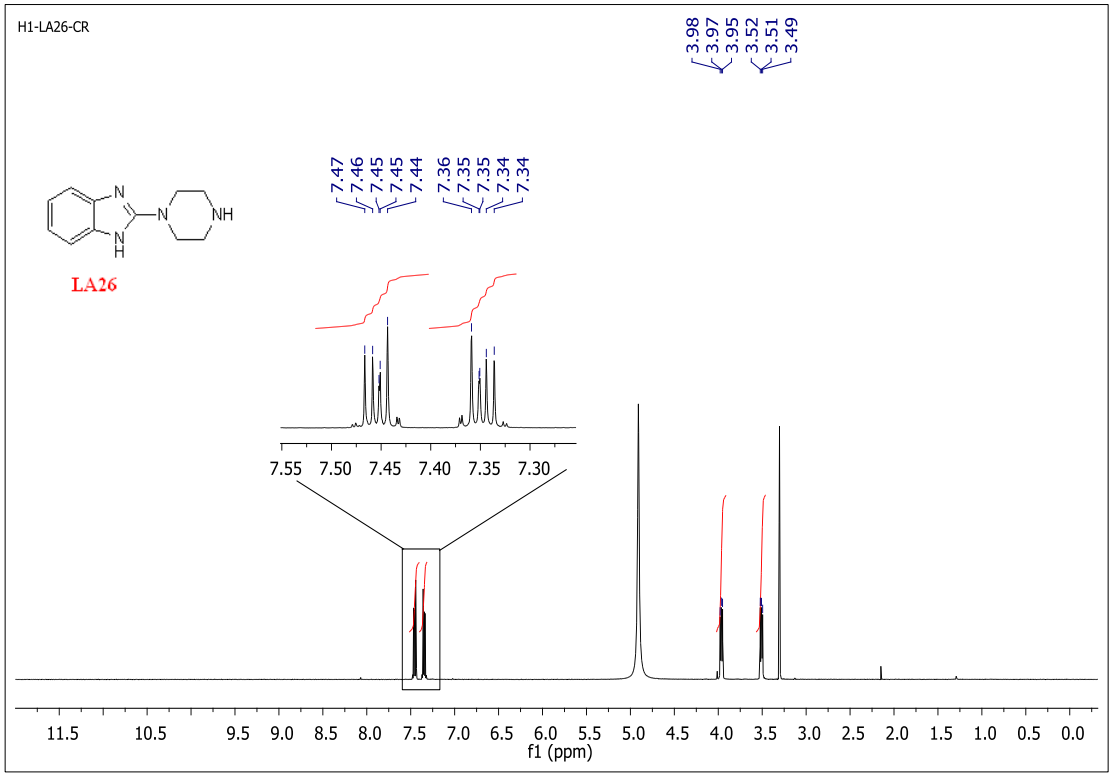


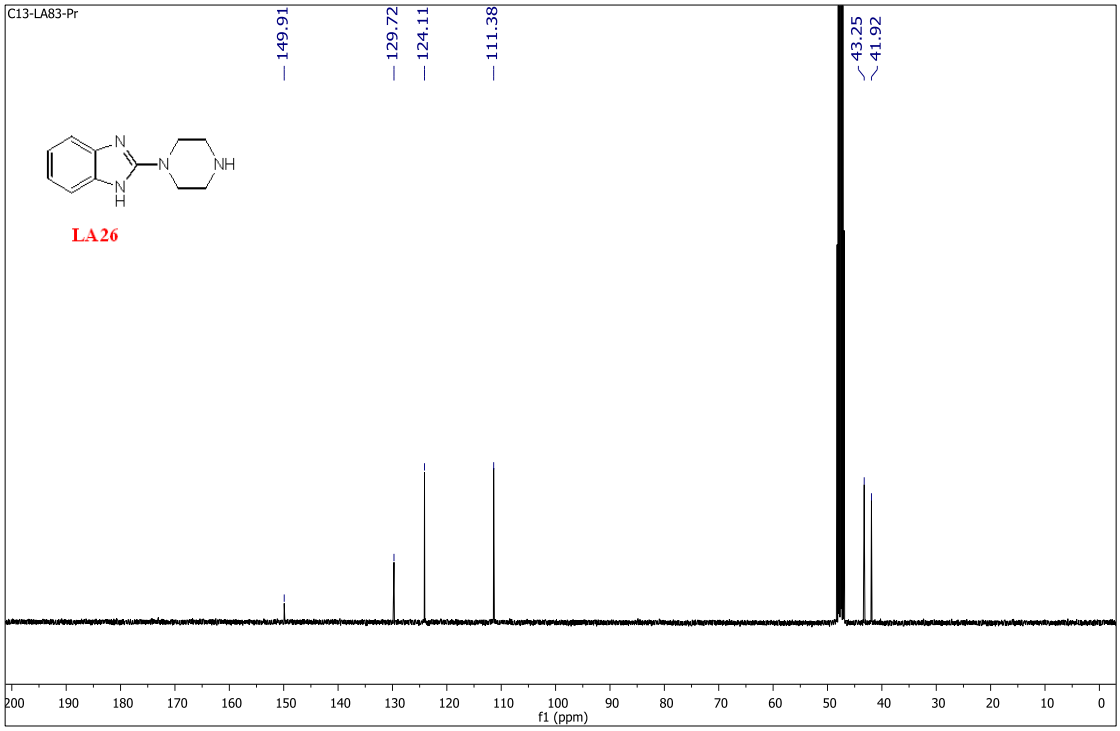


Figure 41: $^{1}H$ and $^{13}C$ spectrum for 56

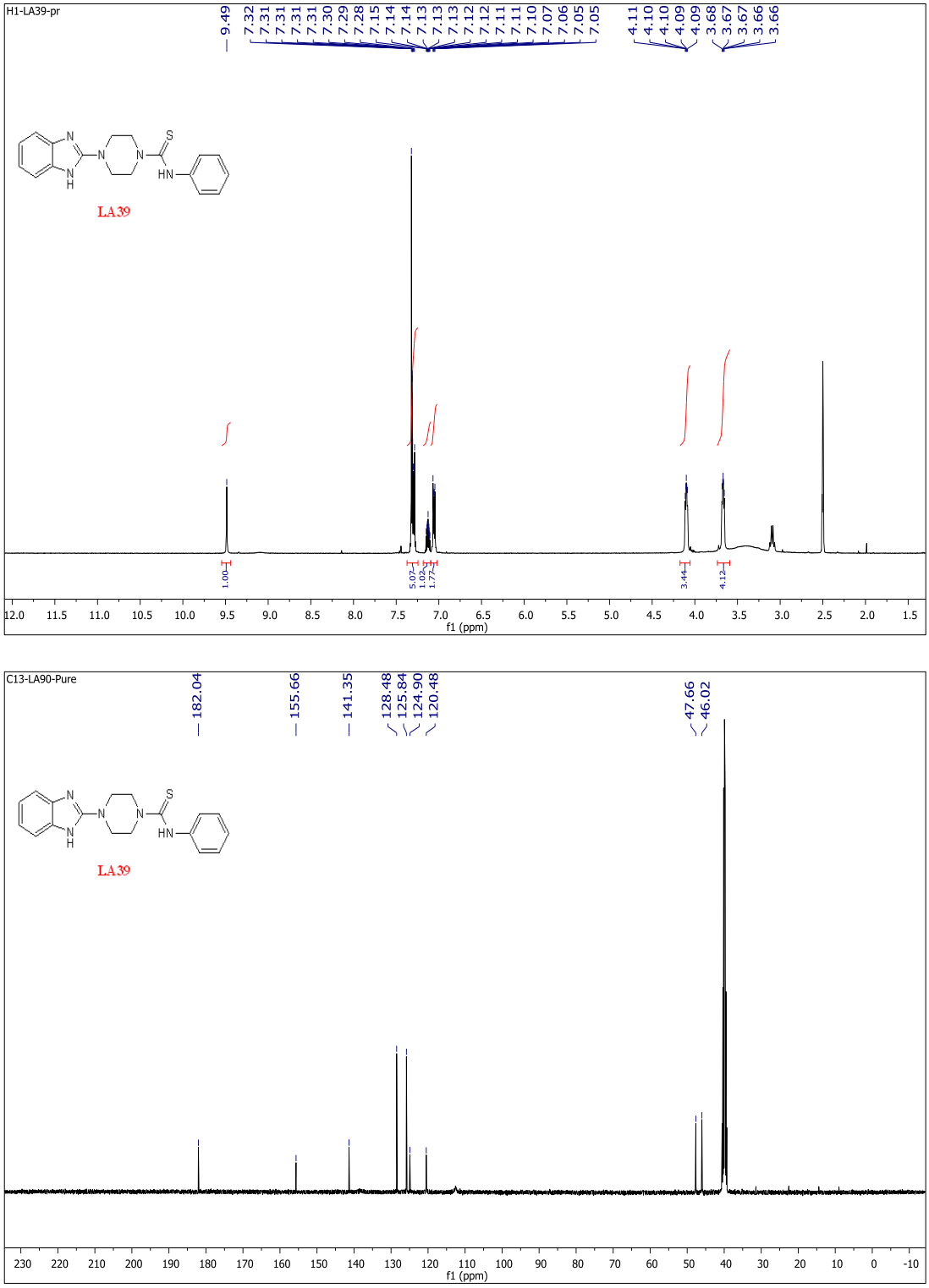


Figure 42: $^{1}H$ and $^{13}C$ spectrum for 57a

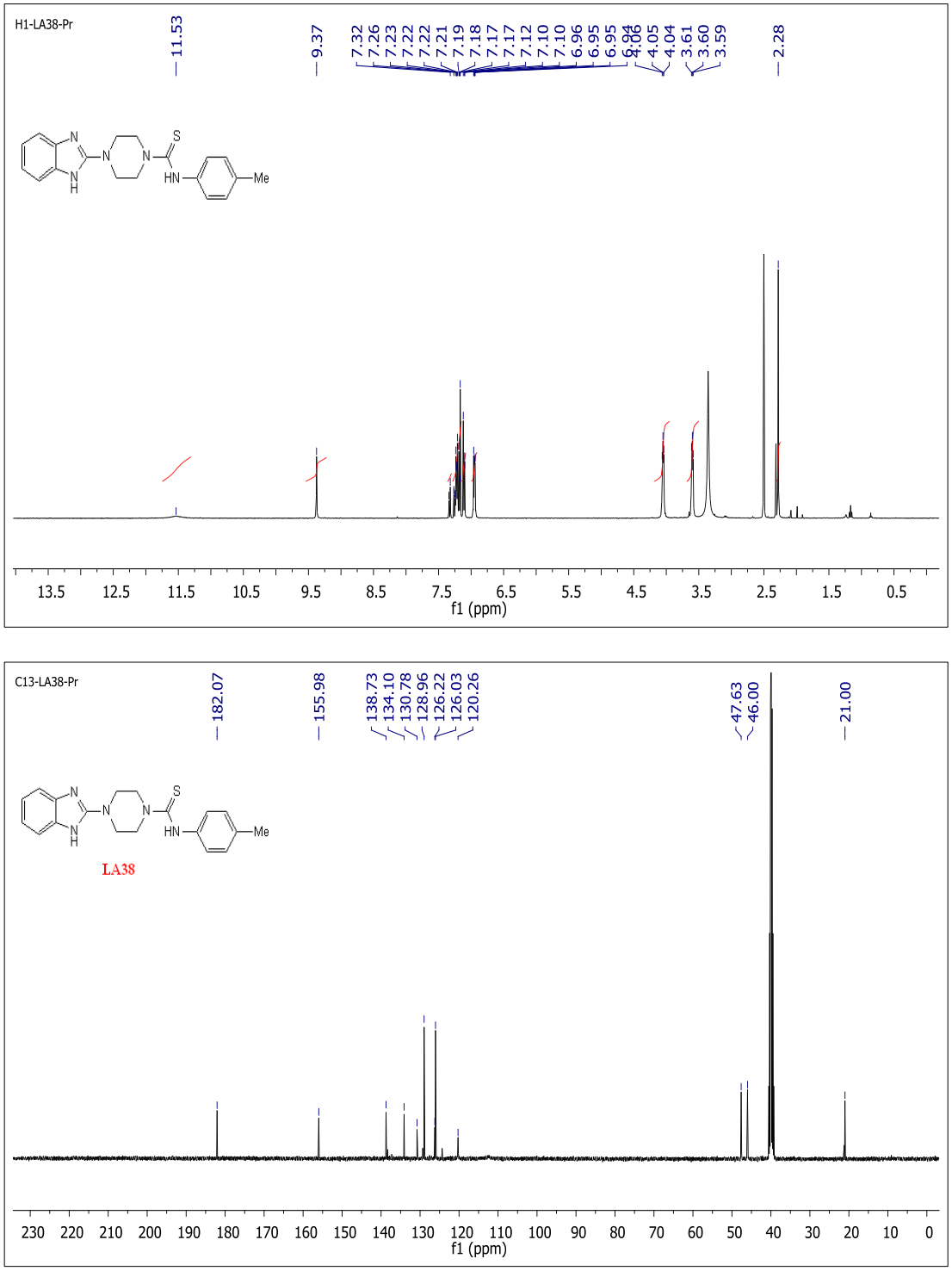


Figure 43: $^{1}H$ and $^{13}C$ spectrum for 57b

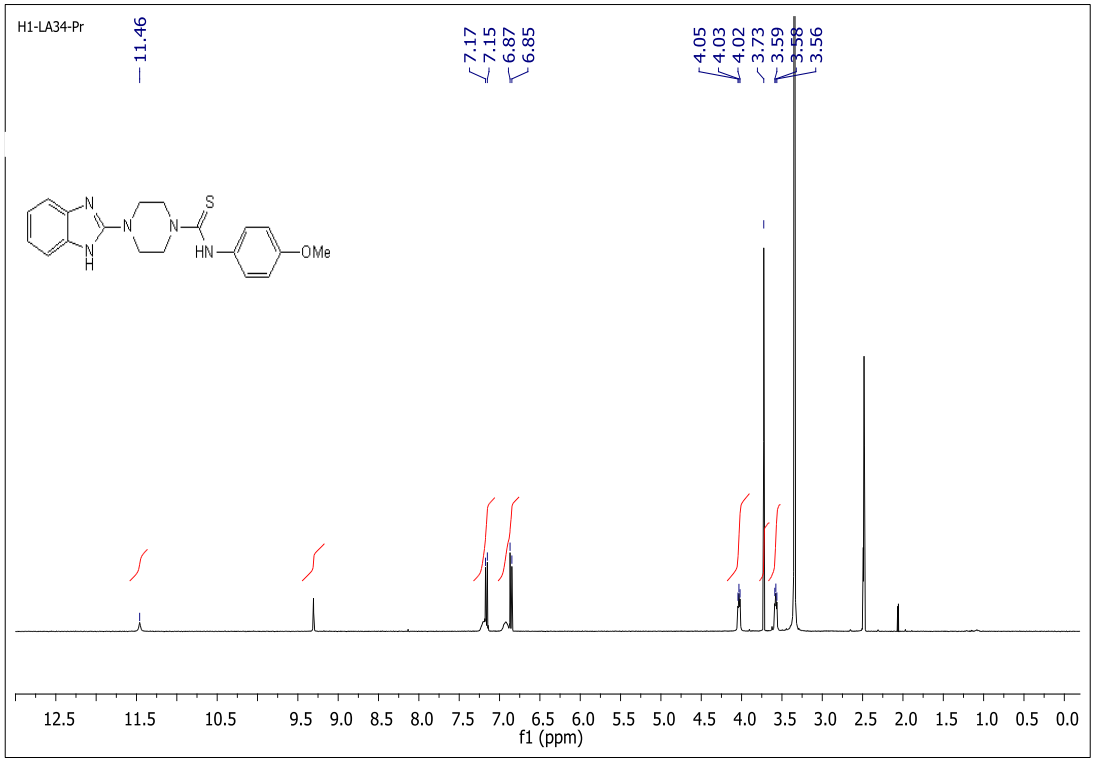


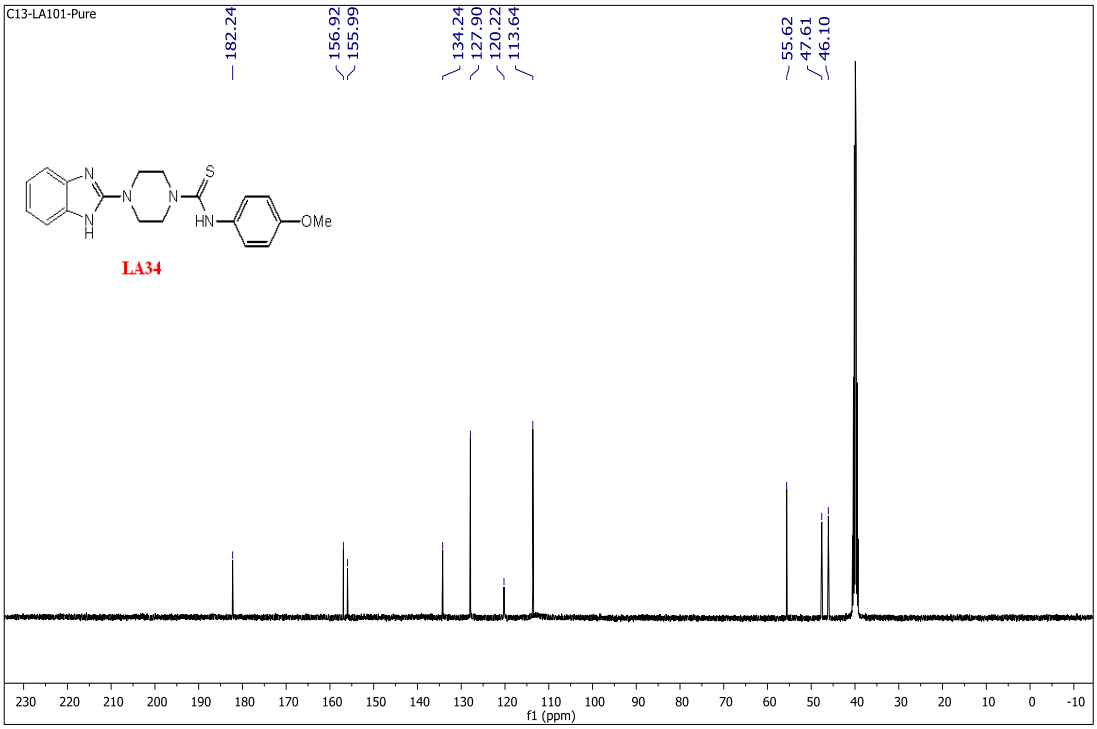


Figure 44: $^{1}H$ and $^{13}C$ spectrum for 57c

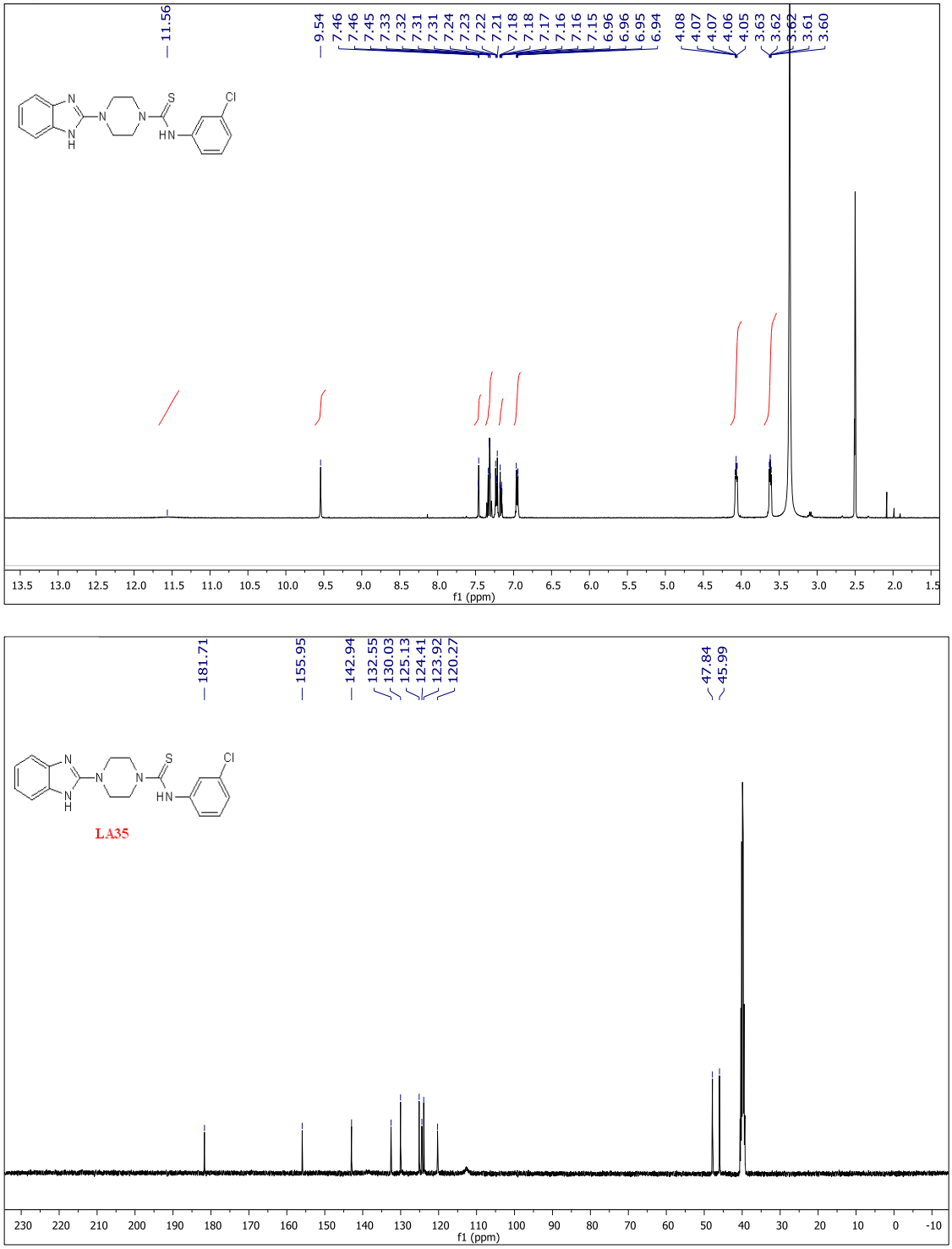


Figure 45: $^{1}H$ and $^{13}C$ spectrum for 57d

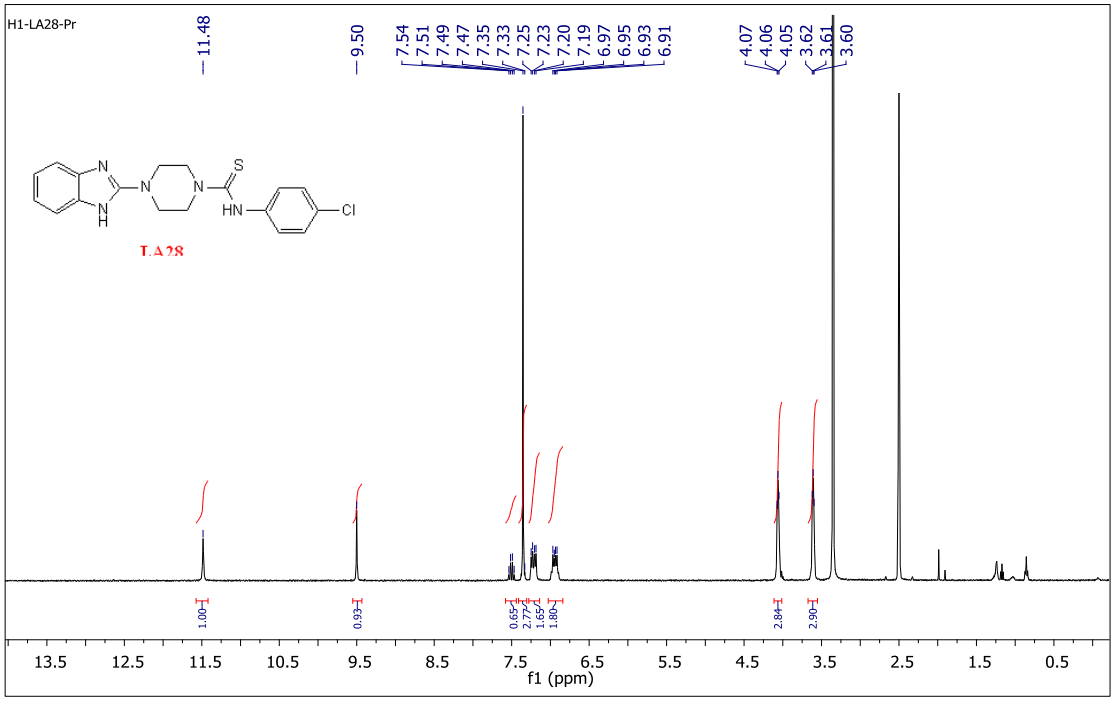


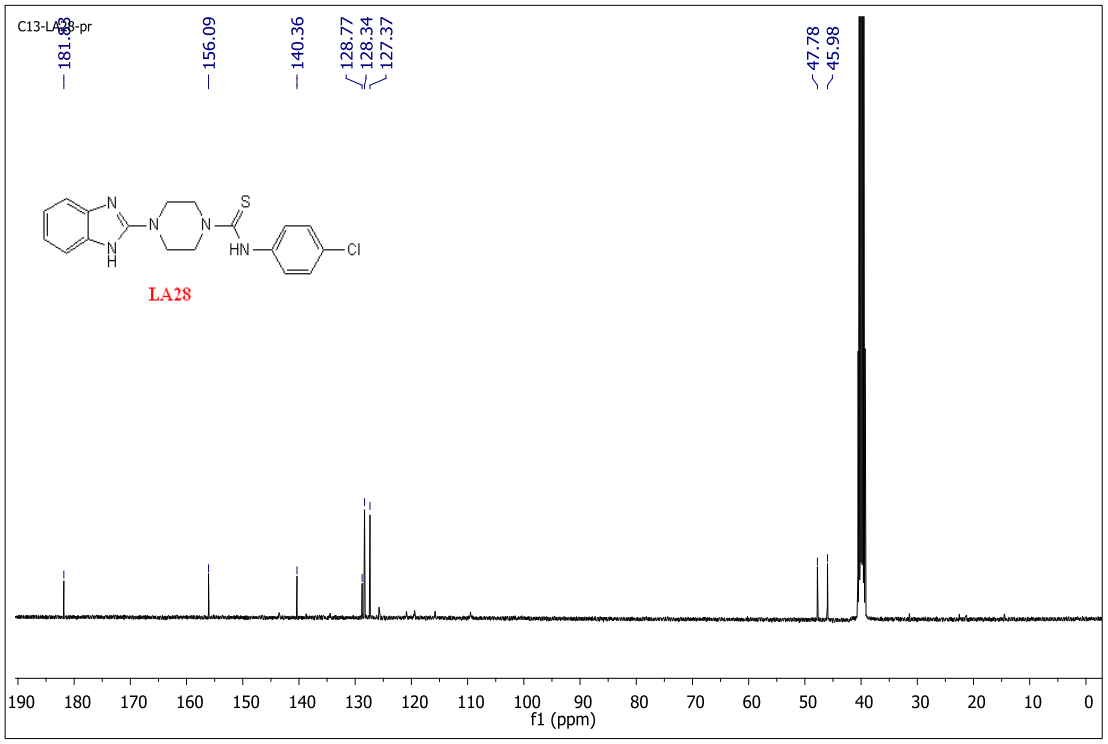


Figure 46: $^{1}H$ and $^{13}C$ spectrum for 57e

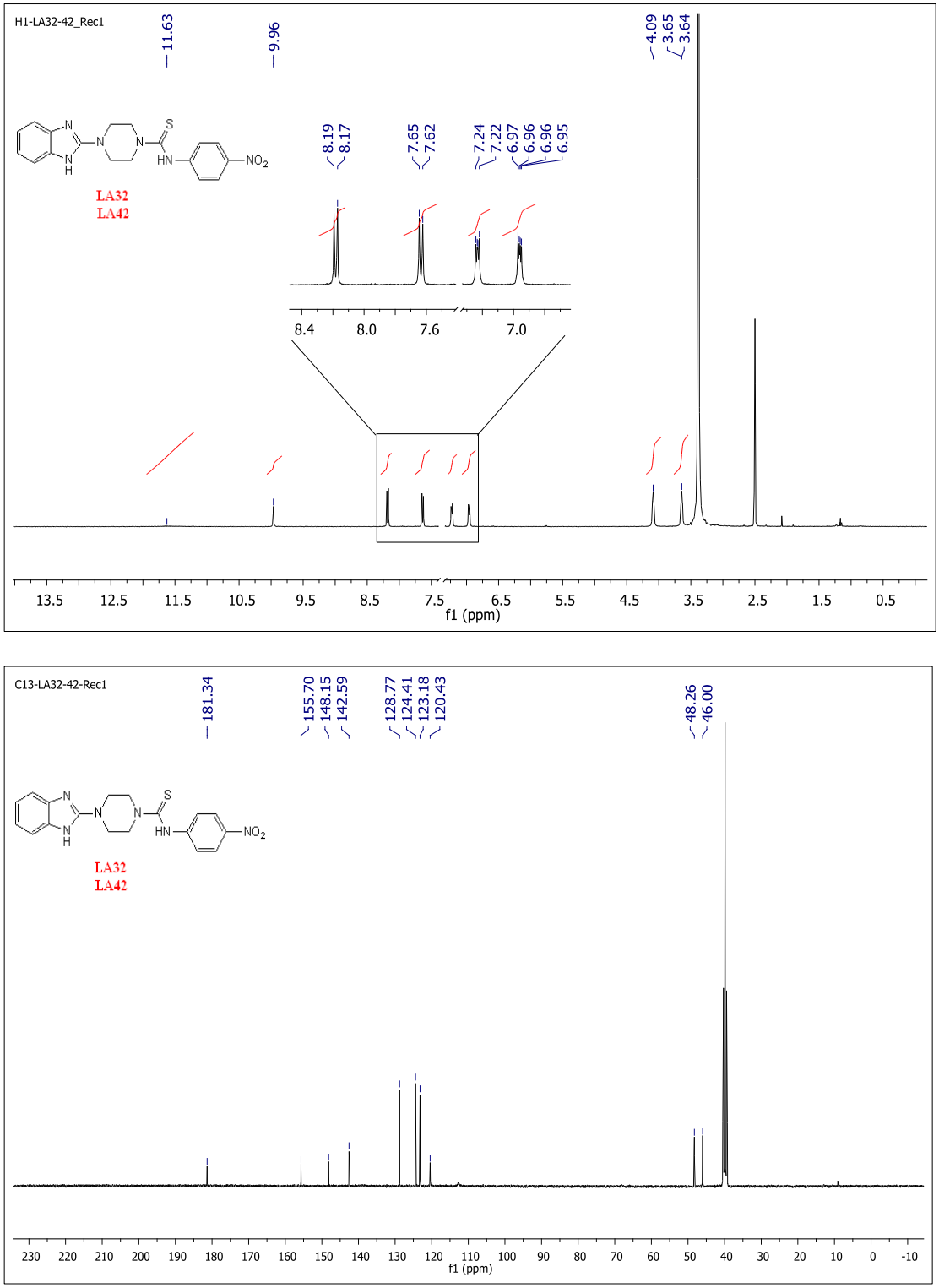


Figure 47: $^{1}H$ and $^{13}C$ spectrum for 57f

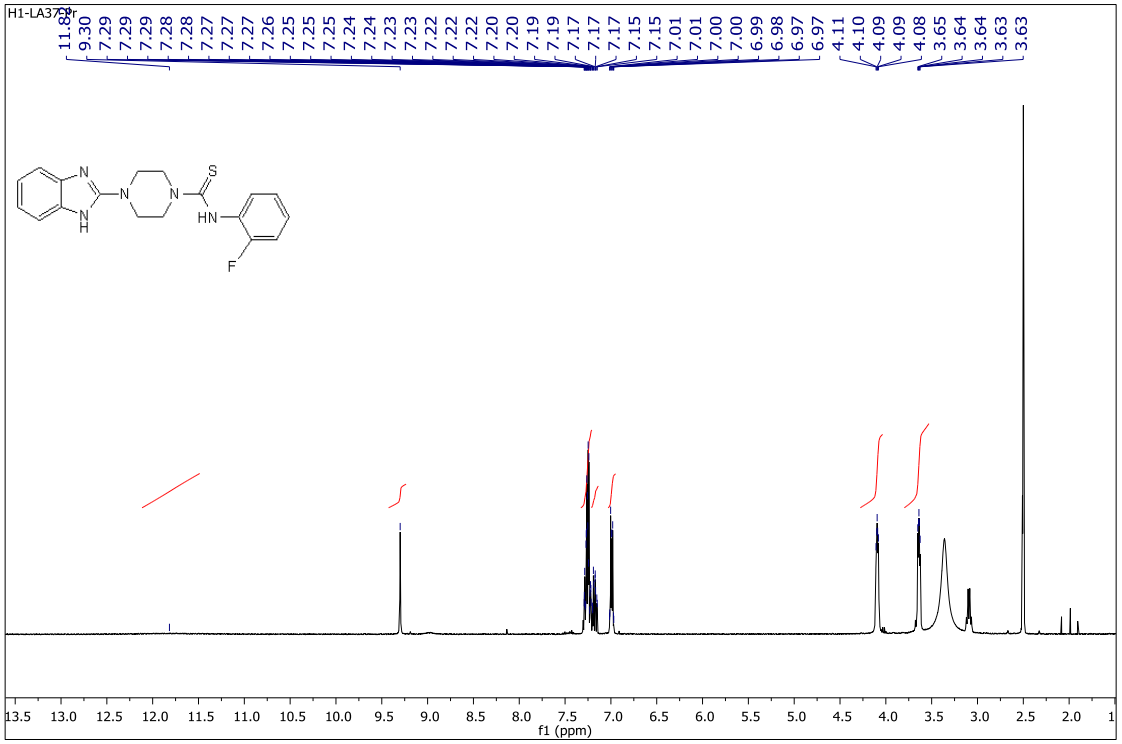


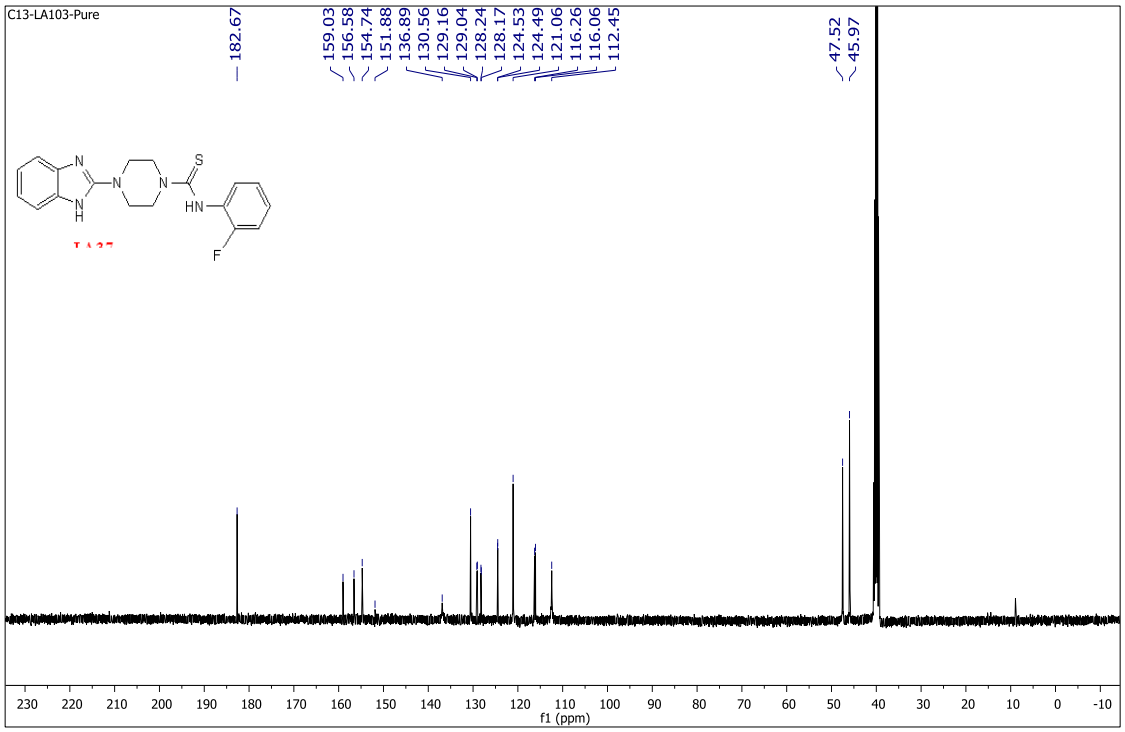


Figure 48: $^{1}H$ and $^{13}C$ spectrum for 57g

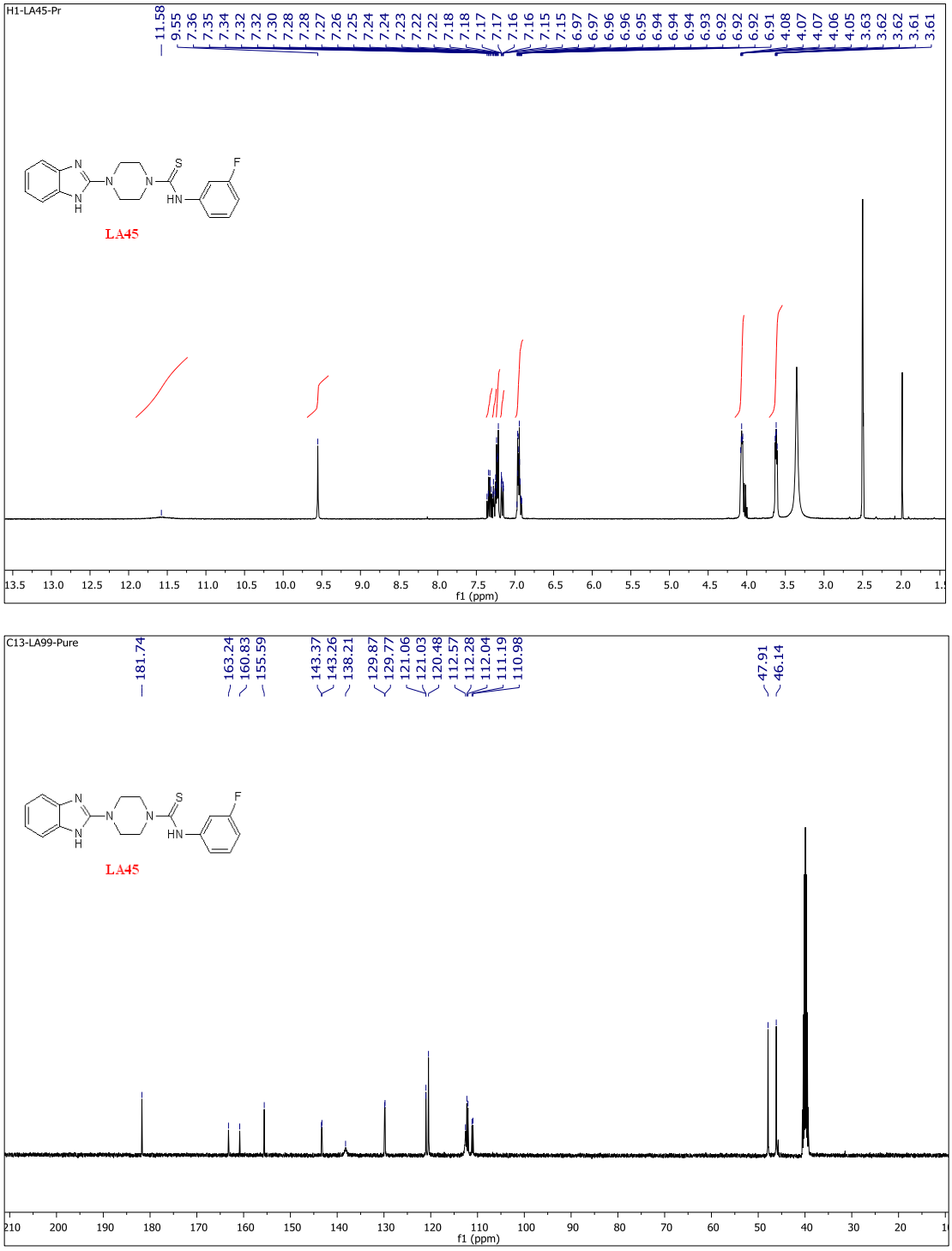


Figure 49: $^{1}H$ and $^{13}C$ spectrum for 57h

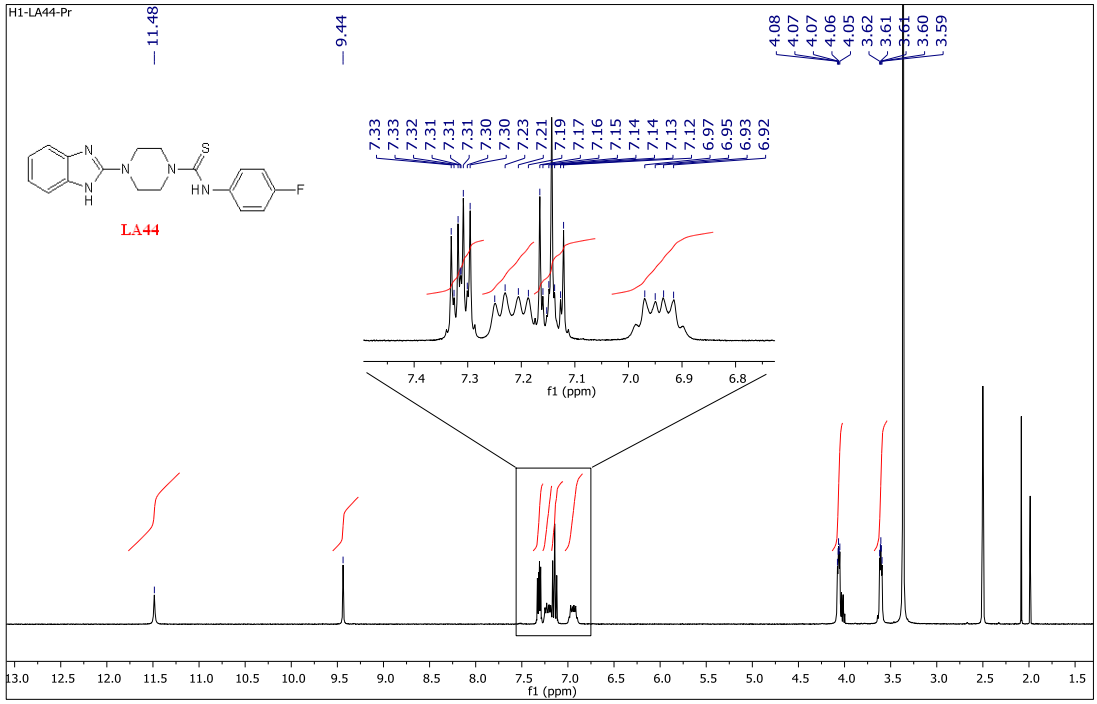


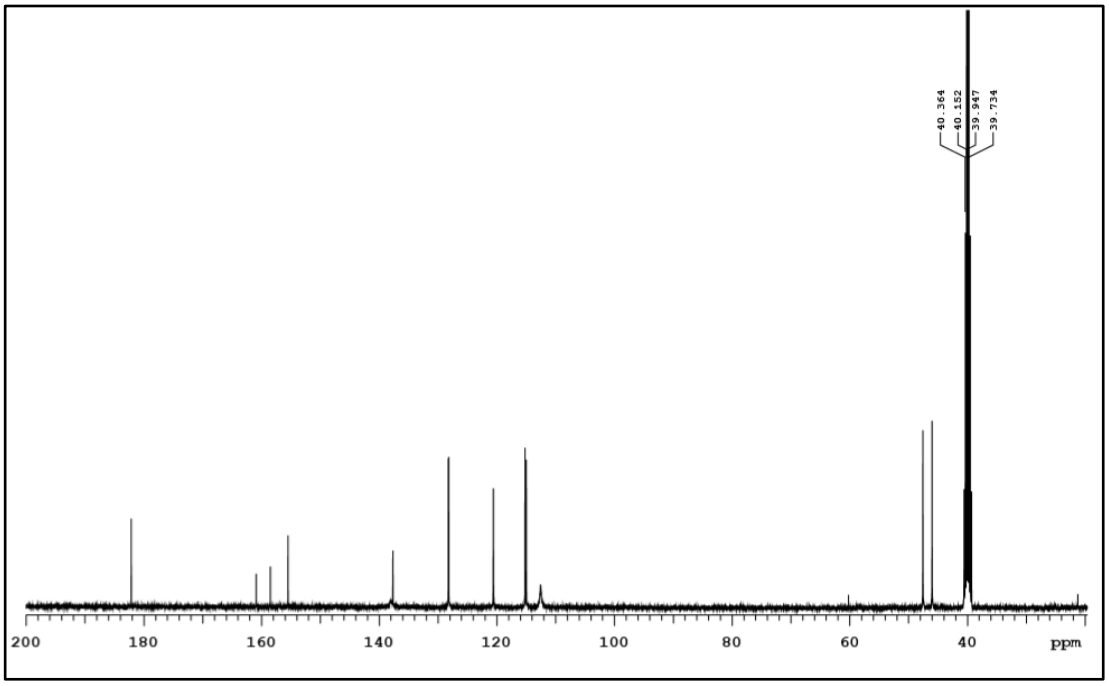


Figure 50: $^{1}H$ and $^{13}C$ spectrum for 57i

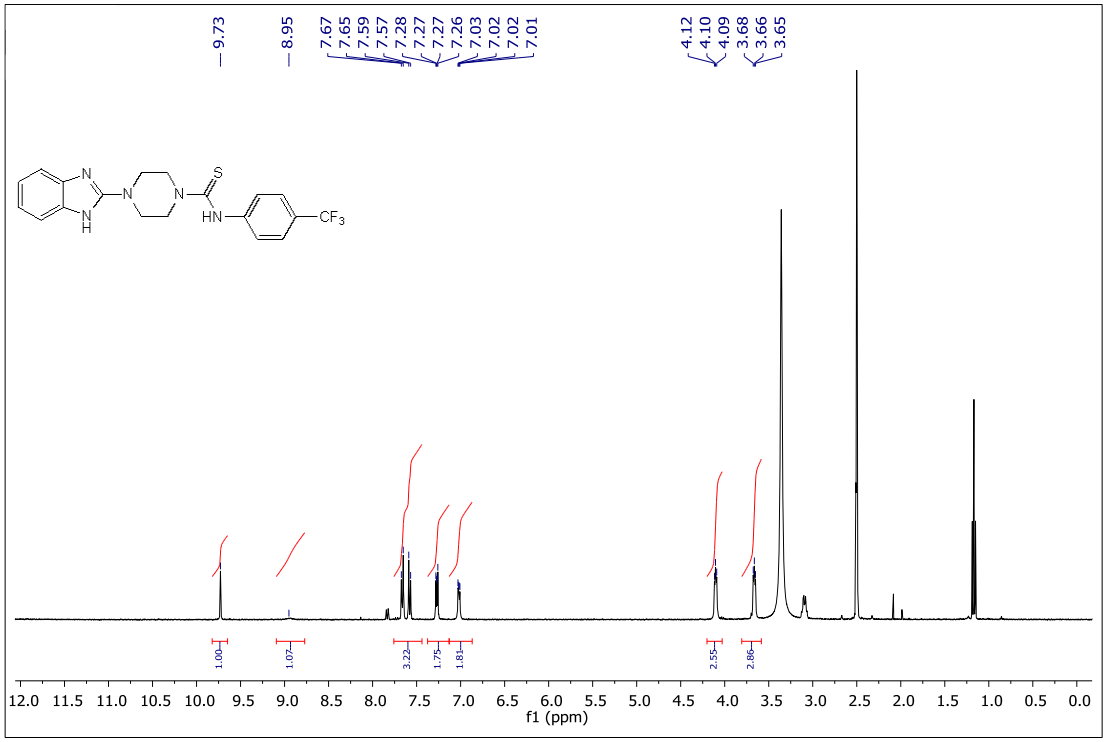


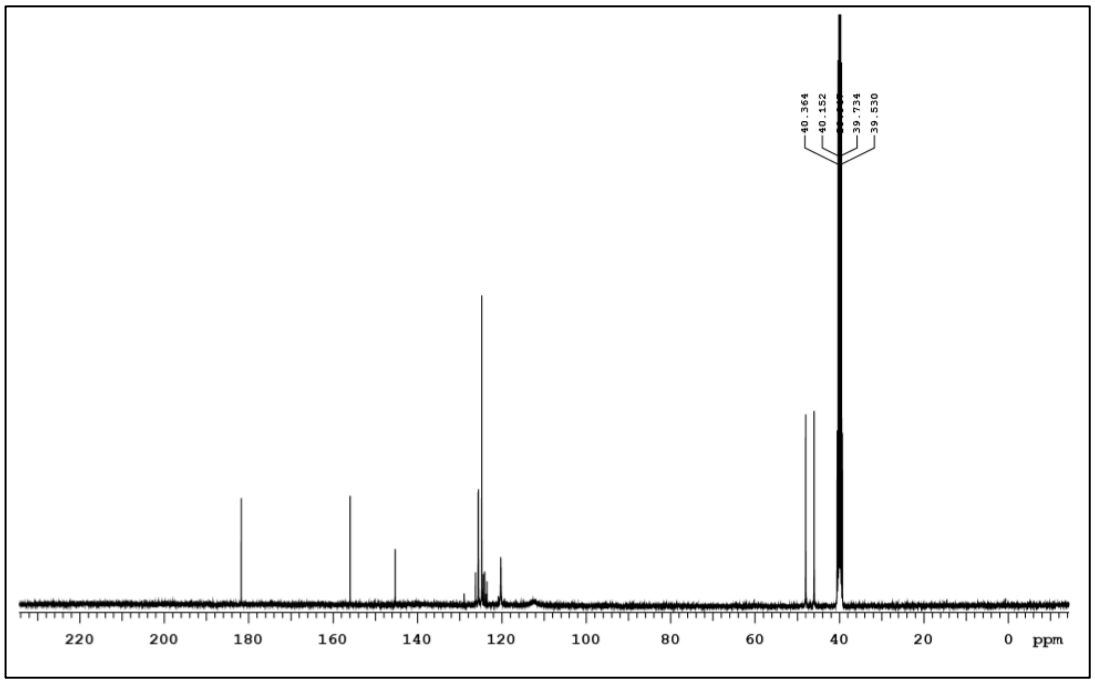


Figure 51: $^{1}H$ and $^{13}C$ spectrum for 57j

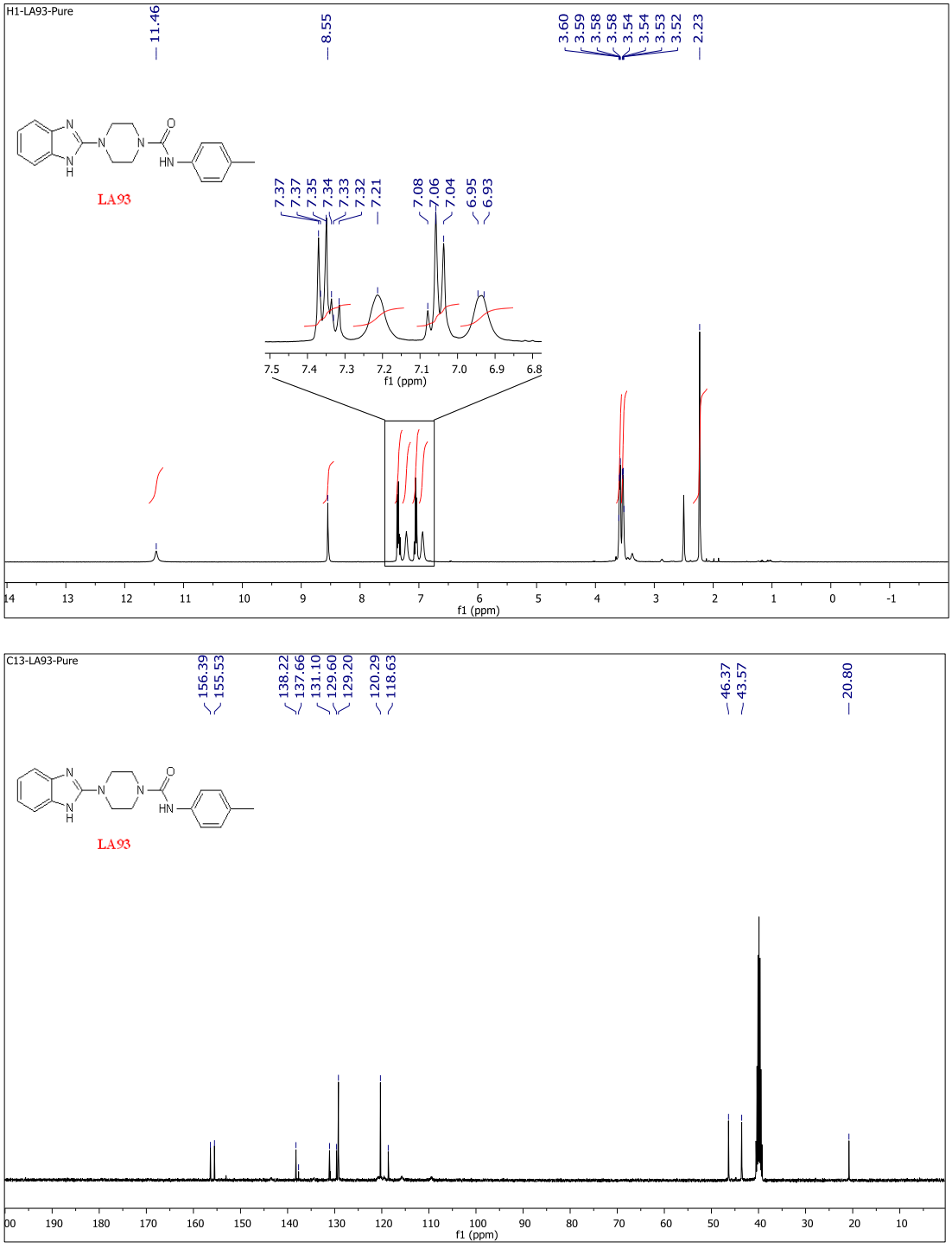


Figure 52: $^{1}H$ and $^{13}C$ spectrum for 58a

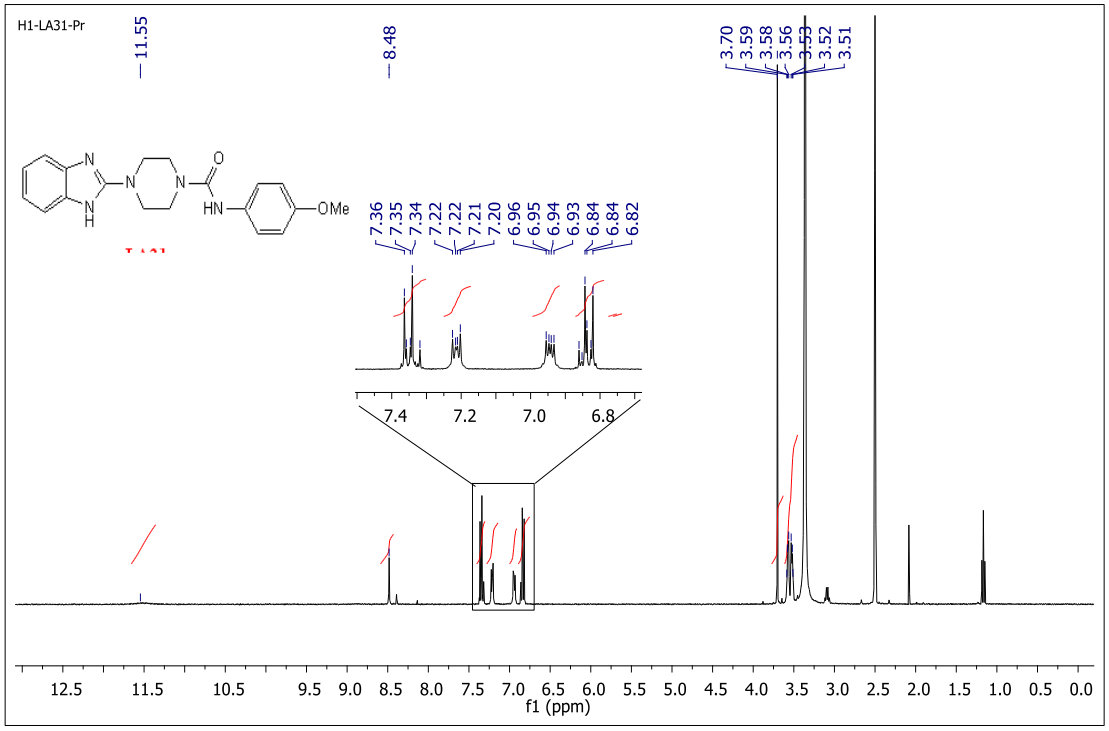


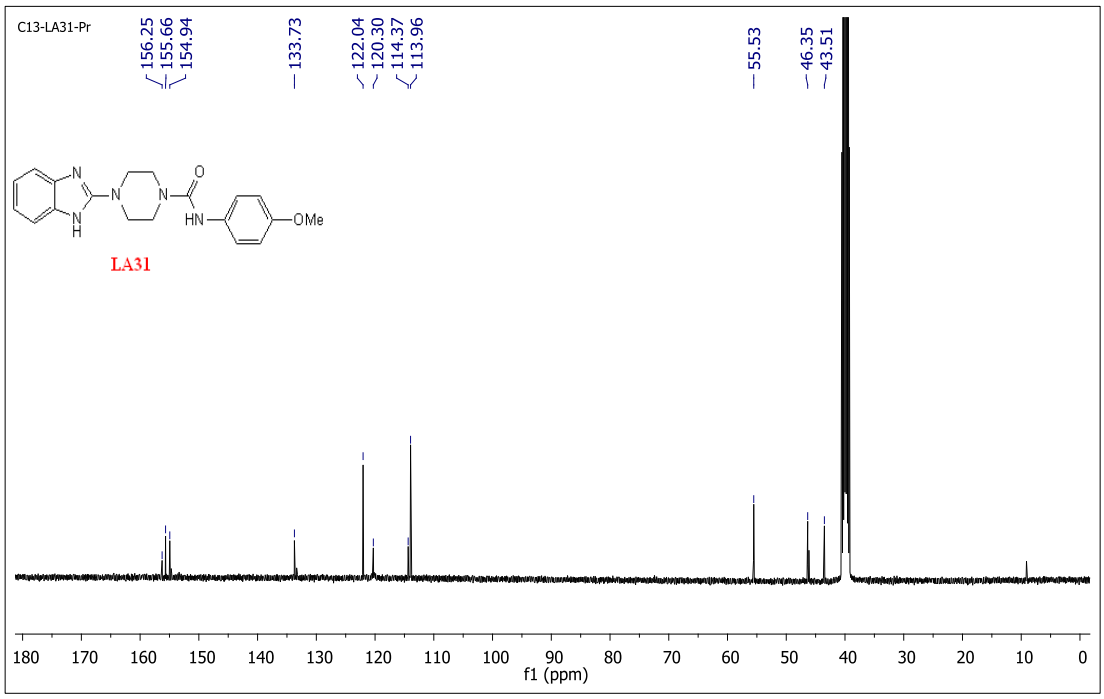


Figure 53: $^{1}H$ and $^{13}C$ spectrum for 58b

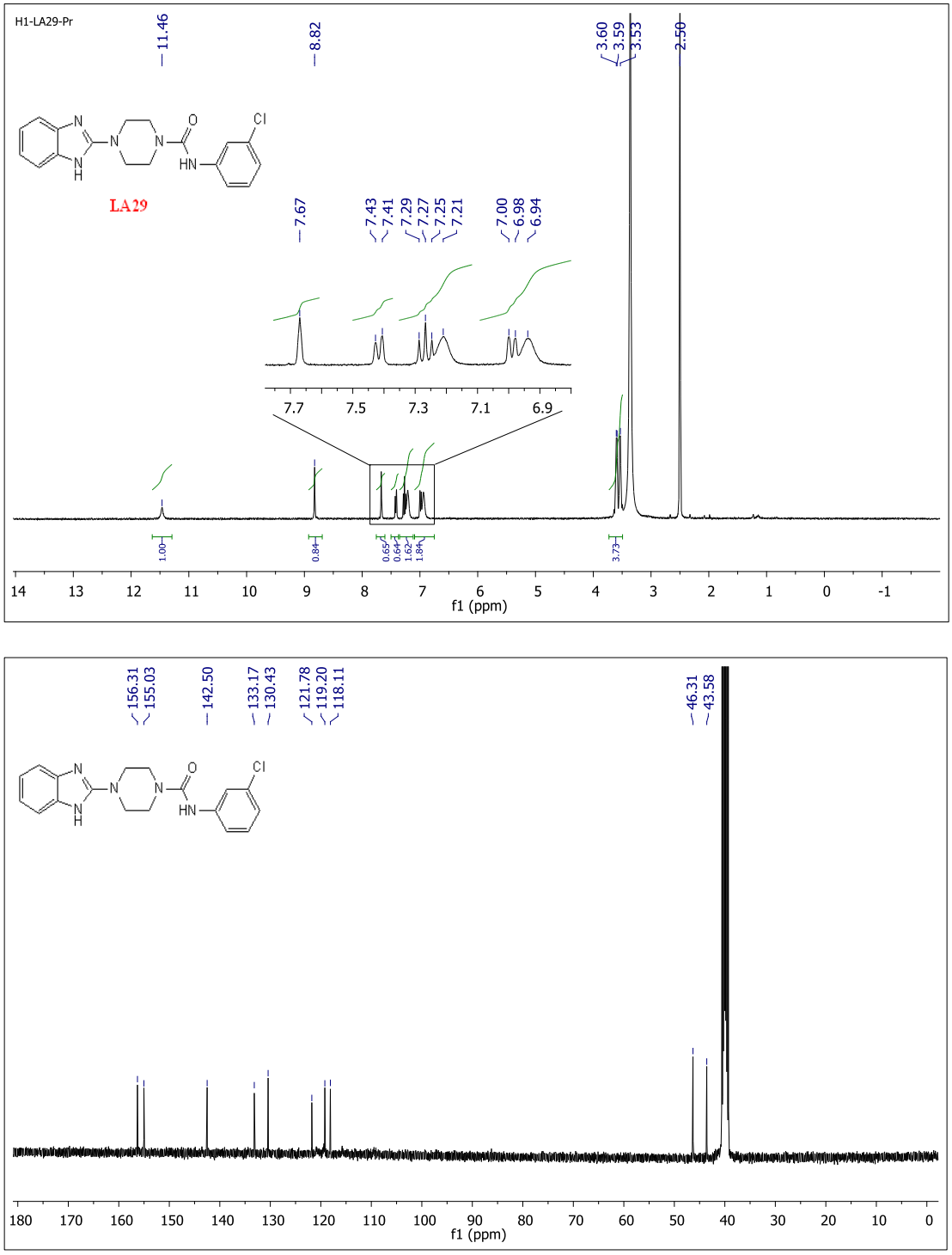


Figure 54: $^{1}H$ and $^{13}C$ spectrum for 58c

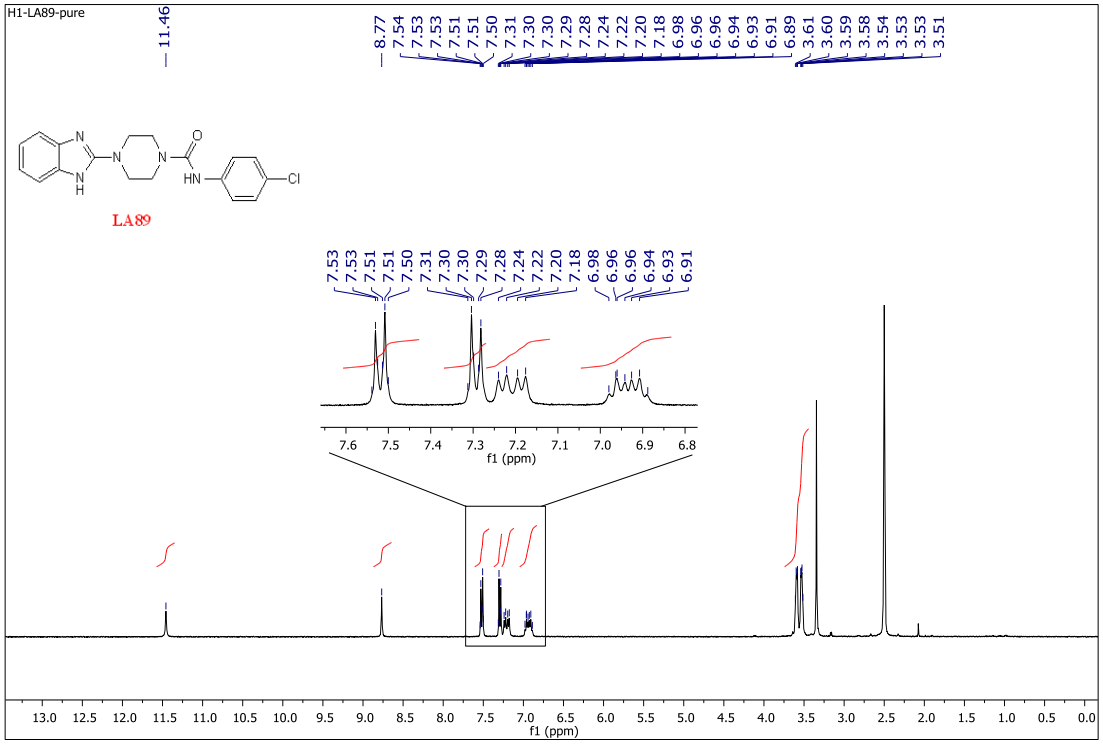


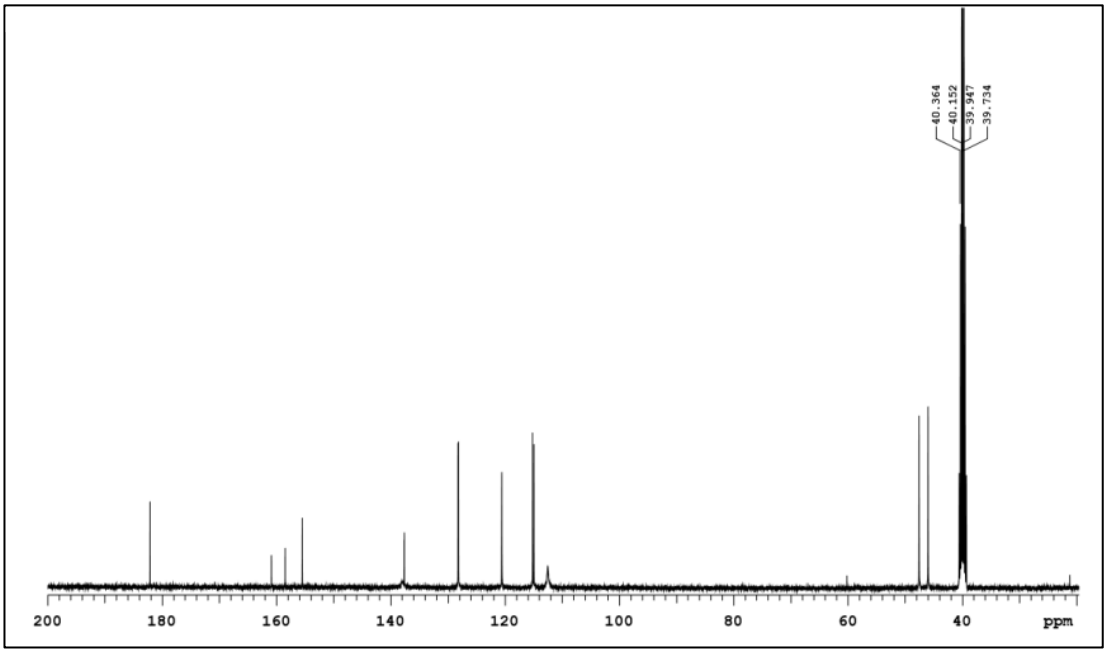


Figure 55: $^{1}H$ and $^{13}C$ spectrum for 58d

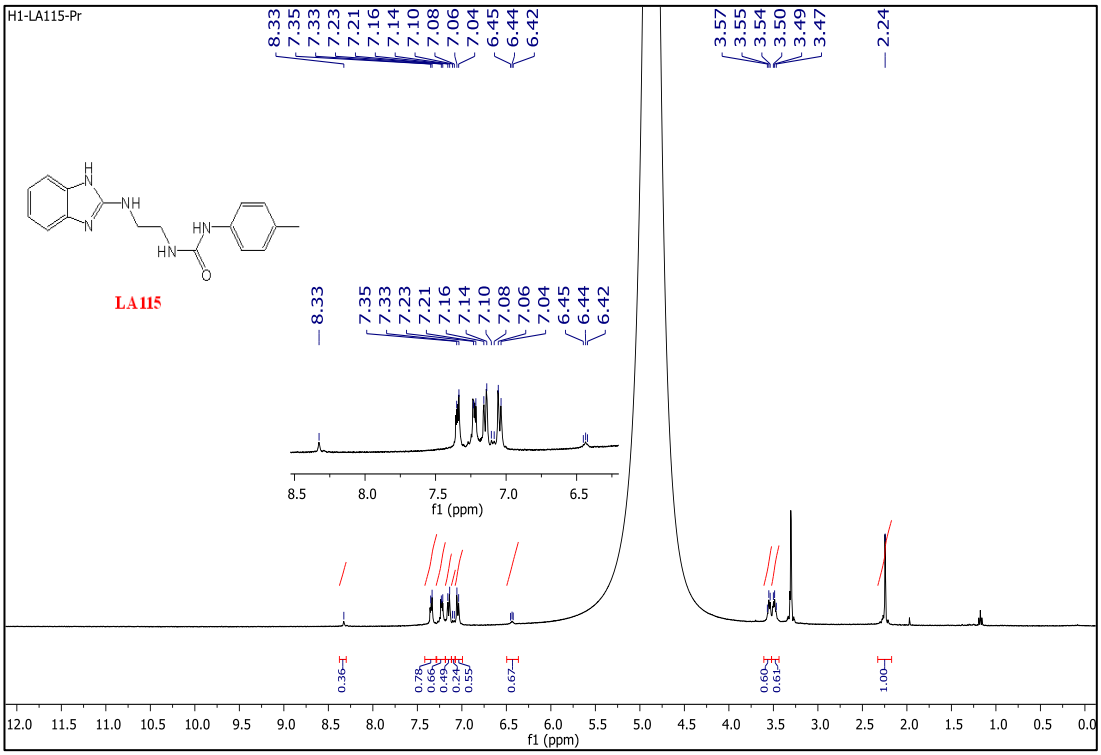


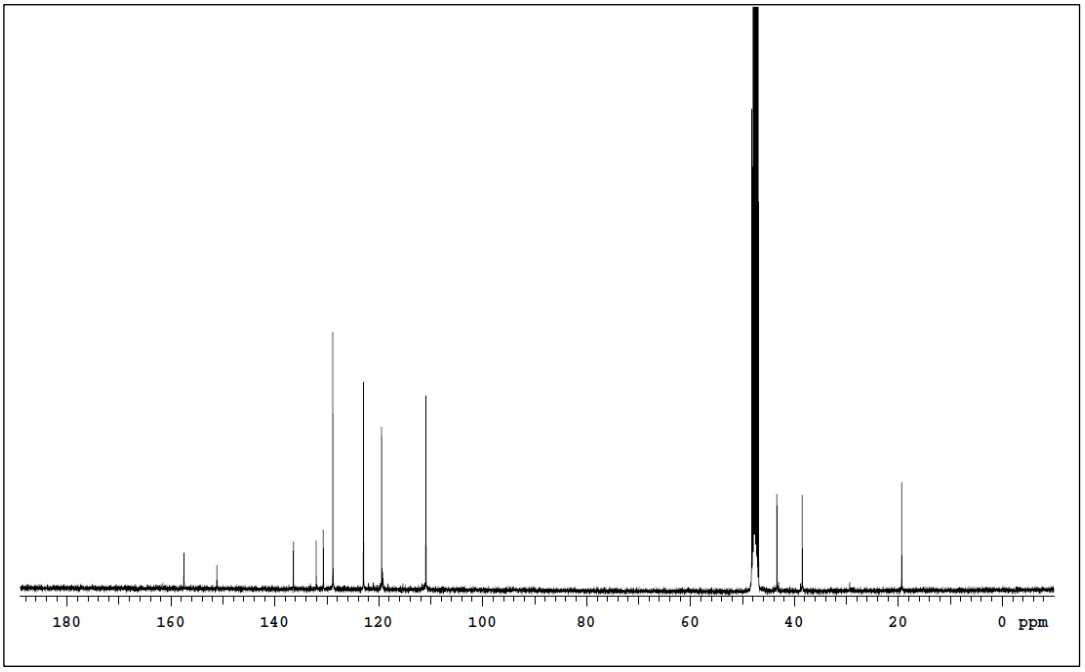


Figure 56: $^{1}H$ and $^{13}C$ spectrum for 62

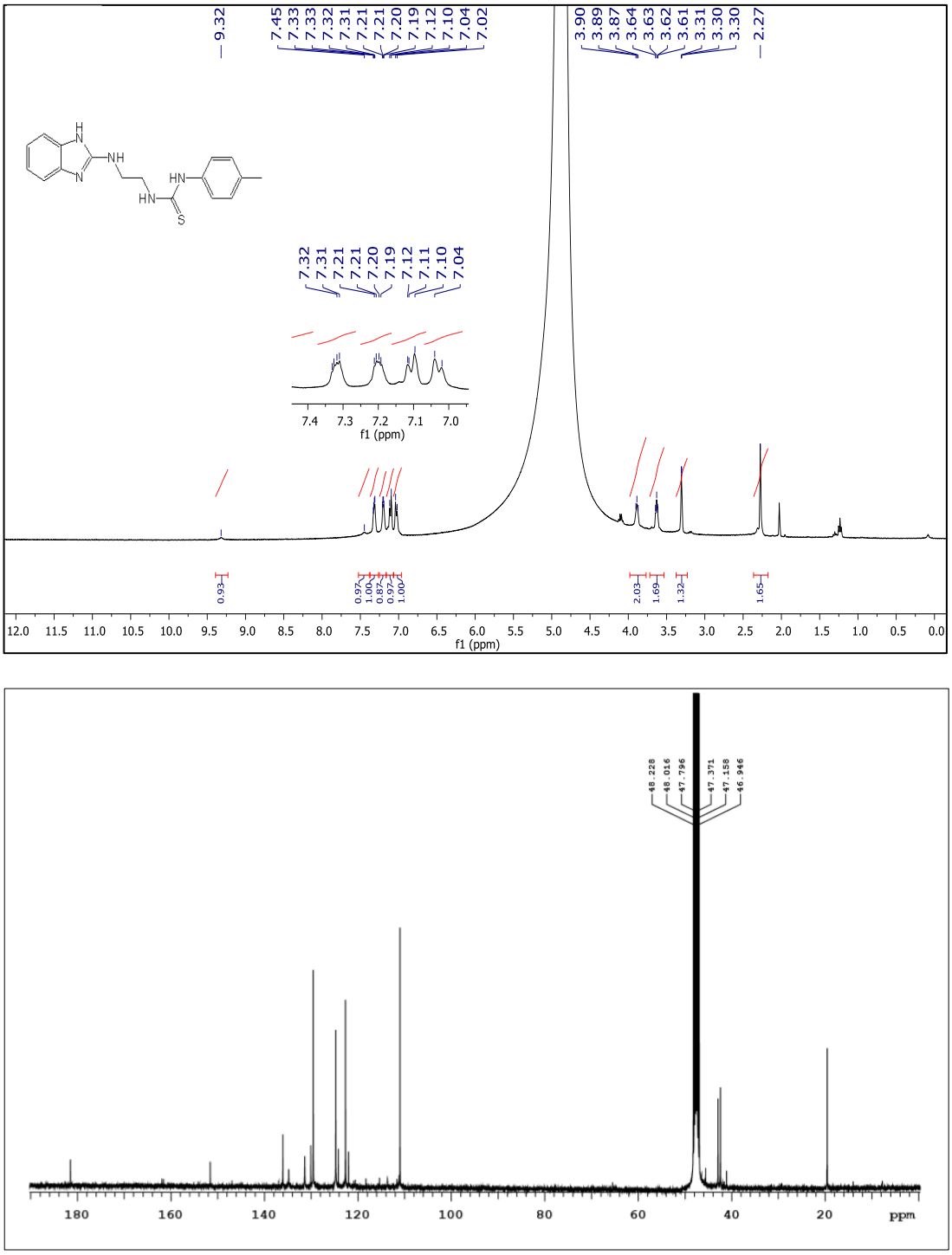


Figure 57: $^{1}H$ and $^{13}C$ spectrum for 63

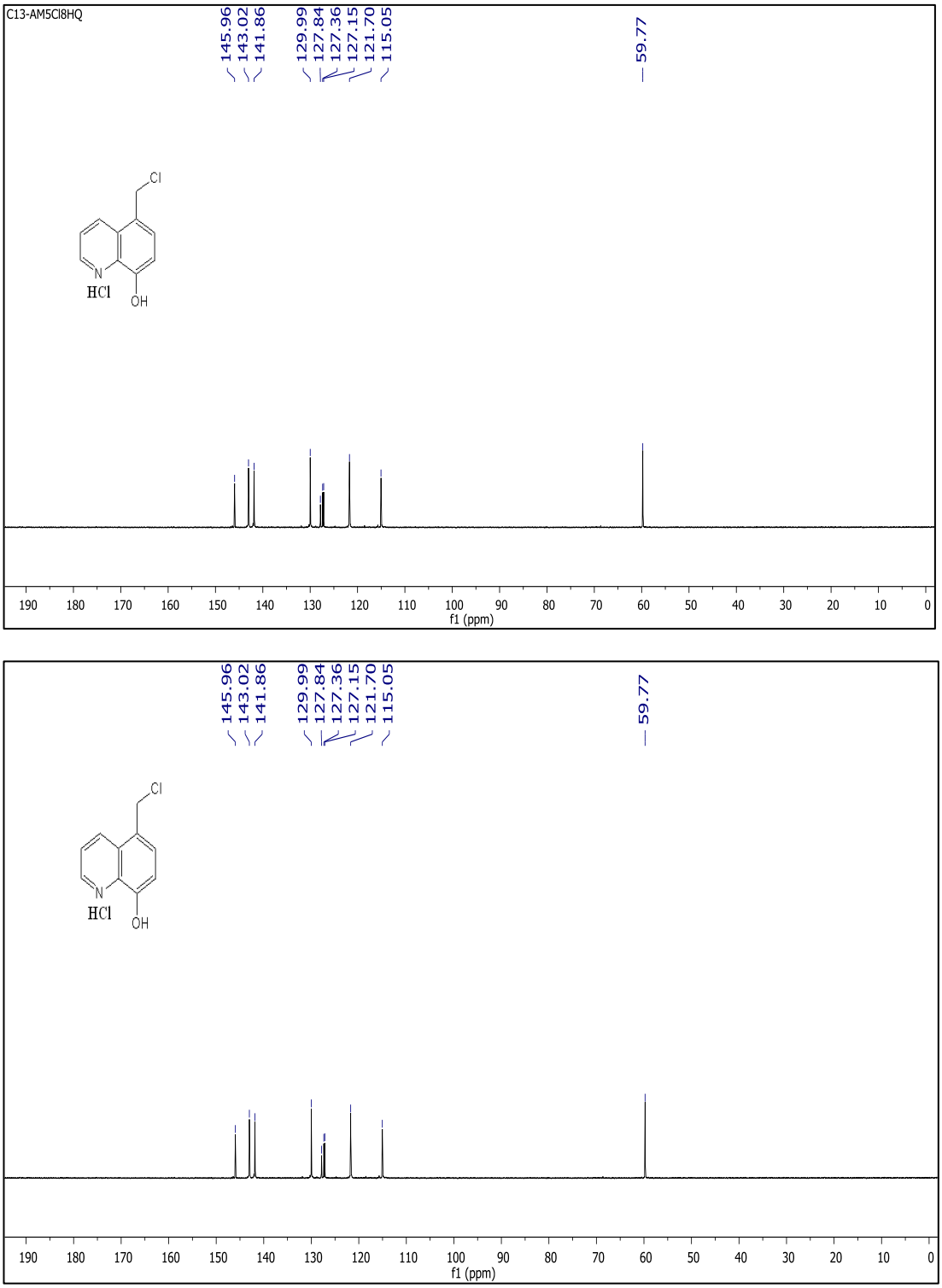


Figure 58: $^{1}H$ and $^{13}C$ spectrum for 64

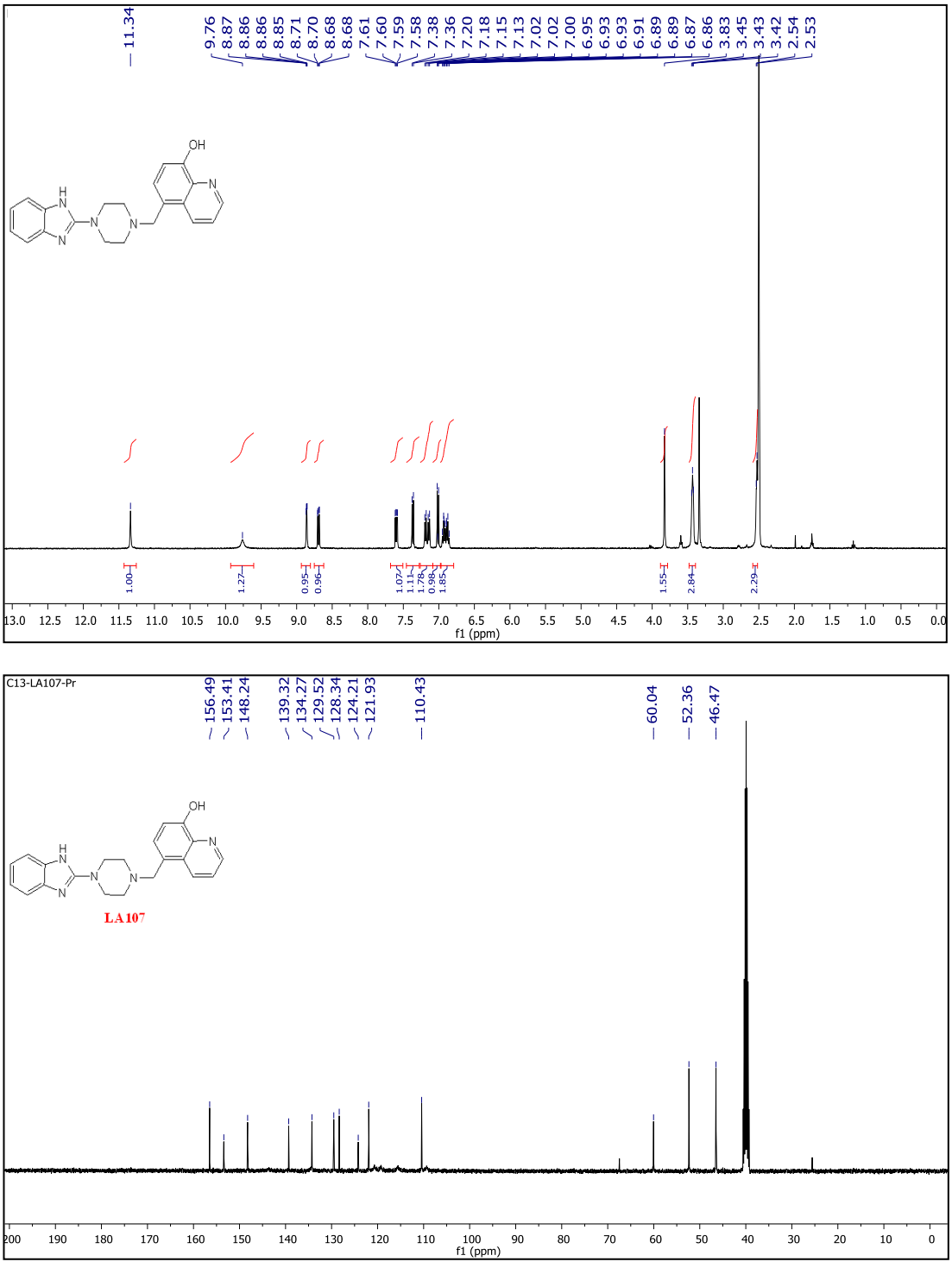


Figure 59: $^{1}H$ and $^{13}C$ spectrum for 65

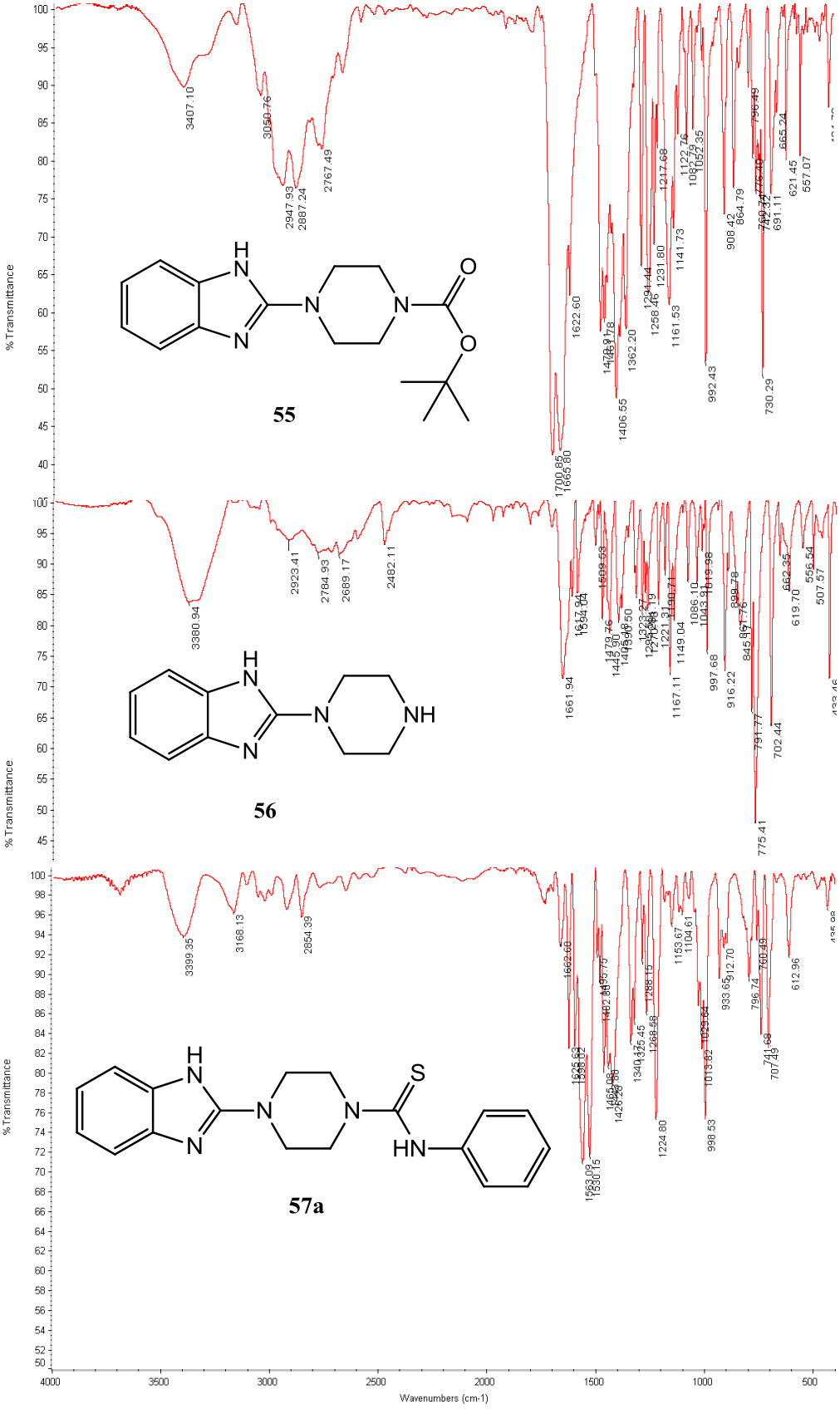


Figure 60: Infrared spectra for (55), (56) and (57a)

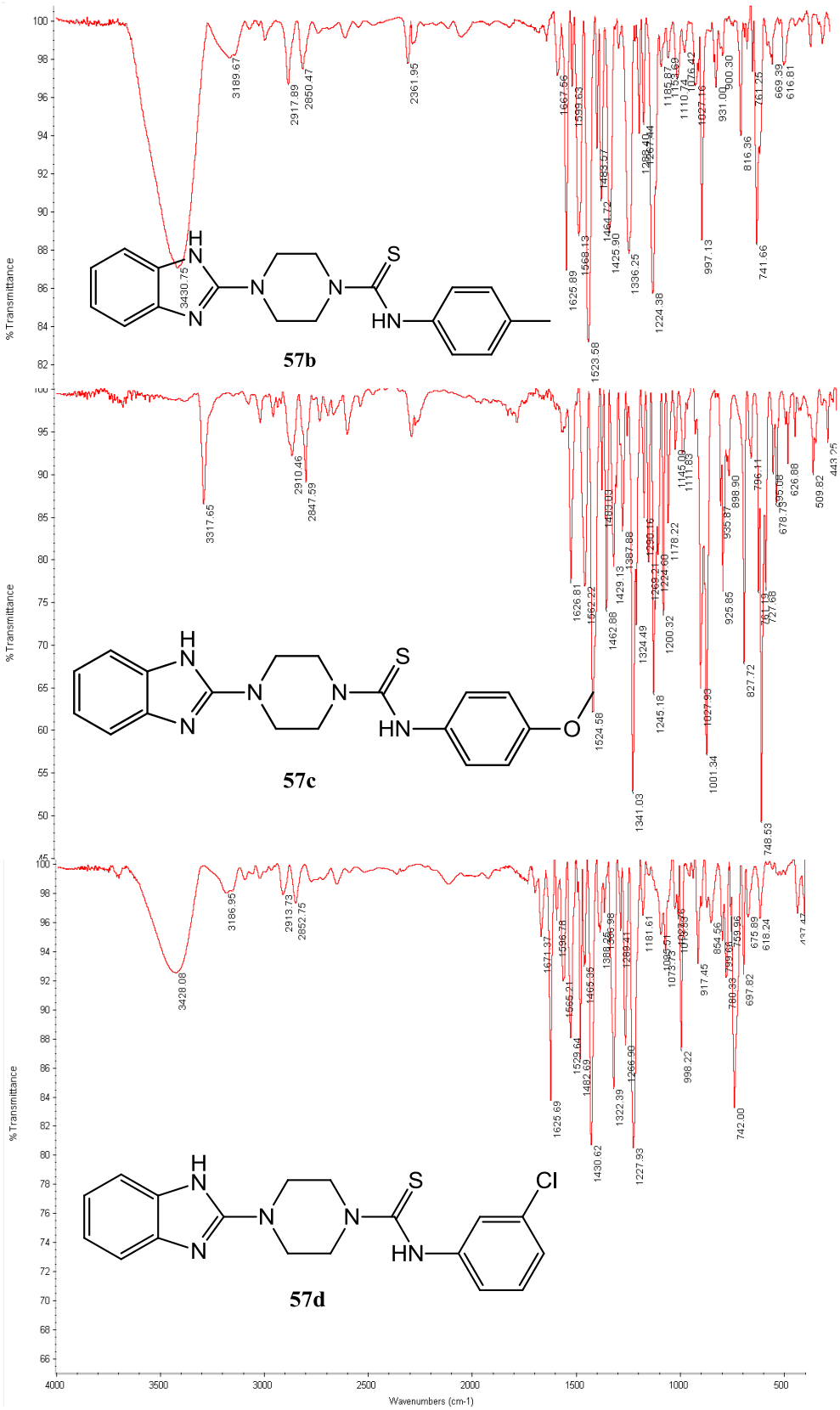


Figure 61: Infrared spectra for (57b), (57c) and (57d)

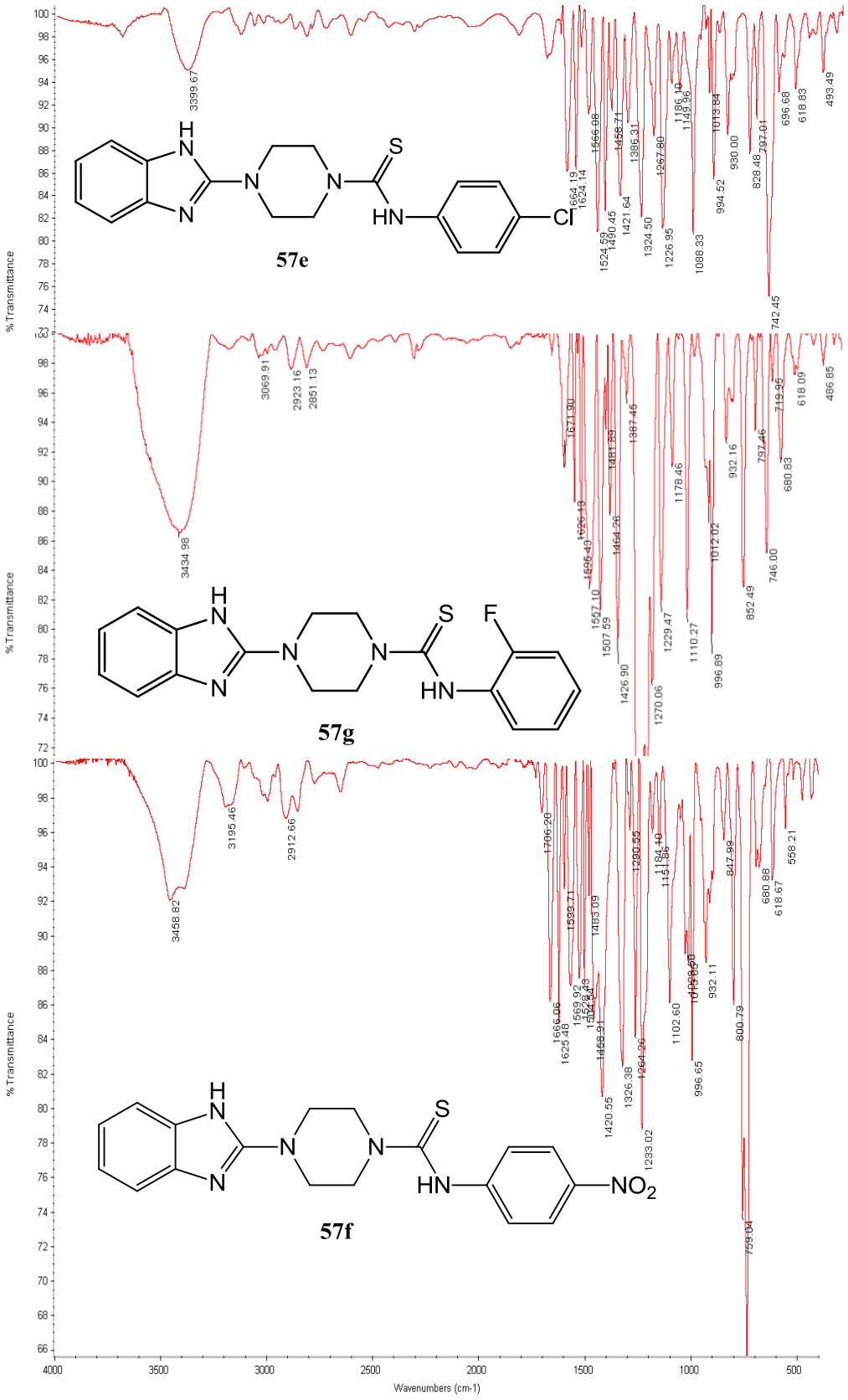


Figure 62: Infrared spectra for (57e), (57g) and (57f)

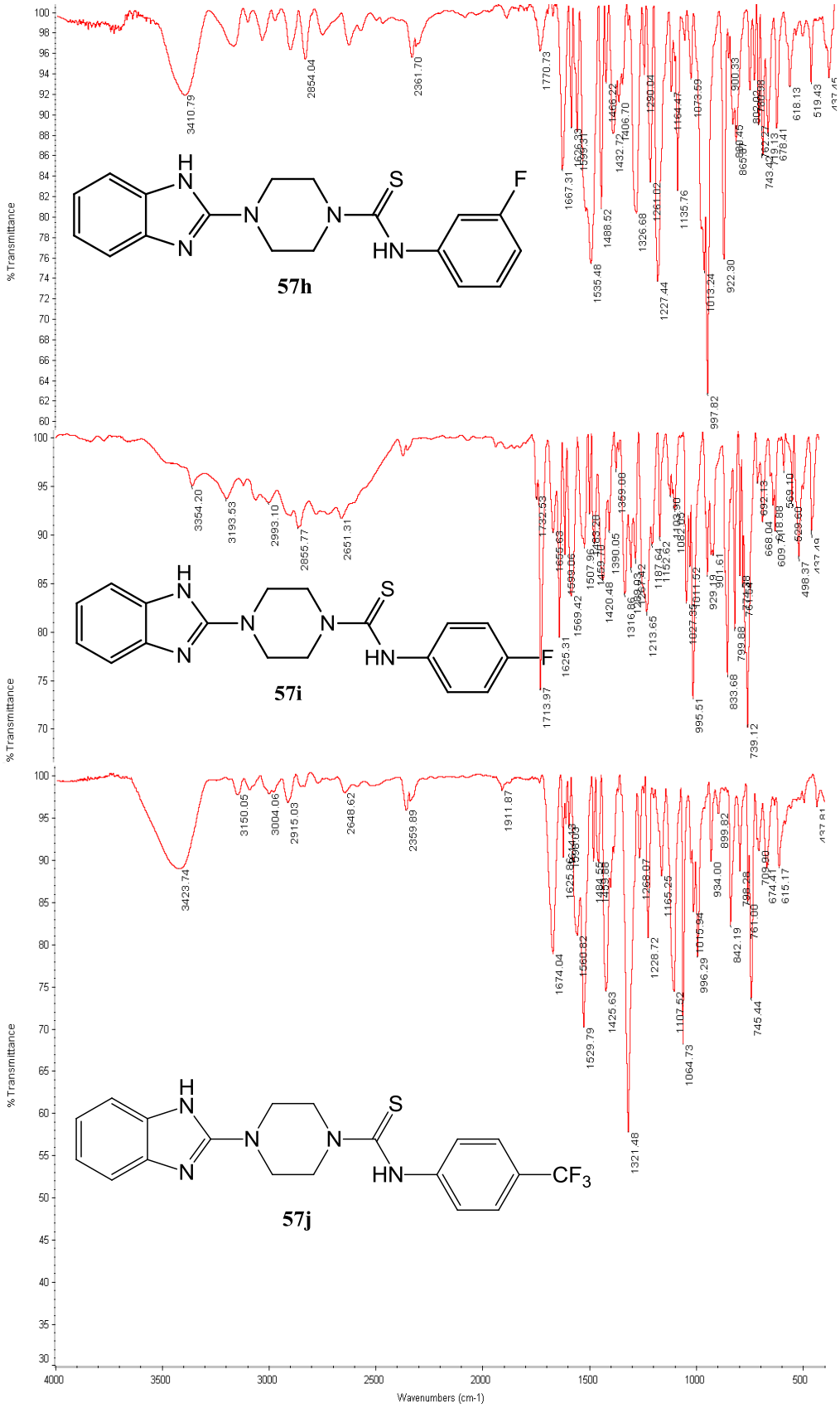


Figure 63: Infrared spectra for (57h), (57i) and (57j)

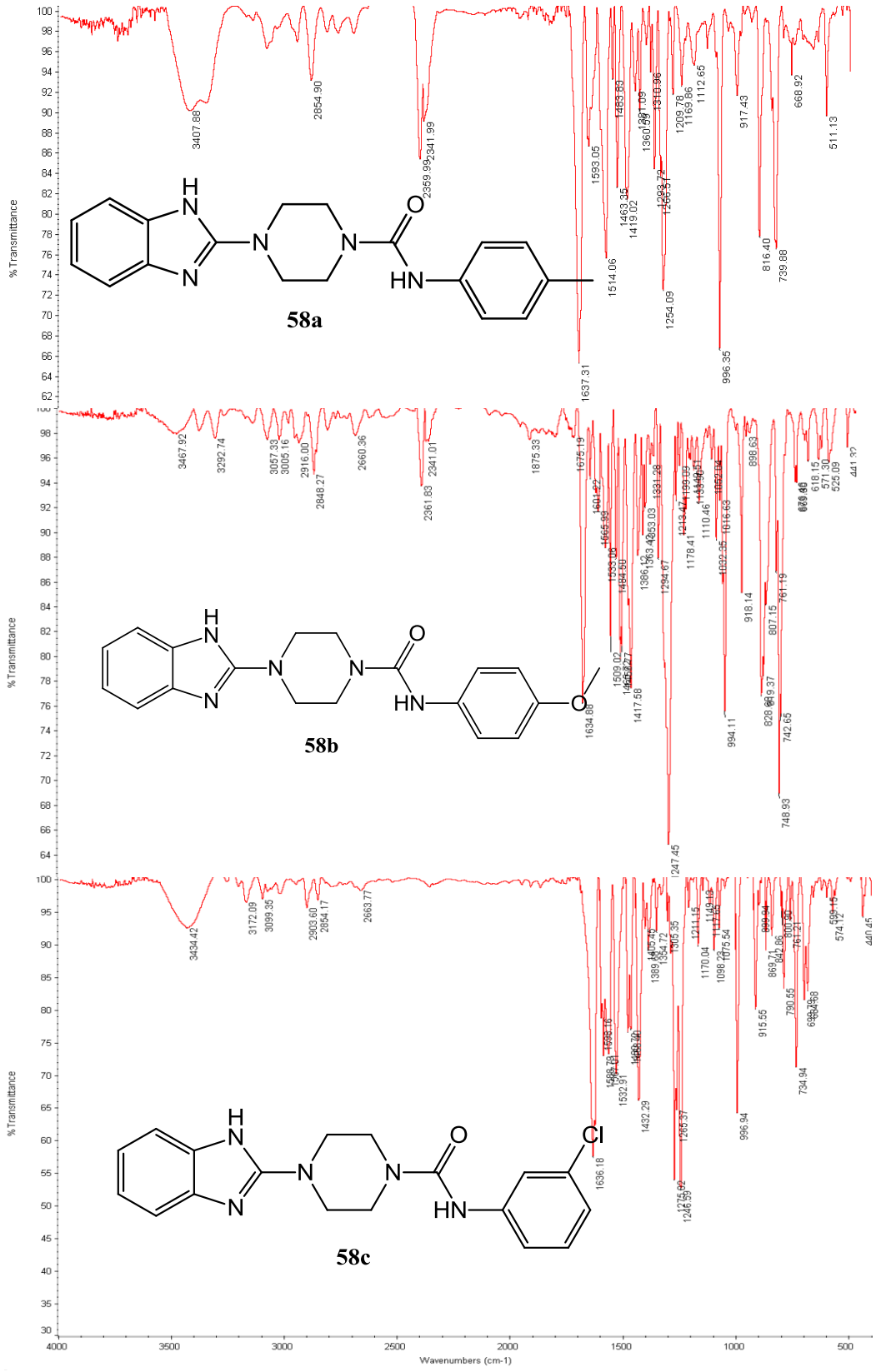


Figure 64: Infrared spectra for (58a), (58b) and (58c)

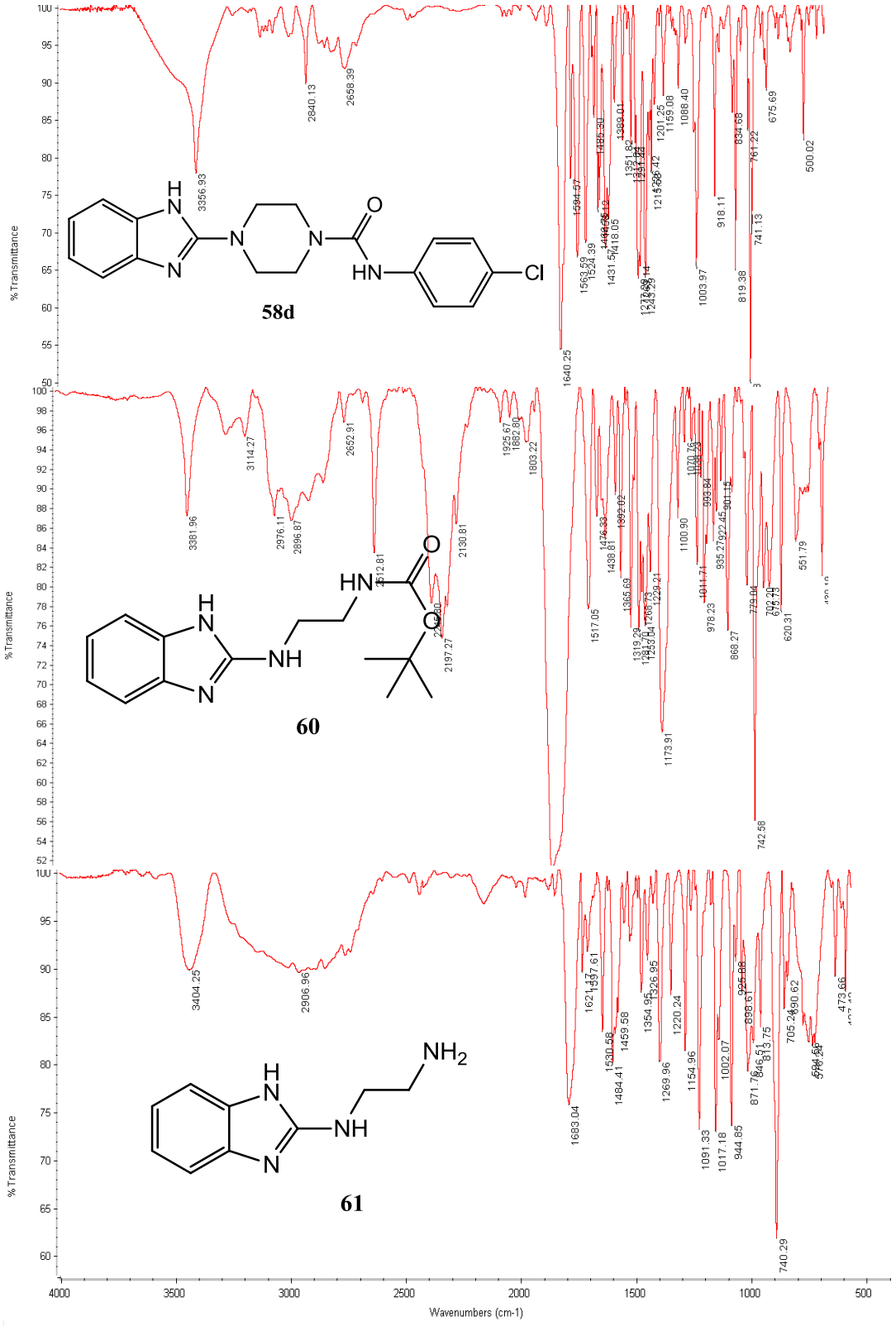


Figure 65: Infrared spectra for (58d), (60) and (61)

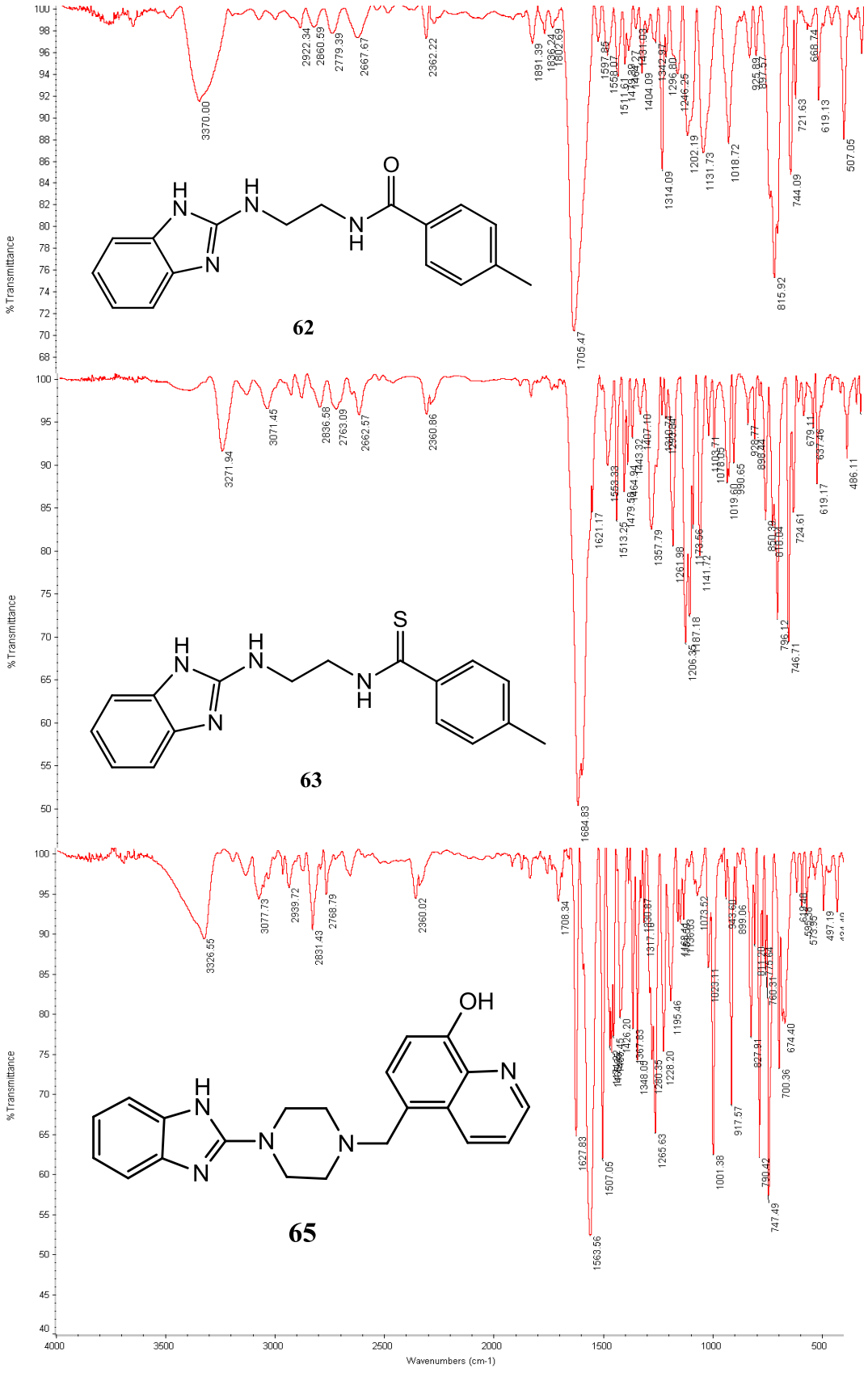


Figure 66: Infrared spectra for (62), (63) and (65)